A Data-Driven Approach for the Development of a Decision Making Framework for Geological CO_2 Sequestration in Unmineable Coal Seams

Ilija Miskovic

Dissertation submitted to the faculty of the Virginia Polytechnic Institute and State University in partial fulfillment of the requirements for the degree of

Doctor of Philosophy

In

Mining Engineering

Michael E. Karmis

Gerald H. Luttrell

Erik C. Westman

Jack C. Pashin

Nino S. Ripepi

December 14, 2011

Blacksburg, VA

Keywords: CO_2 Sequestration, Unmineable Coal Seams, Decision Making

A Data-Driven Approach for the Development of a Decision Making Framework for Geological CO_2 Sequestration in Unmineable Coal Seams

Ilija Miskovic

ABSTRACT

In today's energy constrained world, carbon capture and sequestration can play an essential role in mitigating greenhouse gas emissions, while simultaneously maintaining a robust and affordable energy supply. This technology is an end-of-pipe solution that does not contribute to a decrease of the production of greenhouse gases, but is very useful as a transition solution on the way towards other sustainable energy production mechanisms.

This research involves the development of a comprehensive decision making framework for assessing the techno-economic feasibility of CO_2 sequestration in unmineable coal seams, with the Central Appalachian Basin chosen for analysis due to the availability of empirical data generated through recent characterization and field validation studies. The studies were conducted in order to assess the sequestration capacity of coal seams in the Central Appalachian Basin and their potential for enhanced coal bed methane recovery.

The first stage of this research involves assessment of three major sequestration performance parameters: capacity, injectivity, and containment. The assessment is focused on different attributes and reservoir properties, characteristic of deep unmineable coal seams in the Central Appalachian Basin. Quantitative and qualitative conclusions obtained through this review process are used later in the identification of the minimum set of technical information necessary for effective design and development of CO_2 storage operations.

The second section of this dissertation analyzes economic aspects of CO_2 sequestration. This segment of the research uses a real options analysis to evaluate the impact of major sources of uncertainty on the total cost of developing and operating a CCS project in a regulatory environment that expects implementation of carbon taxes, but with uncertainty about the timing of this penalty.

Finally, all quantitative and qualitative information generated in the first two stages of this research were used for development of a decision making framework/matrix that summarizes the interactions between major technical and economic parameters and constraints, and their impact on overall feasibility of CO_2 sequestration in unmineable coal seams. This framework will provide user with capability to address complex problems in a more systematic way and to analyze the most efficient way to utilize available resources.

DEDICATION

For Marija and Dušan...

ACKNOWLEDGEMENTS

I would like to thank the many people who helped make completing my postgraduate studies possible. I would like to thank my mentor, Dr. Michael Karmis, for invaluable comments and guidance throughout the Ph.D. process, as well as for being a wonderful person without whose help my life might have taken a different direction. The research skills I have developed working under his guidance on this and a number of other projects have made me a much improved researcher. The other members of committee - Dr. Gerald H. Luttrell, Dr. Erik C. Westman, Dr. Jack C. Pashin, and Dr. Nino S. Ripepi - helped shape this research with their valuable insights and feedback throughout the research process.

I could not have completed this work without help of Steven Schafrik, Margaret Radcliffe, Brad Kelley, James Waddell and other colleagues working at the Virginia Center for Coal and Energy Research and Mining Engineering Department.

I would like to acknowledge the U.S. Department of Energy's National Energy Technology Laboratory (NETL) for project funding. This research would not have been possible without the assistance of individuals from Marshall Miller & Associates, CNX Gas, the International Energy Agency, KanORS Consultants, the Geological Survey of Alabama, and Praxair.

Finally, I would like to thank my family and friends for their continuous support. First, I would have never finished this journey without the love and support of my wife Sanja. Throughout all of the highs and lows over the last few years she has always been there for me and made this possible. I would be careless to not thank my daughter Marija for providing the occasionally much-needed distraction during long days and nights sitting and working at my desk.

Nothing of this would be possible without love and encouragement of my parents, Marija and Dušan Mišković. I thank them for loving me unconditionally, always believing in me, and pushing me to be all that I am and more.

TABLE OF CONTENTS

LIST OF FIGURES

LIST OF TABLES

Chapter 1.
INTRODUCTION

1.1 BACKGROUND

Climate change is currently at the forefront of environmental, social, and technological concerns of the 21st century. There is a growing concern about the extent of the climate change and how this change will impact human societies and natural ecosystems around the world. While there are several factors that can shape the Earth's climate and significantly contribute to climate change, such as variations in solar radiation, variations in the Earth's inclination and revolution, mountain-building, and continental drift, most global warming scientists believe that the most significant factor today is anthropogenic greenhouse gas (GHG) emissions.

Since the beginning of the industrial revolution, the level of CO_2 in the atmosphere has risen by more than a third, from pre-industrial 280 ppm to 379 ppm in 2005, and today is increasing faster than ever before [1]. The Intergovernmental Panel on Climate Change (IPCC) has estimated that in the next hundred years, with current trends in emissions showing a rise of about 2 ppm per year, CO_2 concentrations will be three times higher than pre-industrial CO_2 levels [2].

According to the U.S. National Academy of Sciences [3], increased concentrations of GHGs in the Earth's atmosphere directly correlate with the increase in global temperatures. The scientific consensus is that climate change is actually

happening, and scientists worldwide agree that the main reason for this phenomenon is increased level of CO_2 in the atmosphere caused by anthropogenic activities, especially burning of fossil fuels for energy, industrial processes, and transportation.

It is observed that global temperatures have already risen 0.77°C since the early 1900s, with much of the warming occurring in the last 30 years alone. If this trend continues it is expected that global temperatures will rise at least another 1.1°C, and potentially more than 6°C, over the next 100 years [4]. It is not possible to predict future consequences of the rise in CO_2 concentrations, but we can expect different adverse scenarios including ocean acidification, sea level rise, climate perturbations, and ecosystem disruption [5, 6].

There is no shortage of theoretical options and suggestions for how to address potential impacts of climate change. The more challenging task is determining what technological solution, or mix of solutions, will slow down current trends and reduce GHG emissions on the scale of what is needed to avoid adverse impacts of climate change. A complicating factor in addressing climate changes is the world's heavy dependence on fossil fuels, especially coal. As a relatively cheap and abundant resource, coal plays a very important role in today's energy constrained world. Taking into consideration its relative cost stability and wide availability, coal is expected to remain a major fuel for electricity generation at least in the near-term time horizon.

According to U.S. Energy Information Administration (EIA), coal accounts for about 45% of electricity generation in the United States and it is expected that by 2035, coal will continue to be the dominant fuel used for electricity generation, as shown in

Figure 1 [7]. Moreover, coal is used to produce more than half of the electricity in many countries, including South Africa, Poland, China, Australia, and India [8].

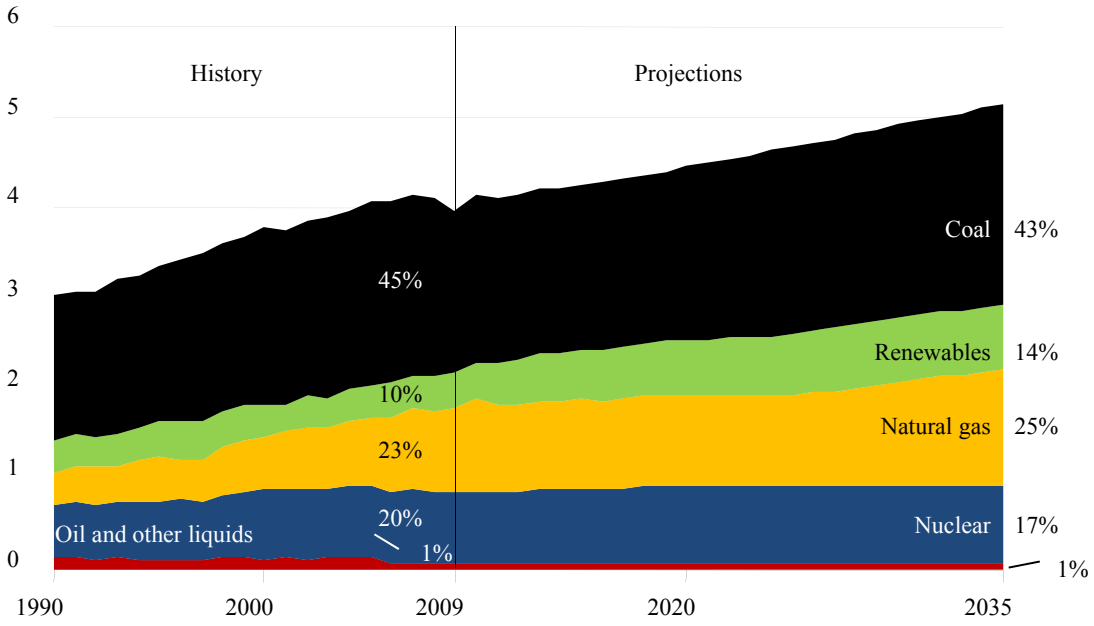

Figure 1: U.S. Net electricity generation (trillion kWh per year) by fuel, 1990-2035. Sources: History: EIA, Annual Energy Review 2009. Projections: National Energy Modeling System, run REF2011. D120810C.

The current global CO_2 emissions associated with energy production and consumption are 29.7 billion metric tons carbon dioxide equivalent (CO_2e), with the U.S. contributing 6.2 billion metric tons of the overall energy-related emissions [10].

Of the total amount of GHGs emitted in the U.S. in 2006, about 5.9 billion metric tons were CO_2 from energy consumption. Nearly 60% of these emissions are emitted from stationary sources, particularly power plants and industrial processes, such as cement and limestone production facilities. The stationary nature of these sources allows CO_2 emissions to be captured and potentially stored in geologic formations instead of being released to the atmosphere. The family of technologies that uses such abatement is referred to as Carbon Capture and Sequestration (CCS). Alongside CCS, there are four

additional options for reducing energy-related CO_2 emissions that can help achieve the sustainable energy systems of the future [9]:

1. Improvements in the efficiency of energy use;
2. Increased use of renewable energy such as wind, solar, and biomass;
3. Expanded electricity production from nuclear energy; and
4. Switching to less carbon-intensive fossil fuels such as natural gas.

Even if a future increase in global energy demand is met by increasing a share of low-carbon sources in the energy mix, there would be no significant reduction in CO_2 emissions because fossil fuels will continue to be a primary source of energy, especially in developing nations with rapid economic growth. As shown in Figure 2, it is expected that consumption of fossil fuels in the U.S. will decrease only 9% over the next 20 years.

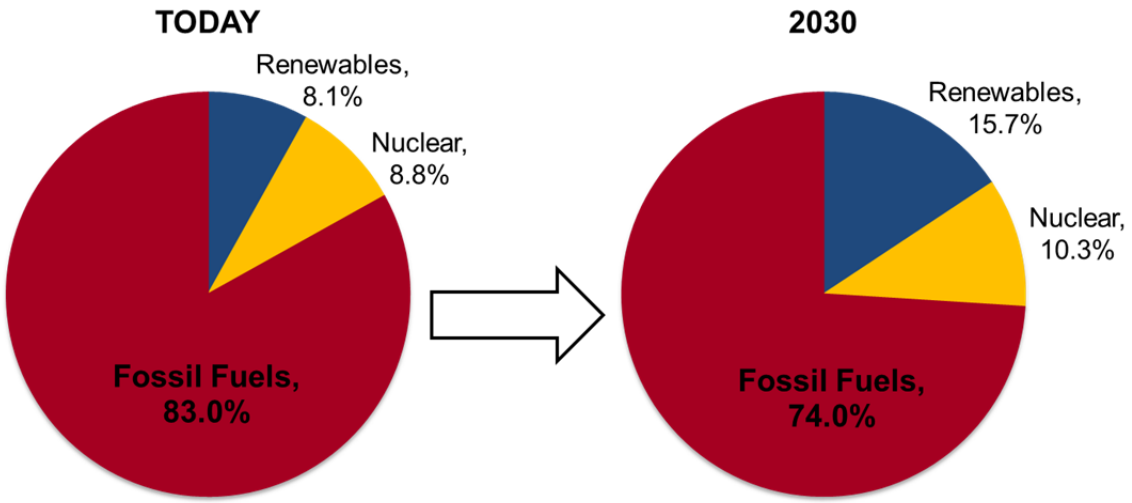

Figure 2: Expected changes in the U.S. energy mix 2010-2030. Source: EIA, Annual Energy Outlook 2011

Compared to other mitigation options, CCS has the potential to reduce CO_2 emissions in the short term. It is an end-of-pipe solution that does not contribute to a

decrease of the production of greenhouse gases, but it is very useful as a transition solution on the way towards other sustainable energy production mechanisms. In this context, CCS has emerged as the most promising large-scale approach for reducing GHG emissions in the next 20 to 50 years for several reasons [10]:

1. The potential storage capacities are enormous. Formal estimates of global storage potential vary substantially but are likely to be sufficient for storing between 3,000 and 10,000 gigatons (Gt) of CO_2. This presents significant capacity if compared with the annual global CO_2 emissions of 25 Gt.
2. CCS is based on existing technologies. CO_2 has been separated from industrial waste streams for nearly 100 years and has been injected underground for over 30 years.
3. CCS is actionable. In the U.S. and many other industrial countries, large CO_2 sources, like power plants and refineries, lie near prospective storage sites.

1.2 RESEARCH OBJECTIVES

It is widely recognized that large scale reductions in CO_2 emissions are required during this century in order to limit the extent of climate change. To meet this long-term goal of atmospheric stabilization, a major technological transformation must occur in the energy sector. One of the possible options to achieve this goal is carbon capture and sequestration.

CCS is an emerging technology that has significant potential and it can be an essential tool for achieving most of the short- and long-term GHG reduction goals. Although current CCS technology is based on a combination of well-known and emerging technologies and processes, many performance and safety aspects must be addressed before CCS is introduced to the market and commercially deployed. Much work remains, but a wealth of information from public and private sectors on what needs to be done is already available. Expert tools that can analyze available data and provide accurate and timely information, reduce costs, and make CCS more transparent and accepted by the public, can aid in the smooth and efficient implementation of CCS technology.

To be most effective, the design of a CCS project must begin with the characterization and careful choice of appropriate storage system(s)/formation(s) and analysis of the feasibility of alternative solutions. The decisions related to this process must take into account both technical and economic goals of the project, while considering risks and safety issues associated with CCS. Furthermore, decisions about selection of the best capture technology and choice of the most efficient transportation option are just adding to complexity of the design, and make CCS decision making process more uncertain.

Because of complex and multiple interactions between different components in the CCS chain, there is a need for a systematic decision support framework that can help project designers, policymakers, and other parties involved in CCS process to evaluate all available data and make knowledgeable decisions.

With this in mind, this research effort is focused on the development of a decision making framework designed to assist in evaluation of direct benefits and costs of entering into contracts for geological CO_2 sequestration. The long-term goal for this research is to create a comprehensive system of indicators that can provide quantitative and qualitative information about various performance characteristics of each component in the chain.

Although this decision making framework does not provide a decision rule or a "right" solution to a set of complex problems expected in commercial CCS operations, it can help provide a view of the different perspectives, facilitating an examination of the necessary trade-offs and leading to responsible decisions.

By aligning research findings and knowledge gained through pilot CCS studies with short- and long-term business objectives, this framework will provide the user with the capability to address complex problems in a more systematic way and to analyze the most efficient way to utilize available resources. This research focuses on the creation of a cohesive decision making framework that integrates technical and economic aspects of geologic CO_2 sequestration into the decision making process.

1.3 RESEARCH CONTRIBUTION

The research will offer a decision making methodology developed to assist technical and economic assessment of potential CO_2 storage projects, with the focus on CO_2 storage in coal seams.

This framework provides a holistic approach to assessment of potential CO_2 storage in unmineable coal seams. The techno-economic assessment and design recommendations addressed in this dissertation take into consideration a number of

technical and economic constrains that a designer or project manager may face through the design process, especially in early characterization and site selection phases.

The framework was designed to be flexible and expandable so that new modules and empirical data can be easily incorporated. The modular approach provides a potential user with capability to develop and implement new modules based on current knowledge and available data, and furthermore, to build a computer-based decision support system that can automatize the entire process.

1.4 DISSERTATION ORGANIZATION

This dissertation has five chapters that are organized in the following way:

Chapter 1 - INTRODUCTION:

Defines the problems in the area of the study, and presents the research objectives and methodology used to accomplish these objectives. Chapter 1 also explains contributions of the research and limitations of this study.

Chapter 2 – LITERATURE REVIEW:

Provides the general review of fundamental knowledge in the area of CCS and decision science and focuses on the identification of the critical techno-economic factors and risks related to CO_2 sequestration.

Chapter 3 – TECHNICAL ASPECTS OF CO_2 STORAGE IN UNMINEABLE COAL SEAMS:

This chapter gives a comprehensive analysis of technical aspects of CO_2 sequestration in coal seams. This analysis identifies technical issues related to CO_2 sequestration in coal

seams such as: capacity estimation; injectivity and enhanced coal bed methane recovery; and reservoir containment.

Chapter 4 – ECONOMIC ASSESSMENT:

Describes and illustrates a real option analysis methodology used to evaluate financial aspects of CO_2 storage in unmineable coal seams and related enhanced coal bed methane recovery.

Chapter 5 – DECISION MAKING FRAMEWORK:

Describes the structure, critical issues, major components, and the general decision process used in this framework. This chapter also discusses the use of assessment criteria and corresponding algorithms in the framework.

Chapter 6 – CONCLUSIONS AND RECOMMENDATIONS:

Summarizes the research and its contributions and gives future research recommendations.

Chapter 2.
LITERATURE REVIEW

Compared to other mitigation options, carbon capture and storage has the potential to reduce CO_2 emissions in the short term. It is an end-of-pipe solution that does not contribute to a decrease in the production of greenhouse gases, but it is very useful as a transition solution on the way towards other sustainable energy production mechanisms. CCS consists of three major steps, namely, capture and concentration of CO_2 from residual gases at a large point source, transport to on-shore or off-shore storage site, and the storage of CO_2 in deep geological formations [11].

2.1 CO_2 CAPTURE

In the CO_2 capture process, a concentrated stream of CO_2 is separated and conditioned before transportation to the storage site. There are three main technologies to capture CO_2 emitted form large point sources that utilize primary fossil fuel (coal, natural gas, or oil), biomass, or mixtures of these fuels for energy conversion [4]:

1. Pre-combustion systems;
2. Post-combustion systems; and
3. Oxyfuel combustion systems.

2.1.1 PRE-COMBUSTION CAPTURE

The first of the three capture technologies, pre-combustion, allows operators of power plants to capture CO_2 and at the same time maximize power output. In this method, an air separation unit produces a stream of almost pure oxygen (Figure 3). The oxygen flows into the gasifier and reacts with the primary fuel (e.g., pulverized coal) to form a gas mixture composed mainly of carbon monoxide (CO) and hydrogen (H_2), or "syngas." This process is known as the gasification step.

In the second step, steam is added to the Syngas in a water-gas shift reactor, converting the CO to H_2 and CO_2. Using a physical wash, the CO_2 is then captured from the gas stream and after compression and dehydration, is ready for transport and storage [12]. The hydrogen rich stream can be used as a fuel in a gas turbine combined cycle plant. The flue gas that leaves from the hydrogen-powered turbines passes through a heat recovery steam generator, which powers steam turbines re-using this energy and optimizing energy output.

Today, the hydrogen is burnt in power turbines and makes electricity; tomorrow, it could also be used, after extra conditioning (e.g., Pressure swing adsorption (PSA)), for use in fuel cells or as a vehicle fuel [4, 12].

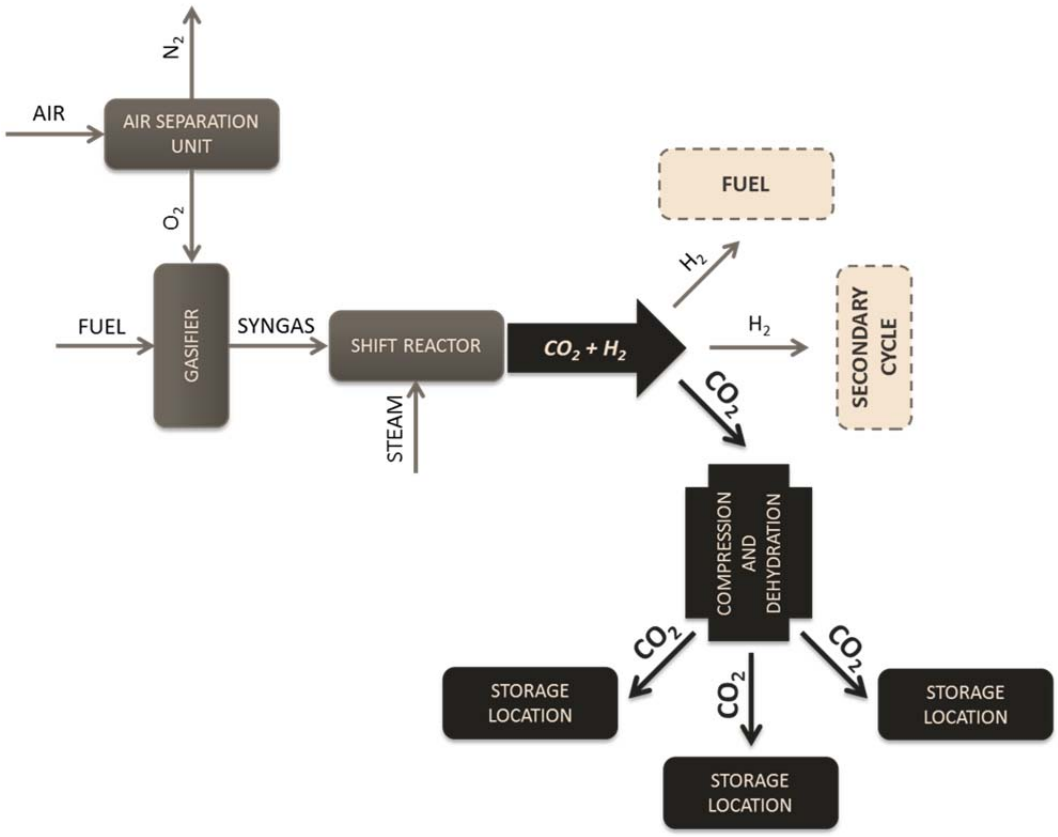

Figure 3: Schematic representation of pre-combustion cycle.

2.1.2 POST-COMBUSTION CAPTURE

Capture of CO_2 from flue gases produced by the combustion of fossil fuels is referred to as post-combustion capture (Figure 4). This technology can be applied with both existing and future power plants and industrial processes.

In post-combustion capture, a solvent is typically used to chemically absorb the CO_2 from the flue stream after the combustion process. In the first step of the post-combustion process, a mixture of primary fuel (coal or gas) and air is injected into the boiler and ignited. Usually, before it is fed into the boiler, the coal passes through a series of "washing" steps, where coal is treated with liquids of varying densities in order to remove unwanted matter and make the coal burn more efficiently. In the second step, the

flue gas, a by-product of coal combustion, is separated from the boiler and filtered. After the generated steam has passed through the turbine, it arrives at a condenser. This unit is used to condense steam back into water, allowing it to be piped back into the boiler and re-heated.

In the next step, a "clean" flue gas enters the CO_2 absorber, where water is used to lower the temperature of the flue gas. Here, the gas stream is typically passed through a liquid sorbent, which reacts with the CO_2, chemically binds with it, and removes it from the flue gas. Once the CO_2 is captured, the sorbent is moved to a desorber to be regenerated, which usually involves heating the sorbent to release the captured CO_2 [13].

Reactive absorbents are the preferred choice in post-combustion due to the low partial pressure of CO_2 (between 3-15 kPa) in the flue gas. Other techniques, such as membranes and adsorption are not as mature and efficient as the absorption process and require further development [14].

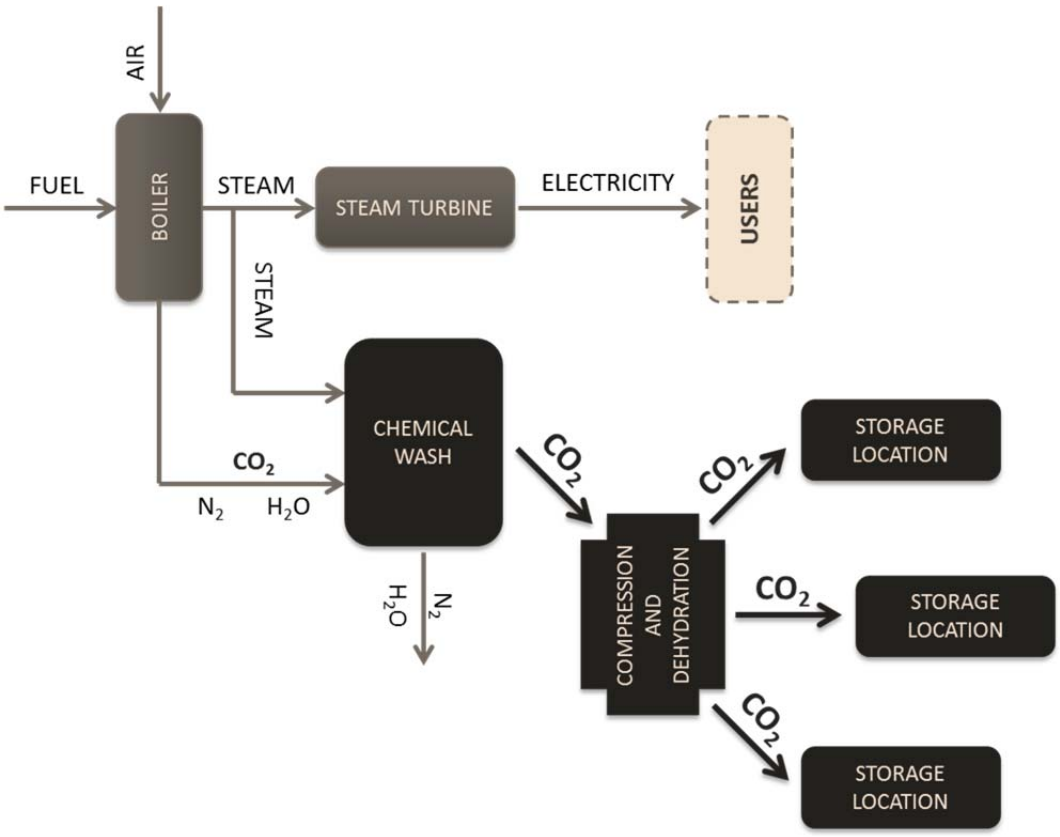

Figure 4: Schematic representation of post-combustion cycle.

2.1.3 OXYFUEL COMBUSTION

The third capture technology, oxyfuel combustion, consists of burning fuel in a mixture of pure oxygen and recirculated flue gas instead of air. This is done to increase the CO_2 concentration in the flue gas, thereby making it more efficient to remove before processing for transport and storage. Theoretically, this system is capable of capturing nearly all produced CO_2, but the need for additional gas treatment systems required to remove inert phases and pollutants, such as SO_2 and NO_X, from flue stream, lowers the capture efficiency to slightly more than 90% [4]. Oxyfuel combustion deploys an air separation unit that removes nitrogen from the air, while producing oxygen.

Generated oxygen is injected, alongside with the fuel, into a boiler where combustion takes place. Generated steam is used to power turbines and make electricity. Meanwhile, the flue gas, CO_2, and water vapor are re-circulated in the system in order to regulate boiler temperature and to gradually cool before CO_2 dehydration and compression [15, 16]. This leaves the captured CO_2 to be ready for transport and storage.

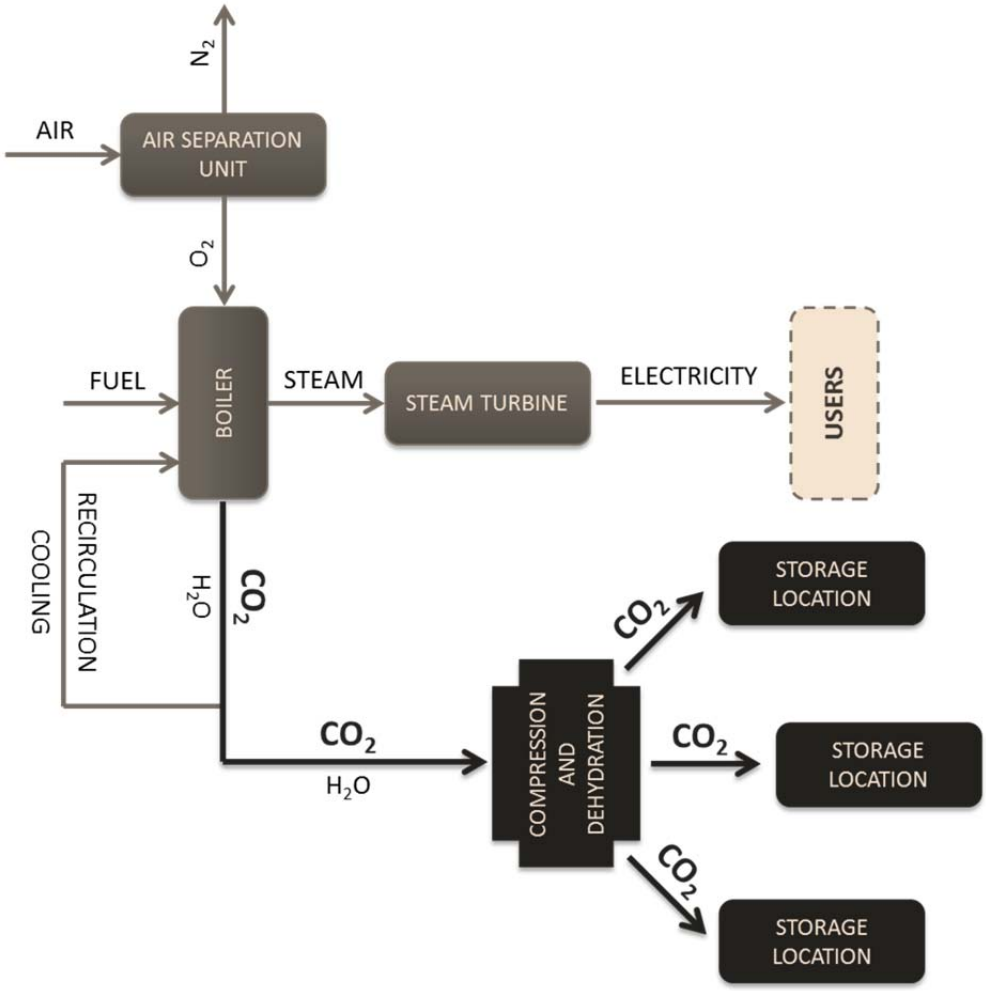

Figure 5: Schematic representation of oxyfuel cycle.

2.2 CO_2 TRANSPORT

Since the early 1970s, the U.S. oil and gas industry has been transporting and re-injecting CO_2 into oil fields to maintain or enhance production. Because of this activity,

there are already about 5,000 kilometers of pipeline network in North America alone transporting CO_2 from natural reservoirs and anthropogenic sources to oil fields. The largest pipeline network supplies oil fields in Texas with more than 40 $MtCO_2$ per year, where the CO_2 is used for enhanced oil recovery (EOR) [17].

Except when stationary sources of CO_2 are located directly above a geological storage site, captured CO_2 must be transported from the point of capture to a storage site. After CO_2 is separated and captured from the flue gas, it is compressed to about 10 MPa at the compression station, which is usually part of the capture facility, and transported to the storage site. The CO_2 pressure in pipelines should be kept above 8 MPa through the entire pipeline trajectory in order to avoid two-phase flow regimes and to increase the density of the CO_2, thereby making it easier and less costly to transport [18].

CO_2 is preferably transported by pipeline, with other means of transport being used when a source of CO_2 is offshore or amount of CO_2 is too small and uneconomical for transport by pipelines. Other options for CO_2 transport include ships, road and rail tankers that carry CO_2 as a liquid in insulated tanks at a temperature well below ambient and at much lower pressures. Sometimes transport of the CO_2 by ship is more feasible than utilization of pipelines, particularly when the CO_2 has to be transported over large distances or overseas. Road and rail tankers are also technically feasible options. These systems transport CO_2 at a temperature of -20ºC and at 2 MPa pressure. However, they are uneconomical compared to pipelines and ships and are unlikely to be relevant to large-scale CCS [4].

2.3 GEOLOGICAL CO_2 STORAGE

Geological CO_2 storage shows great promise because a large number of potential geologic sinks worldwide have the potential to store many hundreds to thousands gigatons of CO_2 [4, 19]. CO_2 storage involves essentially the same geological basins that have already been the focus of oil and gas exploration and development. Depleted reservoirs provide one of the most promising solutions for CO_2 storage today because these reservoirs have been thoroughly characterized and consequently there is a large amount of data available that can be applied to understanding dynamics of future CO_2 storage projects. Also, due to their physical and chemical characteristics, they offer suitable pressure regimes for CO_2 injection and storage [20]. Furthermore, existing wells allow immediate access to the reservoir, although potential well integrity problems may require additional evaluation, monitoring, and remediation.

2.3.1 GEOLOGIC FORMATIONS

There is a variety of different storage systems that can be used for CO_2 storage. Of these, three main options are deep saline aquifers, mature oil and gas fields, and deep unmineable coal seams [4, 21, 22]. Other options include organic rich shale and basalt formations [23].

2.3.1.1 Deep Saline Formations:

Saline formations are deep layers of porous sedimentary rock saturated with brine waters that are considered unsuitable for human consumption and agricultural or industrial use [24]. They offer an enormous potential for large-scale geological storage of CO_2 due to their wide regional coverage and potential proximity to large point sources.

However, these formations are tipically less understood because they lack the characterization data that is readily available for oil and gas reservoirs. Any assessment of CO_2 storage potential of saline formations typically includes significant uncertainty because of the lack or scarcity of subsurface data.

2.3.1.2 Oil and Gas Reservoirs:

The second option for large-scale geological CO_2 sequestration is storage in mature oil and gas fields. Depleted oil and gas reservoirs are likely to be high-quality sequestration sites since they have the demonstrated ability to contain oil and natural gas, without leaking, over the long-time geologic horizon. CO_2 can be stored in oil or gas reservoirs after they have been depleted and are no longer producing, or it can be used to enhance oil or gas recovery (EOR/EGR) in fields that are still producing. The main technical advantage of storage in depleted oil and gas fields over other potential storage formations (saline aquifers and coal seams) is that the containment potential of these sites have been proven by the retention of hydrocarbons for millions of years, and there are typically large amounts of geological and engineering data available needed for detailed site characterization [4, 24]. However, there are a number of potential drawbacks: potential storage capacity may be limited; it is possible that pore pressure depletion has led to pore collapse, which reduces the potential storage volume; and the presence of existing old wells may provide potential pathways for leakage. [22, 25].

2.3.1.3 Unmineable Coal Seams:

CO_2 can be geologically stored in coal seams that are too deep or too thin to be economically mined, or it can be used to enhance coalbed methane (ECBM) production [26]. Geological CO_2 storage in coal seams is driven by different storage mechanisms

than storage in saline formations or oil and gas reservoirs. In the case of coal seams, the CO_2 is trapped by an adsorption mechanism as opposed to storage in rock pore space (saline or hydrocarbon formations). [4, 21, 22].

All commercial CCS projects that include CO_2 storage in coal seams must be in conjunction with ECBM recovery, so that the methane (CH_4) released from the coal matrix does not leak into the atmosphere as it has a higher greenhouse radiative effect, 21 times stronger by weight than CO_2 [25]. Therefore, CH_4 needs to be captured to ensure a net GHG emission mitigation outcome.

Technical challenges for CO_2 storage in coal seams are generally focused around the feasibility of the CO_2 injection. A major concern is typically low permeability of the coal matrix, which decreases with depth [21]. Moreover, changes during both gas extraction (matrix shrinkage) and injection (matrix swelling) as the coal interacts with the CO_2 present a potential barrier for CO_2 storage with ECBM [4, 22]. In addition, the economic viability of ECBM recovery can be decreased due to the large number of wells required to overcome injectivity issues related to low permeability [21, 22].

Although results from different characterization, laboratory, and modeling studies are promising and show that CO_2 sequestration in unmineable coal seams and associated ECBM recovery are viable, empirical data and experience gained through field/pilot studies are key factors that can provide investors and the general public with assurance that this technology is both commercially feasible and safe.

2.3.2 CHARACTERISTICS OF STORAGE SITES

Each geological unit is unique. For that reason CO_2 storage in deep geological formations should be based on solutions that are tailored to address site-specific issues. For CO_2 storage in deep saline aquifers and oil and gas reservoirs, it is desirable that CO_2 is stored at depths below approximately 800-1,000 m where CO_2 is compressed to a supercritical phase [4]. Storing CO_2 as supercritical fluid enhances both the storage capacity and the storage containment potential via reduced fluid mobility.

Contrary to the situation with deep saline or depleted hydrocarbon formations, storage density is greatest in unmineable coal seams at depths less than 600 m, when injected CO_2 is in the gaseous phase [20].

Success of CO_2 storage in geological formations depends on three major characteristics:

1. *Capacity*. The reservoir must have sufficient pore volume to store all the CO_2.
2. *Injectivity*. The reservoir chemical and physical characteristics must facilitate sufficient injection of CO_2 from the wellbore.
3. *Containment*. An overlaying sealing formation must be present to ensure containment of all fluids in the reservoir.

2.3.2.1 Capacity:

The definition of the pore volume available for containment depends primarily on five parameters [27]: formation thickness, which represents the amount of porous rock available for storage; area of storage formation; rock porosity; the density of CO_2; and

storage efficiency, which is defined as a fraction of pore volume saturated by CO_2 [28]. In most cases, storage efficiency remains relatively constant while other parameters can vary significantly. A key parameter is porosity, which determines how the pore volume is distributed in the formation. In general, the better the porosity, the better the permeability, and thus the better the injectivity [27, 29, 30].

Sufficient formation thickness is another essential factor for a successful injection operation. A formation thickness of around 20 meters would be considered as a minimum requirement for saline and depleted oil and gas reservoirs, but this varies with injection volume requirements [31-33]. Deviated or horizontal drilling can also be used to improve access to the storage formation [34].

2.3.2.2 Injectivity:

Permeability measures the ability of fluids to flow through a formation [25, 35]. High values indicate a well-connected pore space while low permeability values indicate convoluted channels that disconnect the pores [33]. Porous rocks have a wide range in permeability; between 0.1 millidarcy for very tight rocks, to several darcies for very permeable formations. The millidarcy (mD) as a unit for permeability is typically used by the oil industry (1 mD is approximately 10^{-15} m^2, which is the Standard International unit more often used in the groundwater industry).

Ideally, CO_2 storage requires high permeability (>100 mD) to ensure an appropriate near wellbore injectivity required for quick access to the reservoir pore space [24]. However, this is not always possible and near wellbore permeability may need to be enhanced by artificially stimulating the injection well.

While high permeability is generally desirable, very high permeability pathways or channels can enhance CO_2 migration only along concentrated pathways reducing the effective storage within the target formation [35]. CO_2 can also react with rocks and fluids in the formation, and these geochemical reactions can affect permeability. [35].

2.3.2.3 Containment:

Containment primarily depends on the geometry and spatial distribution of rocks, and on pressure conditions that limit fluid flow in the subsurface. In the simplest geometrical case, known as a four-way dip closure, one sealing package drapes and encloses the reservoir and thereby limits fluid flow in the upward direction [36]. In the real world, there are many variations of seal geometries that limit the movement of CO_2 in the subsurface, including lateral and vertical variations in the reservoir and complex geometries of the ultimate seal. This also includes flow barriers such as faults and naturally over-pressurized zones [24, 29, 31, 37, 38].

The role of faults and fractures and their impact on the containment of fluids including CO_2 is complicated and are often misunderstood. The presence of a fault does not necessarily imply a leakage problem [33]. Most rock units are faulted and fractured in some way over geological time [34]. The subsurface extent of hydrocarbon reservoirs may be limited by faults. However, fluids do not directly flow to the surface along the faults because faults are not unimpeded leakage pathways to the surface [39]. In some cases, trace amounts of reservoir fluids do seep very slowly to the surface [40].

2.3.2.4 CO_2 trapping mechanisms:

CO_2 can be trapped as a gas or supercritical fluid under a low-permeability cap rock, similar to the way the oil and natural gas are trapped. Geological storage of CO_2 is achieved through a combination of different physical and chemical trapping mechanisms. There are a number of different trapping mechanisms that facilitate CO_2 storage in deep underground formations [20, 21, 23, 41, 42]:

1. *Physical trapping* in structural or stratigraphic traps, where the free-phase CO_2 is physically trapped by the geometric arrangement of the reservoir and seal rock units, similar to hydrocarbon accumulations;
2. *Hydrodynamic trapping*, where the dissolved and immiscible CO_2 travels with the formation water for very long residence times;
3. *Residual trapping*, where the CO_2 becomes trapped in the pore spaces by capillary pressure forces;
4. *Solubility trapping*, where the CO_2 dissolves into the formation water;
5. *Mineral trapping*, where the CO_2 precipitates as new carbonate minerals; and
6. *Adsorption trapping*, where the CO_2 adsorbs onto the surface of the carbonaceous such as coals and shales.

With the exception of CO_2 adsorption, which is specific to coals, each of these storage mechanisms will be active within most formations but to different degree depending on site-specific characteristics.

2.4 RISKS ASSOCIATED WITH GEOLOGICAL CO_2 STORAGE

The benefits of CO_2 sequestration in geologic formations can be great since CO_2 injected into the deep subsurface can potentially be isolated from the atmosphere over a long time horizon [43]. On the other hand, risks are always present.

The idea of storing CO_2 in geologic formations immediately raises questions about storage containment performance, the environmental risks involved, and necessary monitoring and verification [40]. Some storage reservoirs may not leak at all, while others may do so at an unforeseen rate.

At the moment, insufficient information is available to quantify leakage from CO_2 storage sites. However, it is possible to quantify upper limits for leakage and to draw conclusions from these theoretical limits and the experimental information available to date [44]. There are two types of risk associated with leakage of CO_2 from the storage reservoir [11]:

1. *Local*, site specific, affecting health, safety and the environment;
2. *Global*, resulting from a return of stored CO_2 to the atmosphere.

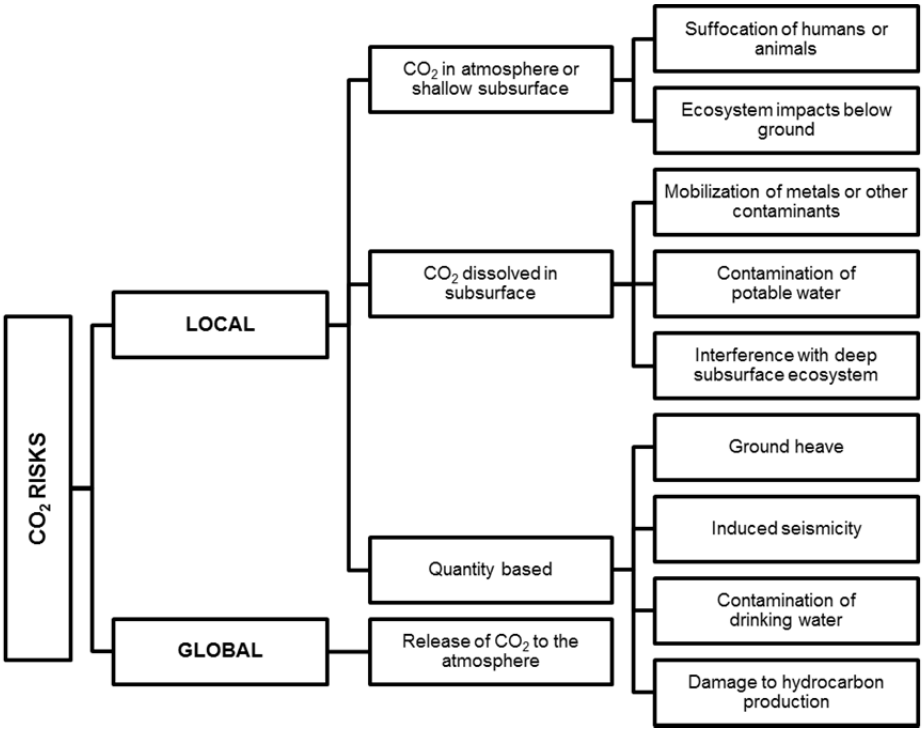

Figure 6: Typology of risks from geologic sequestration (adapted from Metz, 2005) [11].

The majority of constraints imposed on CO_2 storage permanence, and also quality of monitoring, will probably result from the first type, or local risk. At the local scale potentially hazardous impacts may result essentially from three different mechanisms (Figures 6 and 7) [45]:

1. Leakage from the storage location;
2. Alteration of ground and drinking water chemistry; and
3. Displacement of potentially hazardous fluids formerly occupying the pore space being used to store the CO_2.

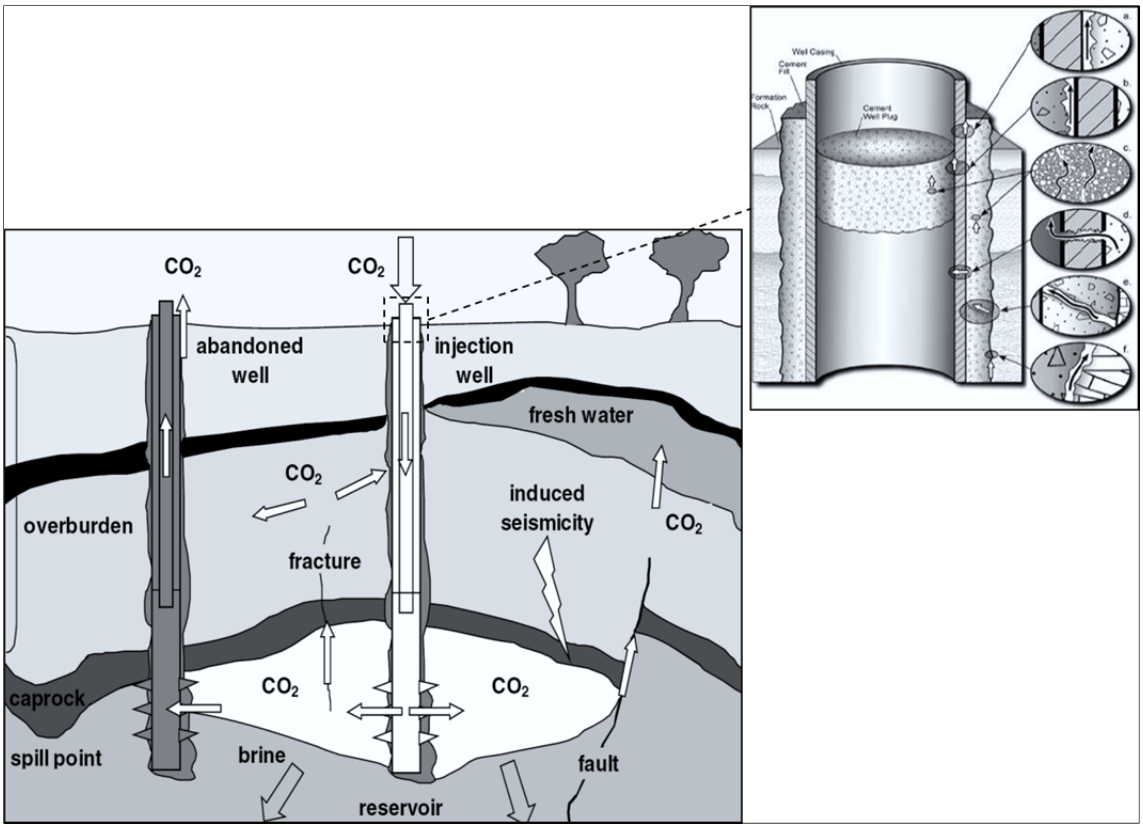

Figure 7: Local risks related to underground CO_2 storage (adapted from Metz 2005, and Damen, 2006) [45].

Rapid release of CO_2 from the storage reservoir through the subsurface into the atmosphere can occur through isolated, catastrophic events, such as an earthquake, or through sustained, slow seepage of CO_2 due to improper storage site selection and preparation. Either of these forms of leakage would result in elevated CO_2 concentrations at the surface or in the shallow subsurface and can negatively impact human health and safety and that of plants and animals in surrounding ecosystems [4]. Currently, we have some understanding of the potential impacts of CO_2 on human beings and flora and fauna, but we are not fully aware of the potential risks to underground potable water.

The local risks of leakage are dependent on both spatial and temporal components of the leakage event. Continuous and dispersed leakage will have very different impacts

than episodic and isolated leakage events. For example, slow but continuous leakage from the reservoir can gradually alter soil ecosystems and surrounding aquifers, and it can cause depressions in the ground and basements of buildings as well. On the other hand, a sudden leakage events such as well blowouts or pipeline ruptures can result in instantaneous disruption [46].

At a global scale, the risk of leakage is dependent only on the average quantity of CO_2 released from the storage site into the atmosphere over time.

2.5 MONITORING, VERIFICATION, AND ACCOUNTING

Although many studies suggest that CO_2 can be stored safely in geological reservoirs for thousands to millions of years, various aspects of CCS need to be studied in more detail [46]. There is a lack of knowledge and data to quantify all processes controlling or causing short- and long-term risks related to underground CO_2 storage. This can be explained by the fact that CCS is a relatively new research field and most studies are still in their early stages [47].

An important aspect of the overall risk management strategy for geological CO_2 storage is the development and implementation of Monitoring, Verification, and Accounting (MVA) protocols. Carefully designed and implemented MVA program can maximize the operational efficiency of the CCS project; maximize the amount of CO_2 stored; minimize the affected reservoir volume; minimize the risk of any unplanned leakage; and minimize the cost of the operation. Furthermore, MVA is necessary to assure continued confinement of CO_2 and verify storage site integrity over the life cycle

of the project; to demonstrate that the storage is performing according to long range predictions; and to foster public acceptance [4].

Standard MVA procedures or protocols are not developed yet, but they are expected to evolve as CCS technology improves [4, 45]. Since all measurement and monitoring techniques currently used in CCS have been adapted from other commercial applications, such as oil and gas production, environmental monitoring, and mining, they need to be tested and evaluated in the context of geological storage (reliability, resolution, and sensitivity).

Given the long-term nature of CCS projects, the development and implementation of new and reliable monitoring tools and protocols, which will enable continuous monitoring of storage over long-term time horizons, is essential to prove that geologic CO_2 storage is both safe and effective [40, 48, 49].

Monitoring spans the entire time horizon of geological storage. It starts with site characterization, and includes extensive baseline measurements before the injection phase. Once injection begins, monitoring addresses injection performance and focuses on the ongoing reservoir and containment properties.

Monitoring activities change intensity as injection stops and subsurface pressures naturally decrease to ensure stability of the injected plume [49]. It continues in reduced manner during the post-closure phase to provide assurance that storage is performing as planned. Successful monitoring depends on selection of the most appropriate monitoring tools and it requires harnessing the appropriate methodologies to provide reliable information about the storage system.

The preferred monitoring combination will depend on site-specific factors such as the depth, temperature, and compositional characteristics of the reservoir, and properties of the injected CO_2 [50]. It will also depend on the type of access permitted, the time frame, the need for repeated measurements, and even cost [50]. The characteristics of the surface above the storage formation also play a huge role in the selection process. Whether on land or offshore, in a desert or forest, farmland or tundra, the surface conditions will impose both practical limitations and technical constraints. Some tools and techniques will be especially useful for certain situations and impractical in others [49, 51, 52].

As shown in Tables 1, 2, and 3, a large and diverse portfolio of standard, "off-the-shelf" monitoring tools and technologies is currently available for monitoring CO_2 storage sites [4]. The challenge is to define and successfully integrate different monitoring tools into one optimized system for a specific CO_2 storage site.

Table 1: List of monitoring objectives and technologies for atmospheric monitoring [50].

	Primary Technologies	***Secondary Technologies***	***Additional Technologies***
Objectives: • Ambient CO2 concentration • CO2 surface flux		**CO_2 Detectors** *(Ambient CO_2 Concentration)*	**Eddy Covariance** *(Surface Flux)*
		Laser systems and LIDAR* *(Ambient CO_2 Concentration)*	**Advanced Leak Detection System** *(Surface Flux)*
			Isotopes

Table 2: List of monitoring objectives and technologies for near-surface monitoring [50].

<table>
<tr><th></th><th>Primary Technologies</th><th>Secondary Technologies</th><th>Additional Technologies</th></tr>
<tr><td rowspan="5">Objectives:
• Groundwater Monitoring
• Fluid Chemistry
• Soil gas monitoring
• Crustal Deformation
• Leak Detection
• Vegetative Stress Monitoring
• Vadose Zone Characterization</td><td rowspan="5">Geochemical Analysis
(Groundwater Monitoring)
(Fluid Chemistry)</td><td>Advanced Water Quality Analysis
• Inorganics & Organics
• Isotopes
• Total Organic and Inorganic Carbon</td><td>Tracers
(Leak Detection)
• Noble Gases
• Mercaptans
• Stable Isotopes
• Perfluorocarbons</td></tr>
<tr><td>Aerial Photography
(Vegetative Stress)
(Crustal Deformation)</td><td>Geophysics
(Leak Detection)
(Vadose zone characterization)
• Conductivity
• Induced Polarization
• Self-Potential</td></tr>
<tr><td>Seismic Surveying
(Vadose zone characterization)
(Leak Detection)
• Shallow 2-D Seismic</td><td>Tiltmeters
(Crustal Deformation)</td></tr>
<tr><td>Soil and Vadose Zone Monitoring
(Gas sampling)</td><td rowspan="2">Remote Sensing
(Crustal Deformation)
• Color IR Transparency Film
• Hyperspectral – multispectral
• Synt. Aperture Radar & InSar</td></tr>
<tr><td>Flux Accumulation Chamber
(Surface Flux)</td></tr>
</table>

Achieving a well-planned, integrated monitoring design can benefit all parties involved. For example, in oilfields, ineffective monitoring might result in missed or lost production that will reflect in lost revenues. For CO_2 storage, inappropriate monitoring might provide either a false sense of security or a false alarm for issues that do not exist [49, 50].

Table 3: List of monitoring objectives and technologies for subsurface monitoring [50].

	Primary Technologies	***Secondary Technologies***	***Additional Technologies***
Objectives: • Groundwater Monitoring • Soil Gas Monitoring • Leak Detection • Subsurface and Reservoir Characterization • Plume Tracking • Well Integrity Testing	**Water Quality Analysis** • Injection Fluid Monitoring • Formation Fluid Monitoring • Water Level	**Seismic Surveying** *(Reservoir Integrity)* • Acoustic (2-D and 3-D) • VSP • 2-D and 3-D	**Geophysical Techniques** *(Leak Detection)* *(Subsurface and Reservoir Characterization)* *(Plume Tracking)* • Crosswell Seismic • Microseismic (Passive) • EMIT • Magnetotelluric Sounding • Resistivity and EM • Electrical Resistivity Tomography • Time-lapse Gravity Survey • Electromagnetic Resistivity • Wireline Logging *(Well integrity and Subsurface Characterization)* • Resistivity
	Caprock Integrity *(Subsurface and Reservoir Characterization)* • Geomechanical Analysis • Core Collection	**Geochemistry** *(Reservoir Integrity)* • Brine/Fluid Composition • Tracer Injection/Monitoring	
	Wireline Logging *(Well Integrity)* • Temperature • Noise • Cement Bond • Density • Gamma Ray • Sonic (Acoustic)	**Injection Well Logging** *(Wireline Logging)* *(Plume Tracking)* *(Reservoir Integrity)* • Temperature Logging • Reservoir Saturation Tool • Optical	
	Physical Testing *(Well Integrity)* • Annulus Pressure • Injection Volume/Rate • Wellhead Pressure • Downhole Pressure • Downhole Temperature		

It is important to note that CO_2 is a fundamental and natural constituent of the biosphere and the subsurface. As such, it is an integral part of our lives and something we breathe. The goal of CCS technology is to significantly slow down and control unbridled anthropogenic CO_2 emissions to the atmosphere [4], not to eliminate them.

Reality is that even with the most advanced monitoring techniques we cannot possibly know the absolute position, concentration, phase, mobility, and migration path of every CO_2 molecule a kilometer below the surface.

2.5.1 MONITORING TOOLS AND TECHNIQUES

Monitoring occurs at many different scales and locations. Some techniques directly measure CO_2 concentrations or other properties such as pressure or fluid composition in the targeted storage formation. Direct techniques usually require access from wellbores that penetrate the containment system into the storage reservoir [50]. Generally, the number of such penetrations must be minimized because they are, by default, potential leakage pathways. On the other hand, direct measurements can also be obtained from monitoring wells at shallower horizons above an expected seal formation [53]. Monitoring wells can provide direct and early indications of unexpected CO_2 movement and that way demonstrate that significant vertical movement is not occurring, and that CO_2 is safely stored in the reservoir [40].

Measuring emissions at the surface above an injection site is another form of direct monitoring. This might be useful if a specific leakage pathway is suspected, but general widespread increase in CO_2 concentration at the surface, high enough to indicate failure of the storage system, should be detected much earlier using other monitoring techniques [49, 50]. Significant baseline studies need to be done in order to quantify and validate the range of CO_2 emissions from the ground so natural emissions related to biological processes at the storage site cannot be attributed to leakage from the reservoir [49, 51, 52].

Most monitoring is accomplished by repeated indirect measurements. The major tools for indirect monitoring are geophysical, and include applications of seismic data, gravity, and even electromagnetics [53]. Surface tiltmeters and satellite-derived surface

elevation data are especially useful for land based storage systems, as opposed to offshore sites [40].

The long-term monitoring of CO_2 behavior in subsurface storage is an intense scientific and operational undertaking [4]. Operators must adapt and improve some fairly sophisticated monitoring techniques developed in the oil and gas and other industries. Regulators need to appreciate "fit-for-purpose" monitoring designs and performance expectations. With operators and regulators working on the same goal, it can be expected that monitoring of even very large commercial-scale CO_2 storage sites will be done in a highly effective manner.

2.6 ECONOMICS OF CCS

The economics associated with CO_2 capture and storage has been the focus of many studies, and a wide range in costs has been reported. The total cost for applying CCS to a coal-fired power plant, or any other non-power industrial facility, can be divided into three main components: capture and compression costs; transportation costs; and storage costs. In general, the bulk of CCS costs, roughly 2/3 of total costs, are associated with carbon capture [54].

Based on recent estimates [54-56], total CCS costs range between US$40 and US$90 per tonne of CO_2 captured and stored, but they are highly dependent on power plant characteristics i.e. fuel and the technology used. For the most cost-effective technologies, capture costs can range from US$20 to US$40 per tonne of CO_2 [56]. Factors such as oil and gas prices, extraction economics and reservoir performance, the benefits from EOR, EGR, or ECBM recovery can offset part or all of the CCS costs.

Assuming reasonable learning rates, it is expected that the total CCS cost for coal-fired plants could fall to below US$25/t of CO_2 captured by 2030 [57].

The cost of CCS from non-power industrial sources may be significantly less than that from coal-fired power plants, and for this reason these industrial facilities may be good candidates for initial CCS demonstration and deployment [54]. However, these facilities have much smaller cumulative CO_2 emissions than coal-fired power plants.

As shown in Table 2, the CCS costs for supercritical pulverized coal (SCPC) power plants are about $52 per tonne of CO_2 [56]. This estimate does not include transport and storage costs, which are site specific [54]. The cost of pipeline transportation strongly depends on the distance and the quantity of CO_2 transported (CO_2 mass flow rate), and whether the pipeline is onshore or offshore. Also, for long pipeline trajectories, additional booster stations are needed, which adds an additional cost [57]. CO_2 transportation by ship is commonly cheaper than pipeline transport for distances larger than 1,000 km [4]. The final cost for large-scale pipeline transportation ranges from US$1 to US$5 per tonne of CO_2 per 100 km [57].

The cost of CO_2 storage depends on storage site characteristics, i.e., location, method of injection, and the cost of monitoring. In general, at around US$1 to US$2 per tonne of CO_2, storage costs are marginal compared to capture costs [54].

According to some recent techno-economic studies a carbon price of about $60 to $65 per metric ton of CO_2 is needed to cover all CCS-related costs and make CCS technology economically viable [58]. On the other hand, adding capture to a power plant raises the cost of electricity by about $0.04 per kWh. This represents an increase in the delivered price of electricity in the 25–50% range [54].

Table 4: CCS costs for SCPC generation (in 2007 U.S. dollars) [56].

Reference power plant

	Units	SCPC
Total plant cost	$/kWe	1910
CO_2 emitted	kg/kWh	0.830
Heat rate (HHV)	Btu/kWh	8868
Thermal efficiency (HHV)		38.5%
LCOE		
Capital	$/MWh	38.8
Fuel	$/MWh	15.9
O&M	$/MWh	8.0
Total	$/MWh	62.6

Power plant with CO_2 capture

	Units	SCPC
Total plant cost	$/kWe	3080
CO_2 emitted at 90% capture rate	kg/kWh	0.109
Heat rate (HHV)	Btu/kWh	11652
Thermal efficiency (HHV)		29.3%
LCOE		
Capital	$/MWh	62.4
Fuel	$/MWh	20.9
O&M	$/MWh	17.0
Total	$/MWh	100.3
$/ton CO_2 avoided		**52.2**

Where:
HHV - higher heating value;
LCOE - levelized cost of electricity;
O&M - operations and maintenance;
SCPC - supercritical pulverized coal.

There are a number of scientific, technological, economic and political uncertainties behind the decision to invest in and build a "capture ready" power plant with a CO_2 storage facility. This decision can be a largely irreversible and requires the investing and possibly raising of a significant amount of capital.

Over the last few decades, it was suggested that energy companies, in evaluation of their decisions about their asset dynamics, should take into account the multi-dimensional structure and the time evolution of the uncertainty in the determinants of asset cash-flows; and how asset structure, including the flexibility that asset managers have to change that structure, influences the effect of underlying uncertainties on asset value [59].

The traditional way to evaluate such decision was to determine the net present value (NPV) of the investment by computing the sum of the anticipated costs and revenues, and discounting them to the present year. At the end of the process, a decision

maker would decide to invest only if the NPV value was positive [60]. However, when not faced with the choice between immediate investment and forfeiture, computing the NPV only in the current period may not result in the best choice [61]. The NPV calculation may not provide an optimal result, because calculating the NPV for the present ignores any possible value of the option to delay investment.

On the other hand, a "real options analysis" (ROA) is a valuation method that is particularly useful in defining an optimal timing for investment decisions under uncertainty. A real option can be defined as "a right – not an obligation – to take an action (e.g., defer, expand, contract, abandon, stage) on an underlying nonfinancial asset at a predetermined cost on or before a predetermined date." [62]

The difference between ROA and traditional NPV project valuation methodologies can be summarized as follows [63]:

"Several interesting implications emerge from the analysis of the option to delay a project as an option. First, a project may have a negative net present value based upon expected cash flows currently, but it may still be a "valuable" project because of the option characteristics. Thus, while a negative net present value should encourage a firm to reject a project, it should not lead it to conclude that the rights to this project are worthless. Second, a project may have a positive net present value but still not be accepted right away. This is because the firm may gain by waiting and accepting the project in a future period, for the same reasons that investors do not always exercise an option just because it is in the money."

2.7 DECISION MAKING AND DECISION SUPPORT SYSTEMS

Making decisions concerning complex systems such as carbon capture and storage is very difficult. Even though individual interactions among a system's variables may be well understood, predicting how the system will react to an external stimulation, such as a policy decision, is often difficult. In the case of CCS, many variables such as energy demand and supply, costs of CO_2 capture, availability of storage potential, and regulatory framework are involved in complex and often delicate interdependencies, and predicting the total outcome may be a challenging task.

Over the last few decades, mathematical and statistical models, numerical algorithms, and computational simulations have been used to gain a better insight into different management problems and to provide decision makers with useful and timely information [64]. The decision support systems (DSSs) are computer-based systems that assist the decision maker in choosing between alternative actions by applying knowledge about the decision domain to arrive at recommendations for the various options [65].

DSS can help a decision maker select among well-defined alternatives based on formal or theoretical criteria defined on technological/engineering principles, principles of engineering economics, operations research, and statistics and decision theory. For problems that cannot be easily processed by formal techniques, artificial intelligence methods can also be employed [66].

Decision support systems have been widely used in diverse domains, including business, engineering, military, medicine, and industrial areas. Furthermore, decision support systems have been used across many process industries, including iron and steel, cement, mining and metallurgy, oil and gas, and pulp and paper [67]. Examples include:

1. A knowledge-based decision support system used to aid operators in selecting petroleum contaminant remediation techniques based on user-specified information [68];
2. An intelligent system that links multiple anaerobic systems for wastewater treatment to a common remote central supervisor via wide area networks. The local control systems have a hybrid structure, which is comprised of algorithmic routines for data acquisition, signal preprocessing, and calculation of plant operation parameters [69];
3. An expert system for a supervisory decision support system for monitoring and control of a water pipeline network [70].

These analogs and experience gained through previous case studies can be used as a good starting point for building DSSs for newly emerging CCS technology.

Chapter 3.

TECHNICAL ASPECTS OF CO_2 STORAGE IN UNMINEABLE COAL SEAMS

3.1 INTRODUCTION

Alongside deep saline aquifers and depleted oil and gas reservoirs, unmineable coal seams are considered to be the third most promising option for geological CO_2 sequestration. When injected into coal seams, CO_2 is expected to be adsorbed and locked permanently in the pore matrix of the coal seam. Injection of CO_2 into deep unmineable coal seams, with high methane content, can enhance coal bed methane (CBM) production and generate revenue that can offset the cost of sequestration.

As a secondary recovery technique, CO_2 injection can help desorb and extract significant amounts of methane left in the reservoir after the primary depressurization and production phase [71-75]. This interaction between CCS and CBM production can extend the operational life of the CBM field, provide additional recoverable reserves, and generate supplementary environmental and economic benefits arising from permanent storage of CO_2.

This chapter focuses on a comprehensive analysis of technical aspects of CO_2 sequestration in deep unmineable coal seams. Based on the experience and data gained

through characterization and pilot-scale validation studies in the Central Appalachian Basin, as well as other similar projects worldwide, this analysis identifies technical issues related to CO_2 sequestration in coal seams and structures the decision process related to those critical issues.

The goal of this research is to provide a quantitative and qualitative assessment of engineering parameters and functional constraints specific to CO_2 sequestration in unmineable coal seams, and to determine their impact on the overall technical feasibility of the project. The variables listed in this chapter will be weighted and ranked and used later in Chapter 5 as components of a new decision making framework. They can be divided into three major performance categories: capacity, injectivity, and containment.

All data and information presented in this chapter are derived from multiple sources including reports published by the Southeast Regional Carbon Sequestration Partnership (SECARB) coal research team, data and maps from industry and government agencies, as well as other publicly available data sources.

The concept of storing CO_2 in geologic formations as a safe and effective greenhouse gas mitigation option requires public and regulatory acceptance and the development of a framework for the management of such facilities. In this context it is important to develop a good understanding of the reservoir performance, uncertainties and risks that are associated with geological storage.

3.2 CAPACITY

The most recent studies show that unmineable coal seams, or seams that are not considered worthy for mining under current technical and economic conditions, can store

up to 112 Gt of CO_2 worldwide [76]. Coal seams targeted for CO_2 sequestration are commonly saturated with water and typically contain large amounts of methane (CH_4) that is adsorbed onto the surface of the coal. The differences in absorption behavior of CO_2 and CH_4 is used as a driving mechanism for CO_2 sequestration in coal seams [77]. One ton of coal can adsorb about 1060 - 1235 ft^3 of CO_2 at pressures from 725 to 1160 psi [78]. One molecule of methane can be exchanged by 1.5 to 5 or 6 molecules of CO_2, depending on the available pressure in the reservoir [79].

Besides adsorption capacity of coal, other major parameters necessary for preliminary assessment and calculation of the CO_2 storage resource are [23]: geographical area that outlines the coal basin or region for CO_2 storage; gross thickness of coal(s); storage efficiency; and CO_2 properties.

3.2.1 GOVERNING EQUATIONS

The following volumetric equation can be used to calculate the capacity for geologic CO_2 storage in unmineable coal seams [23]:

$$G_{CO_2} = A \cdot h_g \cdot C_{s,max} \cdot \rho_{CO_2std} \cdot E_{coal} \qquad \textbf{(Equation 1)}$$

where:

- G_{CO2} – Mass estimate of CO_2 resource of one or more coal beds;
- A – Geographical area that outlines the coal basin or region for CO_2 storage calculation;
- h_g – Gross thickness of coal area(s) for which CO_2 storage is assessed within the basin or region defined by A;
- $C_{ads,max}$ – Adsorbed maximum standard CO_2 volume per unit of *in situ* coal volume (Langmuir or alternative); assumes 100% CO_2 saturated coal conditions; if on dry-ash-free (daf) basis, conversion should be made;
- ρ_{CO2std} – Standard density of CO_2; and

E_{coal} – CO_2 storage efficiency factor that reflects a fraction of the total coal bulk volume that is contacted by CO_2.

3.2.1.1 Reservoir Geometry

The reservoir area is usually estimated based on the assumption that coal seams are laterally continuous. Structural and stratigraphic variations throughout the reservoir determine the three dimensional distribution of the coal. Therefore, data obtained through regional and local geological evaluations can provide valuable information about depth of occurrence, formation geometry (a few thick seams or several thin seams), lateral continuity, and vertical isolation.

Coal seam thickness is the second spatial factor that significantly affects the feasibility of CO_2 sequestration. Thickness of the targeted seam affects the decision of whether to drill a vertical or horizontal injection well, as well as dictates number and spatial distribution of monitoring wells. If the coal seam is thick, then drilling a horizontal well is not considered to be the best economic choice, as the wellbore may not access all parts of the reservoir and that way may decrease the storage efficiency factor.

The depth of targeted coal seam, or multiple seams, is vital parameter in selecting CO_2 injection method since it determines the drilling cost, and it is an important factor in determining the surface injection and bottomhole pressures during the preliminary modeling studies. With an increase in depth, overburden stress, formation pressure, and thermal maturity of coal increase, and in some cases, CH_4 content may also increase [80].

3.2.1.2 Adsorption Capacity

The CO_2 sorption capacity of coal depends on the coal physical and chemical properties including: coal bulk density, moisture and/or ash content, temperature, and

pressure. The maximum CO_2 sorption capacity calculation method calculates maximum CO_2 volume adsorbed per unit of coal volume. It assumes 100% CO_2 saturated coal conditions. It is important to note that this method requires the data about the coal bulk density as well as moisture and/or ash content [23]:

$$C_{ads,\,max} = n_{ads,\,max} \cdot \rho_{c,\,dry} \cdot \left(1 - f_{a,\,dry}\right) \qquad \textbf{(Equation 2)}$$

where:

$n_{ads,\,max}$ – Maximum amount of component adsorbed;

$\rho_{c,\,dry}$ – Dry coal bulk density; and

$f_{a,\,dry}$ – Ash weight fraction.

Another method for calculating sorption capacity is calculating gas excess sorption capacity for coals at low pressures by approximating the Langmuir relationship [81]. Furthermore, this method accounts for a binary CO_2/CH_4 mixture caused by CO_2 injection:

$$n_{ads} = \frac{n_L \cdot p}{P_L + p} = \frac{[mass\ of\ sorbate]}{[mass\ of\ sorbent]} \qquad \textbf{(Equation 3)}$$

where:

n_{ads} – Gas excess sorption capacity or Gibbs capacity;

n_L – Langmuir volume or sorption capacity at infinite pressure;

P_L – Langmuir pressure or pressure at $n_{ads} = n_L/2$; and

p – Formation pressure;

For CH_4 it can be assumed, as a first approximation, a linear relationship between the Langmuir volume and temperature [82]:

$$n^{*}_{ads} = \frac{[n_L + m \cdot (T_i - T_0)] \cdot p}{P_L + p} \qquad \textbf{(Equation 4)}$$

where:

m – Change in sorption capacity with temperature ($\Delta n_L/\Delta T$);

T_i – Coal seam temperature; and

T_0 – Reference temperature.

As mentioned, most of the deep unmineable coal seams contain large amounts of CH_4 adsorbed on the surface of the matrix. After CO_2 injection takes place and CO_2 reaches the targeted formation, it is expected that CH_4 molecules will be desorbed from the coal surface and substituted by CO_2 molecules. In order to account for the presence of a binary CO_2/CH_4 mixture the Langmuir sorption model can be further extended [83]:

$$n^*_{ads,\,i} = \frac{n^*_{Li} \cdot p \cdot y_i}{1 + \sum_j n^*_{L,\,j} \cdot p \cdot y_j} \qquad \textbf{(Equation 5)}$$

where:

$n^*_{ads,\,i}$ – Volume of component "i" adsorbed;

n^*_{Li} – Langmuir volume of component "i"; and

y_i – Molar fraction of component "i".

Average CO_2/CH_4 exchange capacities are assumed to be depth dependent due to the pressure effect. This ratio increases linearly from 1.5 to 4 for depths from 2600 to 6500 ft. and from 4 to 5 for 6500 to 16500 ft. depth [79].

3.2.1.3 Storage Efficiency

The determination of the overall CO_2 storage efficiency for unmineable coal seams is one of the many challenges in estimating coal storage volume. The CO_2 storage efficiency factor reflects the ability of injected CO_2 to contact 100% of available bulk coal volume. This value is a function of six geologic efficiency parameters [23]:

$$E_{coal} = E_{An/At} \cdot E_{hn/hg} \cdot E_A \cdot E_L \cdot E_g \cdot E_d \qquad \textbf{(Equation 6)}$$

where:

$E_{An/At}$ – *Net-to-total area* - represents the fraction of total basin or region area that has bulk coal present. It accounts for known or suspected locations that are within a basin or region outline where a coal area may be discontinuous

$E_{hn/hg}$ – *Net-to-gross thickness* - represents the fraction of total coal area thickness that has adsorption potential.

E_A – *Areal displacement efficiency* - is the fraction of the immediate interfacial area surrounding an injection well that can be contacted by injected CO_2. This term is influenced by spatial heterogeneity such as faults and permeability anisotropy.

E_L – *Vertical displacement efficiency* - is the fraction of the vertical cross section or thickness of the targeted formation, with the volume defined by the area (A) that can be contacted by CO_2 from a single injection well. Vertical displacement efficiency is dependent on variations in the cleat system within the coal. In case that one zone within the reservoir has higher permeability than other zones, injected CO_2 will fill this zone quickly and leave the other zones with less or no CO_2.

E_g – *Gravity displacement efficiency* - is the fraction of the net coal thickness that is contacted by CO2 as a consequence of the density difference between CO_2 and *in situ* fluids in the cleats.

E_d – *Microscopic displacement efficiency* - is the degree of saturation achievable for *in situ* coal compared with the theoretical maximum predicted by the Langmuir model.

The first two parameters, $E_{An/At}$ and $E_{hn/hg}$, are used to estimate pore volume for an entire basin or region. Other terms, E_A, E_L, E_g, and E_d, are necessary for calculating the fraction of pore volume that can be accessed by CO_2 from injection wells.

Due to the fact that a database with information about statistical properties of coal is not currently available, efficiency factors for unmineable coal seams are tentatively calculated based on CBM data and results from computer modeling studies [23]. For this reason, the P_{10}, P_{50}, and P_{90} percent probability ranges for efficiency factors listed in Equation 6 are calculated using the log odds method with Monte Carlo sampling, and

further used for estimating an overall CO_2 storage capacity in unmineable coal seams. The following tables are giving an overview of coal efficiency factors and corresponding probability ranges [23].

Table 5: Parameters used for calculation of overall CO_2 storage efficiency and their P_{10} and P_{90} values

Efficiency Parameter	Symbol	P_{10} Values	P_{90} Values
Net-to-total area	$E_{An/At}$	0.6	0.8
Net-to-gross thickness	$E_{hn/hg}$	0.75	0.9
Areal displacement efficiency	E_A	0.7	0.95
Vertical displacement efficiency	E_L	0.8	0.95
Gravity displacement efficiency	E_g	0.9	1.0*
Microscopic displacement efficiency	E_d	0.75	0.95

**0.999999999999999 used due to inability to divide by zero when using log odds method.*

In case that $E_{An/At}$ and $E_{hn/hg}$ values are determined through preliminary characterization studies they can be used directly in Equation 6. In this instance, only the displacement efficiency factor is needed, which is calculated by multiplying E_A, E_L, E_g, and E_d. The P_{10}, P_{50}, and P_{90} percent probability values for displacement efficiency factor are shown in Table 6.

Table 6: Displacement efficiency factor (DEF_{coal}) and corresponding P10, P50, and P90 percent probability values.

Displacement Efficiency Factor $(DEF_{coal} = E_A \cdot E_L \cdot E_g \cdot E_d)$		
P10	***P50***	***P90***
0.39	0.64	0.77

Finally, Table 7 is giving probability values for overall CO_2 storage efficiency in unmineable coal seams. It is important to note that, because of the limitations in data availability and quality, all parameters and their probability values used for calculation of

overall storage efficiency are considered to be general approximations of efficiency limits, and not precise mathematical conclusions.

Table 7: Overall storage efficiency (E_{coal}) and corresponding P10, P50, and P90 percent probability values.

Overall Storage Efficiency ***(E_{coal})***		
P10	***P50***	***P90***
0.21	0.37	0.48

3.2.1.4 Other Methods for Capacity Estimation

Besides the method suggested by the U.S. DOE, there are three additional capacity estimation methods. First is a volumetric approach (Equation 7), where CO_2 sequestration capacity is a function of coal volume, coal density, and sorption capacity:

$$G_{CO_2} = \text{Coal Volume} \times \text{Coal Density} \times \text{Sorption Capacity} \quad \textbf{(Equation 7)}$$

The sorption capacity in this case is calculated as*:

$$\text{Sorption Capacity} = -13.57 \times \%\ \text{Volatile Matter} + 1130.66\ (ft^3/ton) \quad \textbf{(Equation 8)}$$

Second method is taking into account producible gas in place (PGIP), CO_2 density, and CO_2/CH_4 exchange ratio (e_r) (Equation 9).

$$G_{CO_2} = PGIP \times CO_2\ \text{Density} \times e_r \quad \textbf{(Equation 9)}$$

The PGIP depends on coal volume†, coal density, CH_4 content, recovery factor, and completion factor:

$$PGIP = \text{Coal Volume} \times \text{Coal Density} \times CH_4\ \text{Content} \times \text{Completion} \times \text{Recovery} \quad \textbf{(Equation 10)}$$

* For Central Appalachian coals
† Excluding ash and moisture

The completion factor is an estimation of the fraction of the net cumulative coal thickness within the drilled strata that will contribute to CBM production and subsequently CO_2 storage. The recovery factor is an amount of gas that can be recovered from the targeted coal seams.

Third method is based on CBM production analysis. This method utilizes CBM production decline parameters, including initial decline rate and the hyperbolic exponent. When decline parameters are derived from the production type curves they are used to project the estimated ultimate recovery (EUR) for the certain CBM field. In the final step, EUR is multiplied with the CO_2/CH_4 exchange ratio, which yields a total CO_2 storage capacity.

3.2.2 CASE STUDY: CENTRAL APPALACHIAN BASIN CAPACITY ASSESSMENT

For the purpose of this study six CBM fields in the Central Appalachian Basin were selected for detailed characterization, including estimation of the CO_2 storage capacity and ECBM potential. The primary objective of this study was to provide geologic and reservoir characterization of the Pennsylvanian-age coal beds in Central Appalachia and to identify potential CO_2 storage sites within the Central Appalachian region that have significant potential for long-term, commercial-scale storage of CO_2.

The regional study area was located within the Central Appalachian Basin, a northeast-to-southwest-trending basin encompassing approximately 10,000 square miles (mi^2) in southwestern Virginia and southern West Virginia, as shown in Figure 8. The principal area of investigation for most of the detailed geologic mapping consists of

portions of five counties located within southwestern Virginia including Buchanan, Dickenson, Russell, Tazewell, and Wise Counties and four counties in West Virginia, including Fayette, McDowell, Raleigh, and Wyoming [84].

The geologic data utilized in this study were derived from multiple sources including reports published by the Southeast Regional Carbon Sequestration Partnership (SECARB) coal research team, data and maps from industry and government agencies, as well as other publicly available data sources. The evaluation also required the procurement of CBM databases, coal outcrop data, deep mine boundaries, and geophysical well logs and production data from the West Virginia Geological and Economic Survey (WVGES) and the Virginia Division of Gas and Oil (VDGO).

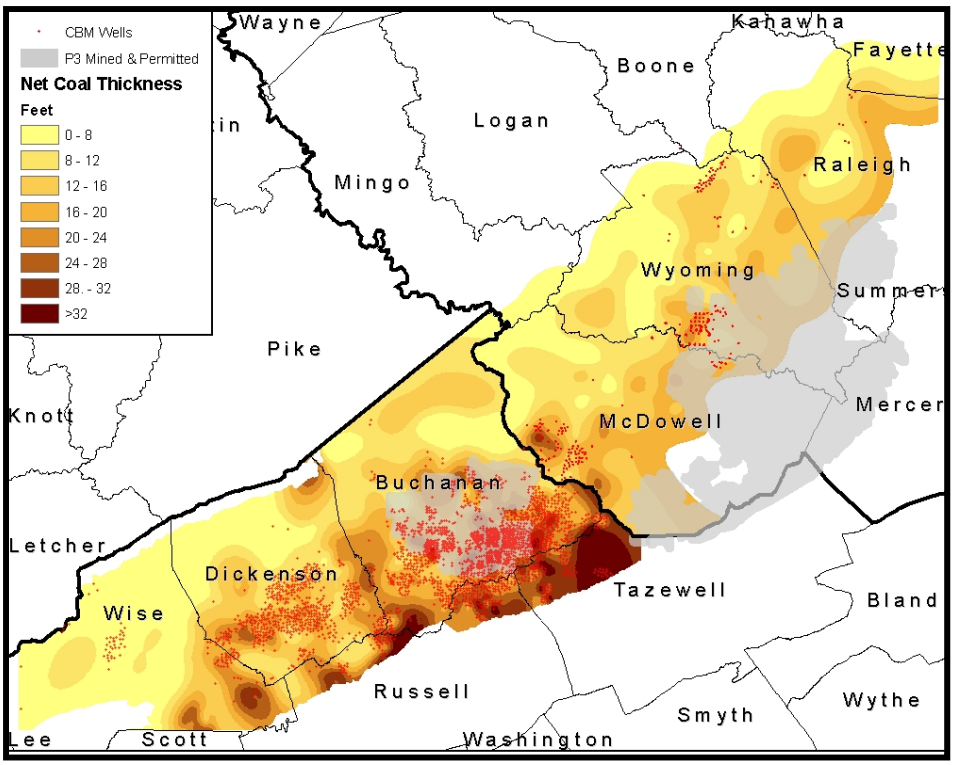

Figure 8: Regional study area (after MM&A, 2011, and Ripepi 2009) [85], [86].

Based on the results from Phase I and Phase II SECARB characterization and field validation studies, four CBM fields located in southwestern Virginia (Figure 9), and two CBM fields located in southern West Virginia were chosen for detailed assessment. However, this section will report only capacity estimates for four CBM fields located in southwestern Virginia: Frying Pan; Sourwood; Lick Creek; and South Oakwood (Table 8).

Table 8: Four CBM fields in southwestern Virginia.

Basin/Field Name	**Lithological unit**	**Average Surface Area** (acres)
Frying Pan/Nora	Lower Breathitt Group	7200
Sourwood/Nora	Lower Breathitt Group	11220
Lick Creek/Nora	Lower Breathitt Group	31020
South Oakwood	Lower Breathitt Group	38400

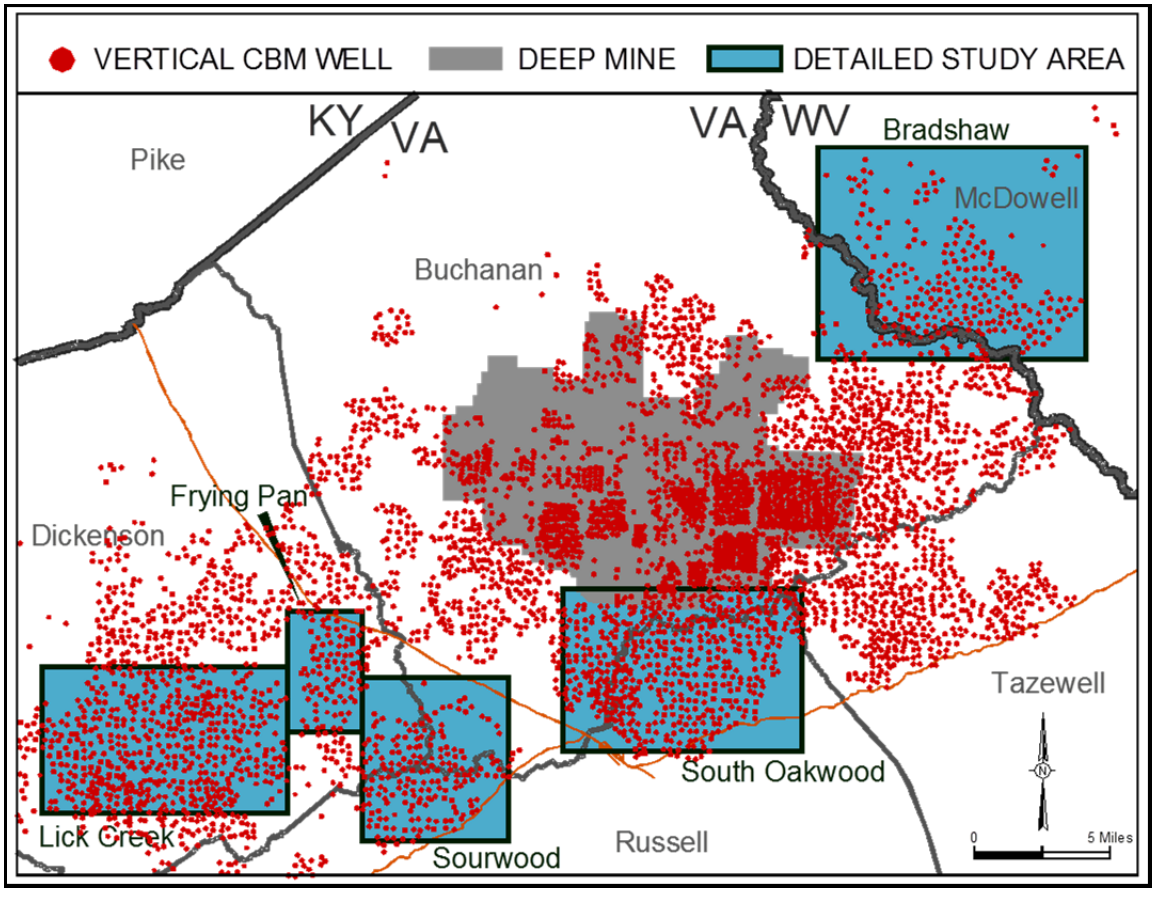

Figure 9: Four CBM fields in southwestern Virginia chosen for detailed characterization study (after MM&A, 2011) [85].

Coal seams producing methane in the Frying Pan, Sourwood, Lick Creek, South Oakwood fields belong to the Lee and underlying Pocahontas formations (Figure 10). The CO_2 storage capacity for each of these fields was estimated based on volumetric CH_4/CO_2 exchange ratio of 1.78 (for every standard cubic foot (scf) of CH_4 desorbed from the coal surface, approximately 1.78 scf of CO_2 can be adsorbed) [86]. This ratio is based on the CH_4 - CO_2 isotherm relationship determined from analyses of coal cores obtained during SECARB's field validation test in the South Oakwood CBM field.

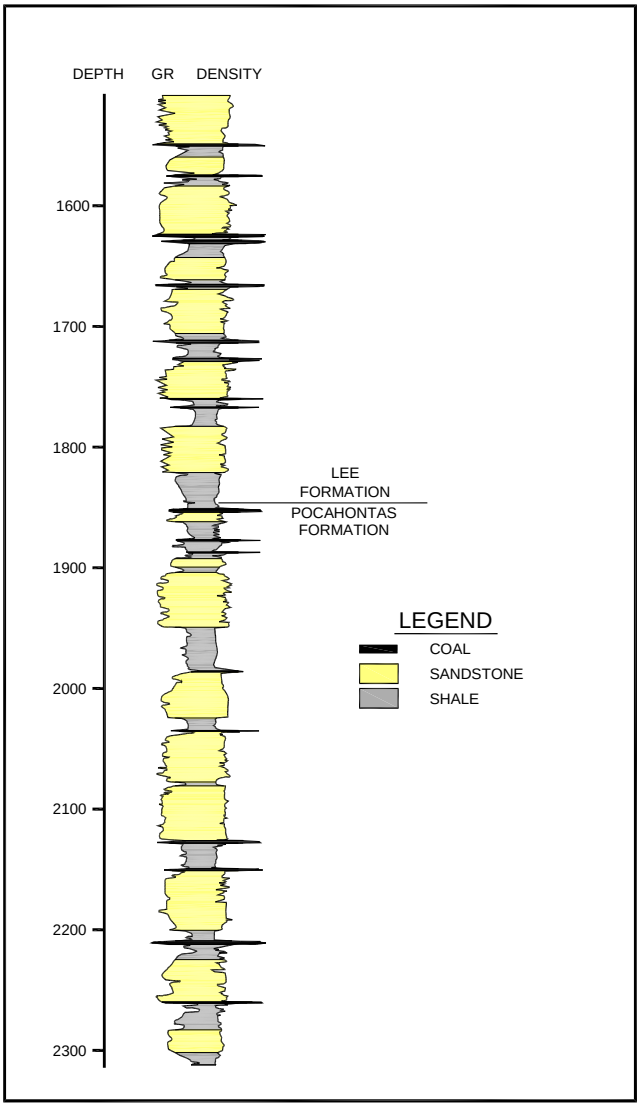

Figure 10: Stratigraphic column for South Oakwood field.

All key parameters and their corresponding values used for preliminary capacity assessment of four CBM fields in southwest Virginia are given in Table 9. All values are based on data provided in the Phase II - Task 10 Final Report published by the SECARB's Coal Group [85, 87].

Table 9: Key performance parameters used for capacity calculations

Parameter	**Frying Pan**	**Sourwood**	**Lick Creek**	**South Oakwood**
Area that outlines the CBM field	7,200 acres	11,220 acres	31,020 acres	38,400 acres
Gross thickness of coal	22 ft.	26 ft.	19 ft.	24 ft.
Mid-point coal elevation	1,489 ft.	1,511 ft.	1,772 ft.	1,583 ft.
Initial pressure (0.31 psia/ft)	460 psia	466 psia	548 psia	489 psia
Current pressure (0.1 psia/ft)	148 psia	150 psia	176 psia	157 psia
Average permeability	11 mD	10 mD	7.5 mD	7.5 mD
Average porosity	1%			
Absolute adsorption capacity	1.77724 ft^3/ton			
Adsorbed maximum standard CO_2 volume per unit of in situ coal volume (Current)	0.0647856 ft^3 CO_2 per 1 ft^3 of coal			
Standard density of CO_2 (supercritical)	0.0222868 ton/ft^3			
Standard density of CO_2 (gas)	5.61852 x 10^{-5} ton/ft^3			
CO_2 storage efficiency factor	P10 = 21% P50 = 37% P90 = 48%			
Average dry coal bulk density	1800 tons/acre-ft.			
Average volatile meter	27.8%			
Average ash weight fraction	11.784%			
Average CO_2/CH_4 exchange ratio	1.78			
Initial CH_4 content	423 ft^3/ton	409 ft^3/ton	351 ft^3/ton	397 ft^3/ton
Current CH_4 content	240 ft^3/ton	240 ft^3/ton	230 ft^3/ton	215 ft^3/ton
Estimated ultimate CBM recovery	35.6 Bcf	55.3 Bcf	231.1 Bcf	321.9 Bcf
PGIP (GIIP)	59.4 Bcf	92.1 Bcf	462.2 Bcf	643.8 Bcf
Recovery factor	60%	60%	50%	50%

The following sections will show CO_2 storage capacity estimates calculated using four different calculation methods presented earlier: "U.S. DOE method", "Volumetric method", "PGIP method", and "CBM production analysis".

3.2.2.1 Method I – U.S. DOE:

As described in Chapter 3.2.1 and based on the methodology suggested by the U.S. DOE in the 2010 Carbon Sequestration Atlas of the United States and Canada, the following capacities for all four CBM fields are calculated using data published in two final reports by the SECARB's coal research team (Table 9).

Frying Pan Field Capacity:

	Storage efficiency		
	P10	P50	P90
	21%	37%	48%
Current CO_2 storage capacity (tons)	2,092,130	3,686,130	4,782,010

Sourwood Field Capacity

	Storage efficiency		
	P10	P50	P90
	21%	37%	48%
Current CO_2 storage capacity (tons)	3,853,000	6,788,620	8,806,860

Lick Creek Field Capacity:

	Storage efficiency		
	P10	P50	P90
	21%	37%	48%
Current CO_2 storage capacity (tons)	7,784,460	13,715,500	17,793,000

South Oakwood Field Capacity:

	Storage efficiency		
	P10	P50	P90
	21%	37%	48%
Current CO_2 storage capacity (tons)	12,172,400	21,446,600	27,822,600

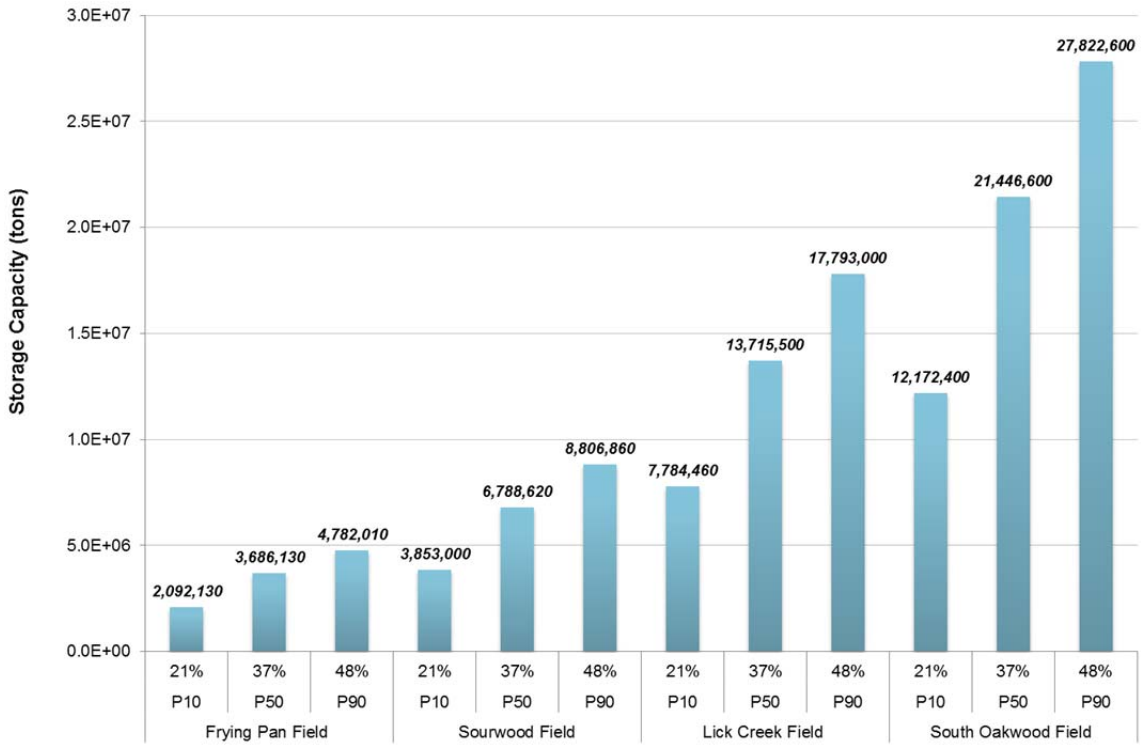

Figure 11: Storage capacity estimates based on the U.S. DOE methodology.

3.2.2.2 Method II – Volumetric Approach:

Frying Pan Field Capacity:

Sorption Capacity = -13.57 x 0.278 + 1130.66 = 1,126.89 ft^3/ton

Area = 7,200 acres

Gross thickness of coal = 22 ft.

Coal Density = 0.0413223tons/ft^3

G_{CO_2}= 1,871,490 tons

Sourwood Field Capacity

Sorption Capacity =1,126.89 ft^3/ton

Area = 11,220 acres

Gross thickness of coal = 26 ft.

Coal Density = 0.0413223tons/ft^3

G_{CO_2}= 3,446,670 tons

Lick Creek Field Capacity:

Sorption Capacity = 1,126.89 ft^3/ton

Area = 31,020 acres

Gross thickness of coal = 19 ft.

Coal Density = 0.0413223tons/ft^3

G_{CO_2}= 6,963,520 tons

South Oakwood Field Capacity:

Sorption Capacity = 1,126.89 ft^3/ton

Area = 38,400 acres

Gross thickness of coal = 24 ft.

Coal Density = 0.0413223tons/ft^3

G_{CO_2}= 10,888,700 tons

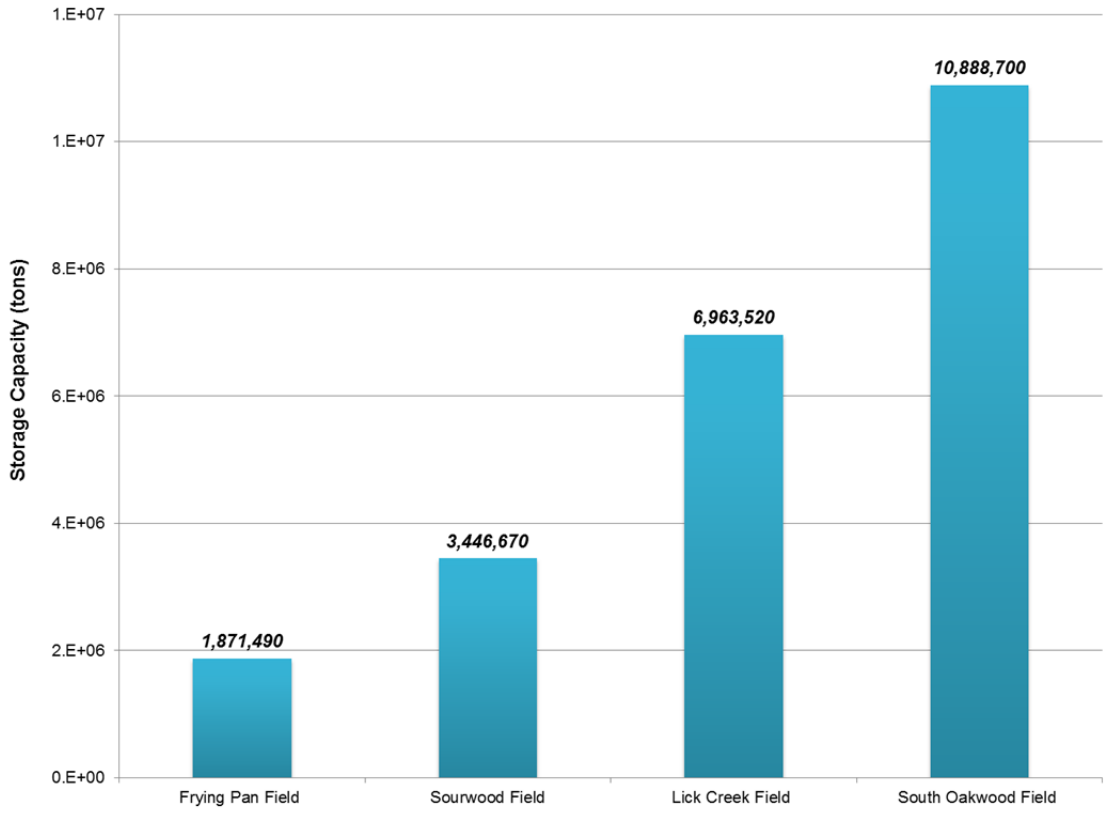

Figure 12: Storage capacity estimates based on the volumetric approach.

3.2.2.3 Method III – PGIP Method:

Frying Pan Field Capacity:

e_r= 1.78

Standard density of CO_2 (gas) = 5.61852 x 10^{-5} ton/ft^3

PGIP (GIIP) = 59.4 x 10^9 tons

G_{CO_2}= 5,940,570 tons

Sourwood Field Capacity

e_r= 1.78

Standard density of CO_2 (gas) = 5.61852 x 10^{-5} ton/ft^3

PGIP (GIIP) = 92.1 x 10^9 tons

G_{CO_2}= 9,210,880 tons

Lick Creek Field Capacity:

e_r= 1.78

Standard density of CO_2 (gas) = 5.61852 x 10^{-5} ton/ft^3

PGIP (GIIP) = 462.2 x 10^9 tons

G_{CO_2}= 46,224,400 tons

South Oakwood Field Capacity:

e_r= 1.78

Standard density of CO_2 (gas) = 5.61852 x 10^{-5} ton/ft^3

PGIP (GIIP) = 643.8 x 10^9 tons

G_{CO_2}= 64,384,200 tons

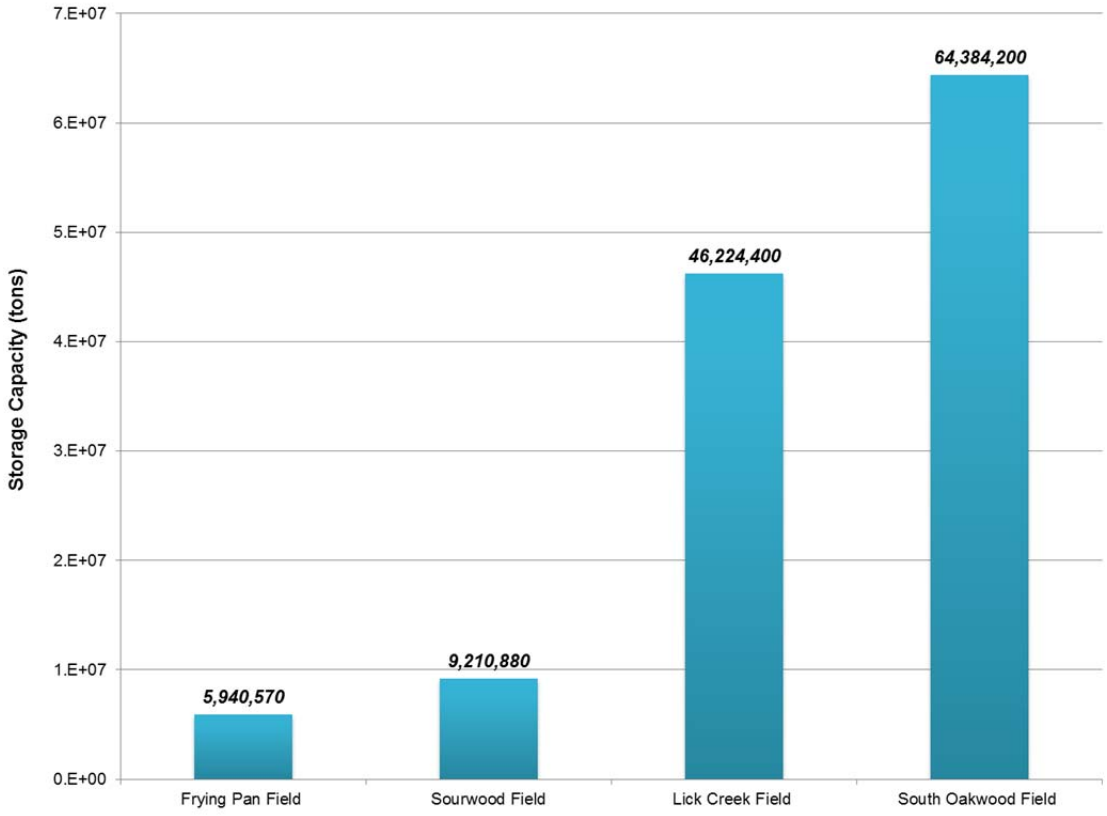

Figure 13: Storage capacity estimates based on the PGIP method.

3.2.2.4 Method IV – Production Type Curve Analysis:

In this case, the CO_2 storage capacity is calculated based on cumulative CBM production volume and CH_4/CO_2 exchange ratio. The final mass capacity is calculated by multiplying the calculated CO_2 storage volume by the conversion factor of 1.0 ton per 17,168 ft^3 (1 ton CO_2 = 17,168 ft^3 CO_2).

Frying Pan Field Capacity:

Table 10 summarizes CO_2 storage capacity estimates for the Frying Pan field. The current CO_2 storage capacity, based on the determined CBM field depletion of approximately 48%, is calculated to be 1,778,000 tons. The total CO_2 storage capacity

for Frying Pan field, assuming that the total estimated ultimate recovery (EUR) for the field is produced (100% depletion), is estimated at 3,703,770 tons [85].

Table 10: CO_2 storage capacity estimates for Frying Pan field

Cumulative Production (MMcf)	Remaining Reserves (MMcf)	Field EUR (MMcf)	Percent Depletion (%)	Current Storage Capacity (tons)	Total Storage Capacity (tons)
17,106	18,537	35,643	48%	1,778,000	3,703,770

Sourwood Field Capacity

Table 11 summarizes CO_2 storage capacity estimates for the Sourwood field. The current CO_2 storage capacity estimate, based on the determined field depletion of approximately 34% depleted, is calculated to be 1,953,300 tons. Assuming 100% depletion, the estimated CO_2 storage capacity for Sourwood field is 5,741,910 tons [85].

Table 11: CO_2 storage capacity estimates for Sourwood field

Cumulative Production (MMcf)	Remaining Reserves (MMcf)	Field EUR (MMcf)	Percent Depletion (%)	Current Storage Capacity (tons)	Total Storage Capacity (tons)
18,795	36,467	55,262	34%	1,953,300	5,741,910

Lick Creek Field Capacity:

Table 12 summarizes the CO_2 storage capacity estimates for the Lick Creek field. The current CO_2 storage capacity estimate, based on the determined field depletion of approximately 35 percent depleted, is calculated to be 8,395,200 tons. The total CO_2 storage capacity for Lick Creek field, assuming 100% depletion, is estimated at 24,011,620 tons.

Table 12: CO_2 storage capacity estimates for Lick Creek field

Cumulative Production (MMcf)	Remaining Reserves (MMcf)	Field EUR (MMcf)	Percent Depletion (%)	Current Storage Capacity (tons)	Total Storage Capacity (tons)
80,807	150,292	231,099	35%	8,395,200	24,011,620

South Oakwood Field Capacity:

Table 13 summarizes CO_2 storage capacity estimates for the South Oakwood field. The current CO_2 storage capacity estimate, assuming the field is approximately 28 percent depleted, is calculated to be 9,408,210 tons. The total CO_2 storage capacity for South Oakwood field, assuming that the total EUR for the field is produced, is estimated at 33,449,600 tons.

Table 13: CO_2 storage capacity estimates for South Oakwood field

Cumulative Production (MMcf)	Remaining Reserves (MMcf)	Field EUR (MMcf)	Percent Depletion (%)	Current Storage Capacity (tons)	Total Storage Capacity (tons)
90,557	231,389	321,946	28%	9,408,210	33,449,600

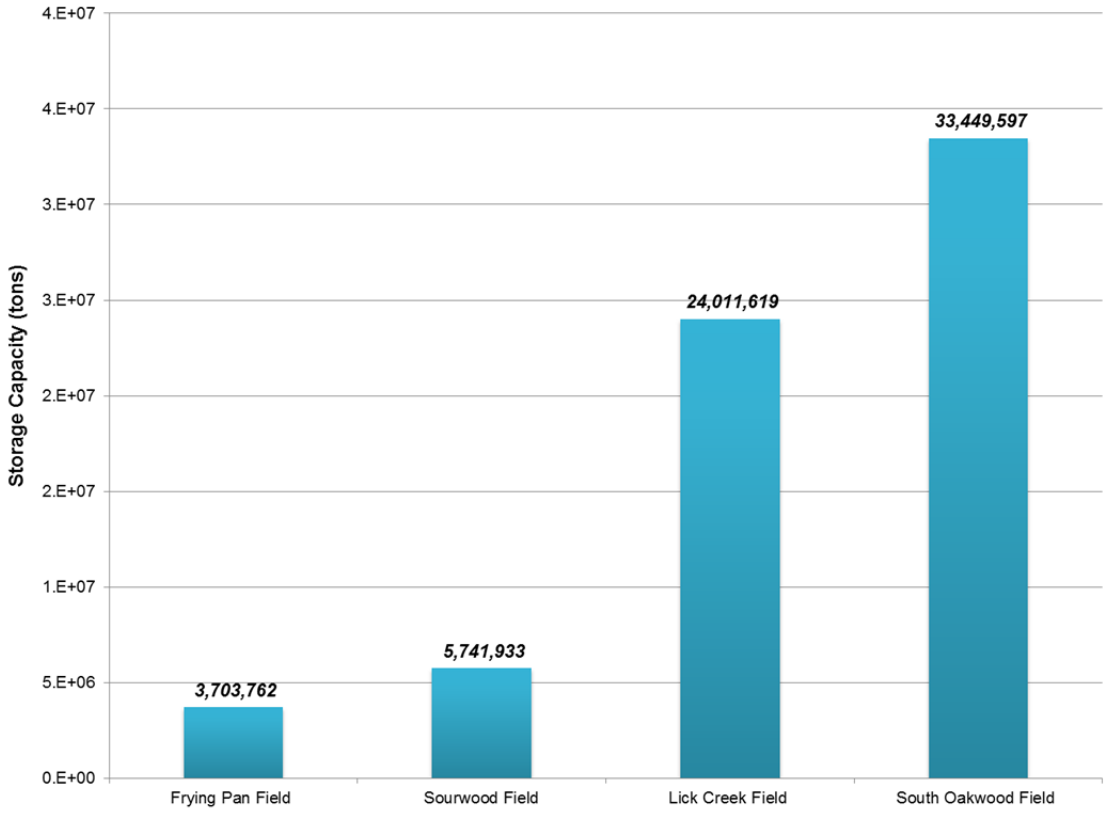

Figure 14: Storage capacity estimates based on the PGIP method.

3.2.2.5 Storage Capacity Summary:

Based on results obtained from four different capacity calculation methods, it was observed that the method for capacity estimation is the main source of the uncertainty, and has the largest impact on the technical feasibility of the CO_2 storage project development. As shown in Figure 15, when using different calculation methods for storage capacity assessment, the capacity estimates significantly differ for the same storage site. It is obvious that procedures that incorporate more variables or performance parameters (i.e., "U.S. DOE" and "Volumetric" methods) yield more conservative results.

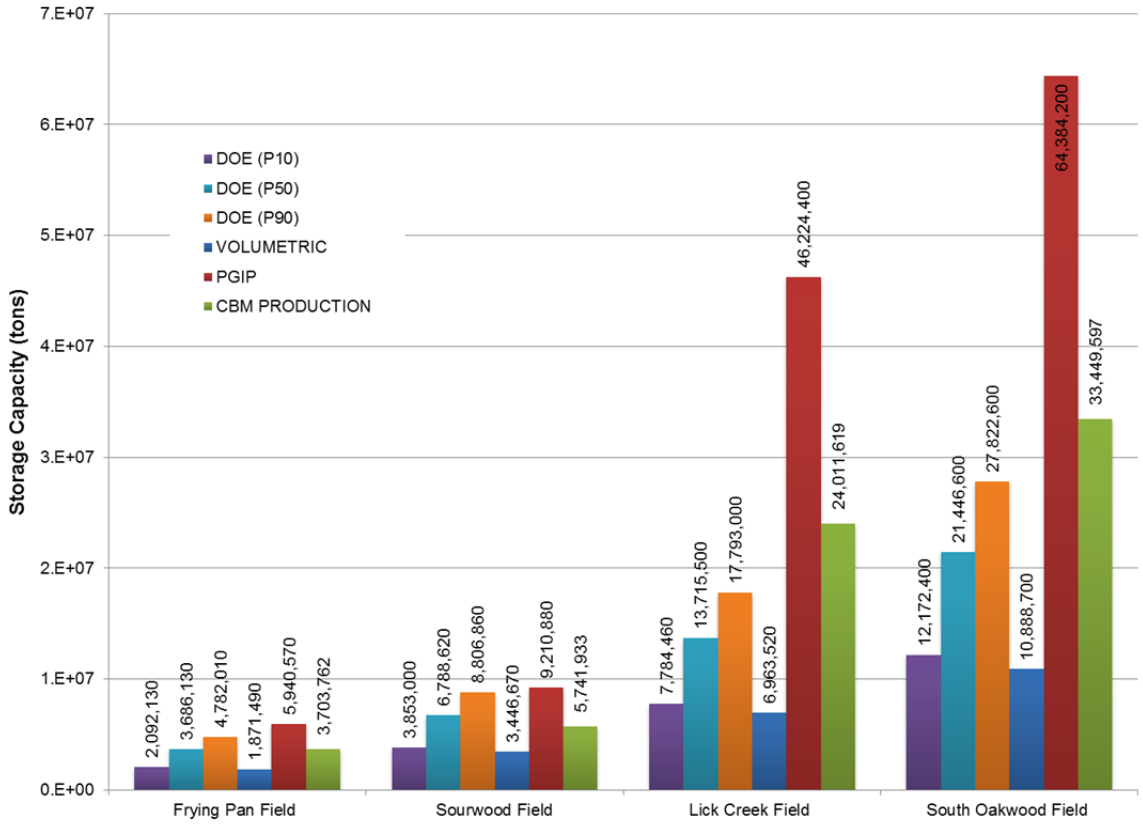

Figure 15: Comparison of the results (storage capacities) obtained with four different storage capacity calculations.

On the other hand, when the number of variables is reduced - the uncertainty about the storage capacity estimate increases. This is common for estimation procedure based solely on the gas production (i.e., "PGIP" and "CBM production" methods), whose results are sometimes 5-6 times higher than results obtained with other calculation methods. This difference is not a linear phenomenon and generally depends on site specific characteristics such as recovery factor, completion factor, estimated ultimate recovery, and CO_2/CH_4 exchange ratio.

3.3 INJECTIVITY AND ECBM RECOVERY

CO_2 sequestration in unmineable coal seams is a distinctively different process from sequestration in conventional hydrocarbon reservoirs and aquifers. The major difference is that; in the case of oil and gas reservoirs and saline aquifers, injected CO_2 occupies the rock pore space as a separate phase or is dissolved in formation water or oil, while an adsorption process at high pressure is the main storage mechanism for coal seams [88-90]. This process provides an opportunity for both: significant reduction of the CO_2 from the atmosphere; and improvement of the efficiency and potential profitability of CBM recovery.

During the sequestration process, injected CO_2 reduces the partial pressure of methane in the reservoir, which promotes CH_4 desorption from the coal matrix [88]. Results from different laboratory- and pilot-scale studies show that coal has a greater affinity for CO_2 than for CH_4. The CO_2 sorption capacity of coal seams is typically between 2 and 10 times that for CH_4 depending on coal rank (thermal maturity) and formation pressure [79] [91].

Desorption of CH_4 molecules from the coal surface and their replacement by CO_2 during the sequestration process sometimes causes profound changes in the coal cleat porosity and permeability. An incremental desorption of CH_4 from the coal surface causes coal matrix shrinkage. During CH_4 desorption, pressure in the coal matrix drops and permeability of the coal increases, sometimes a few orders of magnitude [89]. Opposite to this process, CO_2 adsorption onto coal causes pressure increase and matrix swelling. In this case, permeability decreases [88, 89, 91]. A good example for this phenomenon is the Allison CO_2-ECBM pilot test in the San Juan Basin, New Mexico, where reduction in injection well permeability was over two orders of magnitude [92]. Changes in matrix geometry have significant impact on the cleat system and main flow parameters, which consequently impacts the injectivity of the coal seams, especially at the low pressure range. At higher pressures the permeability increases, but this change will directly influence a higher operational costs (CO_2 injection costs) [93].

Following section reviews results from the SECARB's Phase 2 field validation study in the Central Appalachia conducted by the SECARB coal research team, under research grant DE-FC26-05NT42590 funded by the U.S. Department of Energy's National Energy Technology Laboratory (NETL).

3.3.1 CASE STUDY: FIELD VALIDATION OF THE CO_2 SEQUESTRATION POTENTIAL OF COAL SEAMS IN THE CENTRAL APPALACHIAN BASIN

For the purpose of this sequestration study, an existing CBM well, donated by the CNX Gas and located in their South Oakwood CBM field in Russell County, VA, (37° 5' 15.286" N, 81° 57' 39.106" W) was converted for CO_2 injection (Figure 18). The depth of the injection well (RU-84 - Commonwealth of Virginia designation; or BD-114 - company well designation) was 2,534 feet [86, 87].

The Middle Horsepen coal seam, which represents the top of the shallowest injection zone, lies at an elevation of 707 feet above sea level, 1,420 feet below the surface of the wellhead, or 747 feet vertically below the elevation of the expected deepest potential source of drinking water in the adjacent valley [87]. The proposed injection zone consisted of 19 separate coal seams occurring in the Lee and Pocahontas Formations (Figure 10 and Table 14), totaling 36.3 feet and at depths between 1,420 and 2,259 feet.

As shown in Table 14 and Figure 16, thicknesses of the seams in the proposed injection zone ranged from 0.5 to 3.7 feet, and averaged approximately 1.5 feet per seam. Based on regional permeability and reservoir modeling studies, coal porosity and permeability values were anticipated to range from 0.5% to 1.0%, and from 0.1 md to 20 md, respectively [87]. All targeted coals were expected to have moderately developed face and butt cleats with induced fractures from hydraulic stimulation of the injection well.

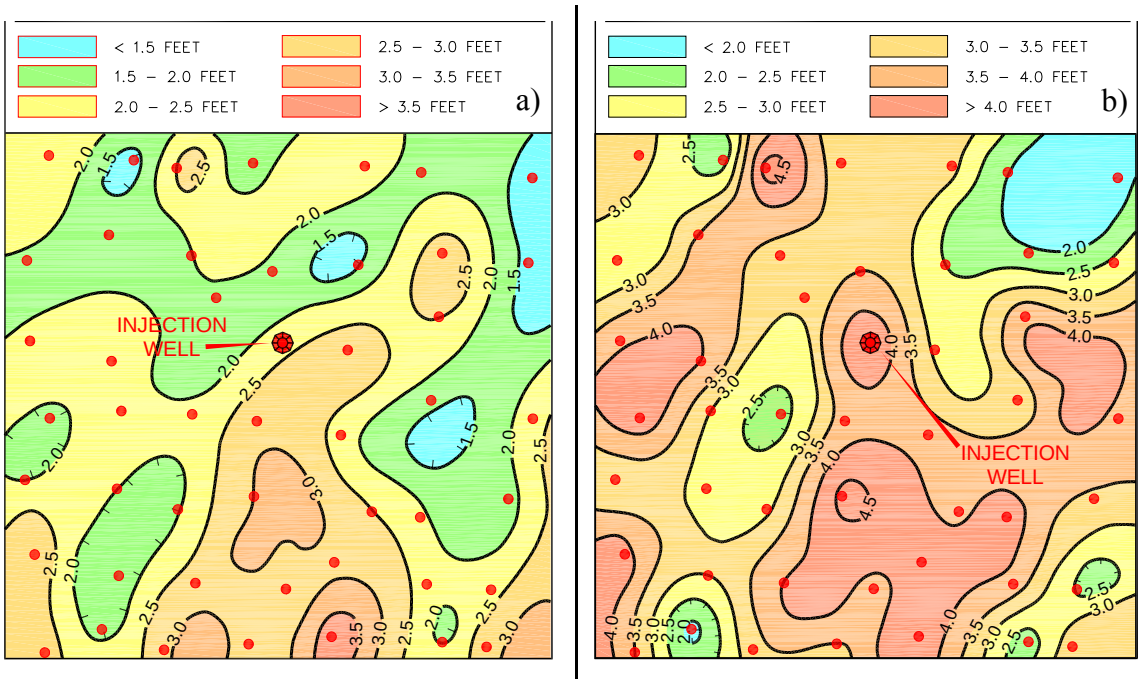

Figure 16: a) Pocahontas No. 3 seam and b) Lower Horsepen seam thickness maps [87].

Table 14: Regional CO_2 storage capacity estimates [85].

Coal Seam	Depth to Coal (feet)	Coal Thickness (feet)
Middle Horsepen 1	1420.5	2.2
Middle Horsepen 2	1497.4	0.7
Pocahontas 11	1547	1.9
Pocahontas 10	1573	1.0
Lower Horsepen 1	1622	2.1
Lower Horsepen 2	1627	1.9
Pocahontas 9	1663.5	1.8
Pocahontas 8-1	1710	2.0
Pocahontas 8-2	1725	1.3
Pocahontas 7-1A	1758.1	0.8
Pocahontas 7-1B	1765.1	0.9
Pocahontas 7-2	1850	1.6
Pocahontas 7-3	1875.1	0.9
Pocahontas 6	1984.1	0.5
Pocahontas 5	2033.3	0.7
Pocahontas 4-1	2125	1.9
Pocahontas 4-2	2148.1	1.1
Pocahontas 3-1	2208	2.4
Pocahontas 3-4	2258.2	1.0
19 Coal Seams		***26.7***

3.3.1.1 Injection and Monitoring Wells

The production well was taken off-line and converted to an injection well in December 2009. Prior to CO_2 injection, two monitoring wells, M1 and M2, were drilled in close proximity to the injection well. The two monitor wells were drilled at 90º offsets from the injection well through the deepest coal seam.

As shown in Figure 17, monitoring well M1 was air-rotary drilled 135 feet from the injection well in the face cleat direction, while well M2 was drilled 285 feet from the injection well in the butt face direction. This well was continuously core drilled from 450 to 2,250 feet. Both monitoring wells were used to monitor the pressure of the plume, as well as composition of gas in the targeted formation.

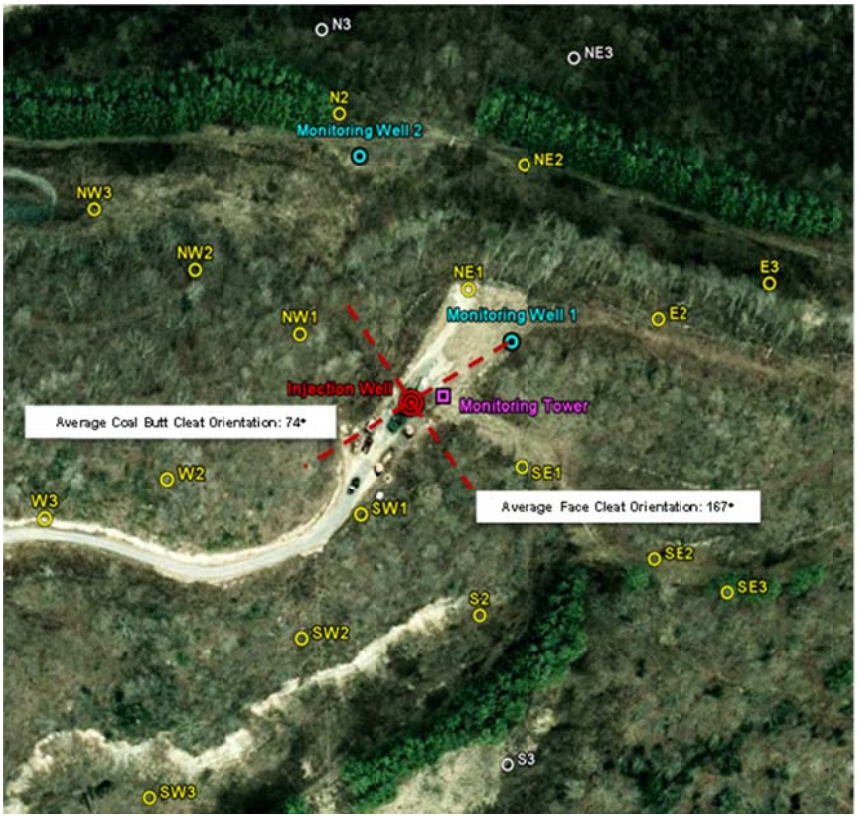

Figure 17: Field validation test site layout, Russell County, VA. (Aerial view) (Source: Google Inc. (2011). Google Earth (Version 6.1.0.5001))

Coal samples from M2 were characterized through a suite of geophysical logs including gamma ray, caliper, density, neutron, induction, and temperature logs [87]. Since all samples analyzed are vertical cores, the results reported in this section reflect only the properties of the seams in the vertical direction.

3.3.1.2 Coal Petrology

Coal seams of both the Lee and Pocahontas Formations are typically high in rank. They are high volatile A to low-volatile bituminous coals with average macerals reflection values of 1.03% (Ro=1.03%) [87]. These thin coals also exhibit considerable variability in ash yield and total sulfur content. Based on all three attributes, it can be concluded that these coal seams can be classified as non-feasible for mining.

3.3.1.3 Coal Petrography

For the purpose of petrographic analysis, core samples of all 24 coal seams were analyzed for maceral content, which is summarized in in Table 15. All coal samples were mostly consisted and high in vitrinite, with some associated macerals of inertinite and liptinite. Obtained petrographic results are in agreement with the petrographic composition of coals of similar rank from other CBM fields in the Appalachian Basin [94].

Table 15: Maceral percentages for analyzed coal samples. All percentages are reported on a mineral-matter free basis [85, 87].

	Vitrinite*	**Liptinite***	**Inertinite***
Maximum	87.6	14.0	30.8
Average	***76.3***	***6.1***	***17.6***
Minimum	56.4	0.8	6.4

High vitrinite content coals are generally considered to have an increased adsorption capacity for methane (CH_4) [95]. Thus, it is expected that coals with high vitrinite contents have significant potential for CBM production, as well as for the CO_2 sequestration.

3.3.1.4 Desorption results

Results from the desorption testing showed very high concentrations of methane gas in place, even after seven years of production from BD-114. On an as-received basis, the gas content of all coal samples ranged from 222 scf/t to 452 scf/t.

3.3.1.5 Adsorption Isotherms

Crushed samples from the Pocahontas No. 3, No. 7, and War Creek (Pocahontas No. 11) coal seams were analyzed for their CO_2 and CH_4 adsorption capacity. It was observed that the average CO_2/CH_4 exchange ratio at 350 psia, for three analyzed samples, was 1.78:1, verifying that these coals preferentially adsorb CO_2 (Figures 18, 19, 20, 21, 22, and 23) [87]. As expected, of all three samples, the Pocahontas No. 3 sample, which is the deepest of three coal seams, had the smallest affinity toward both CH_4 and CO_2. The gas saturation for the coal samples was estimated by comparing the desorption results with the results from adsorption experiments.

Figures 18, 20, and 22 show the amount of gas desorbed from the Pocahontas No. 3, War Creek, and Pocahontas No. 7 coal samples, respectively. These values are plotted below the CH_4 adsorption isotherm at the estimated initial pressure of the formation. The formation pressure was calculated based on the under-pressured gradient of 0.35 psi/ft. The current gas saturations of the Pocahontas No. 3, was 68.8%, while the gas saturation

of the War Creek and Pocahontas No. 7 coal samples was calculated to be 82.6% and 90.8%, respectively.

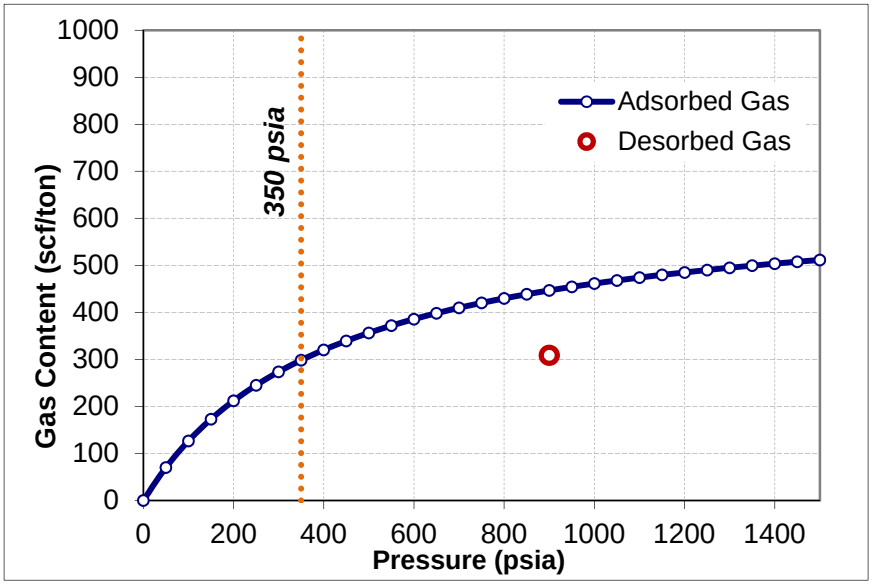

Figure 18: CH_4 adsorption isotherm on dry, mineral-matter free basis (DMMF) for Pocahontas #3 seam (depth 2,099'). Calculated Saturation = 68.8%. [87].

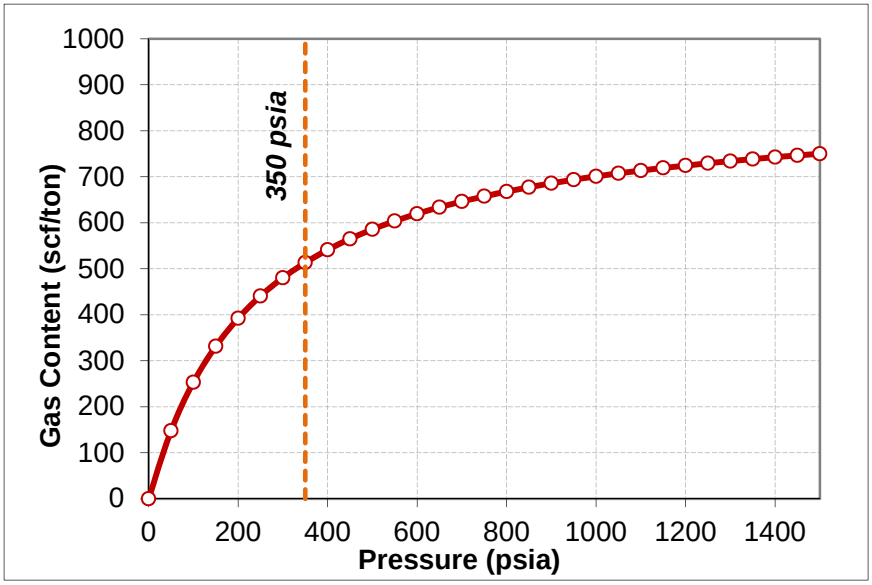

Figure 19: CO_2 adsorption isotherm (DMMF) for Pocahontas #3 seam [87].

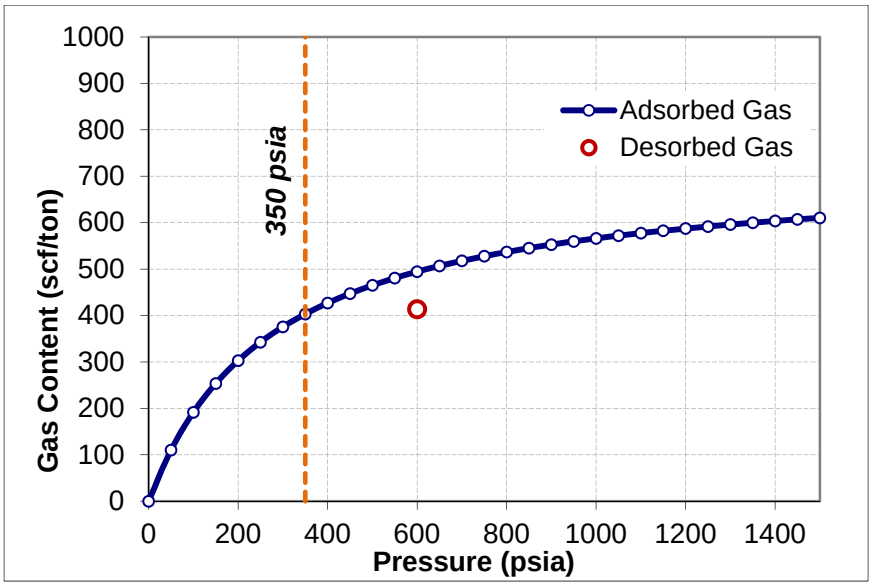

Figure 20: CH_4 adsorption isotherm (DMMF) for War Creek seam (depth 1,440'). Calculated Saturation = 82.6%. [87].

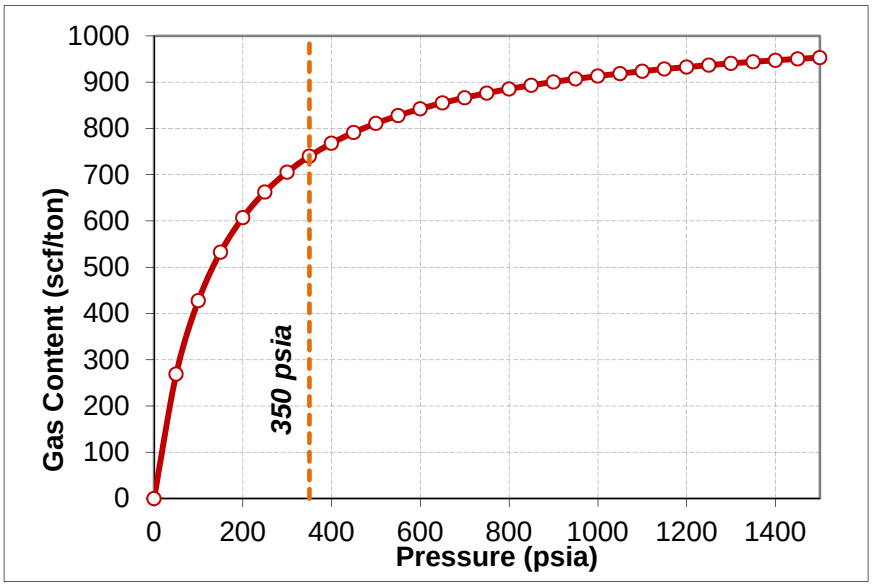

Figure 21: CO_2 adsorption isotherm (DMMF) for War Creek seam [87].

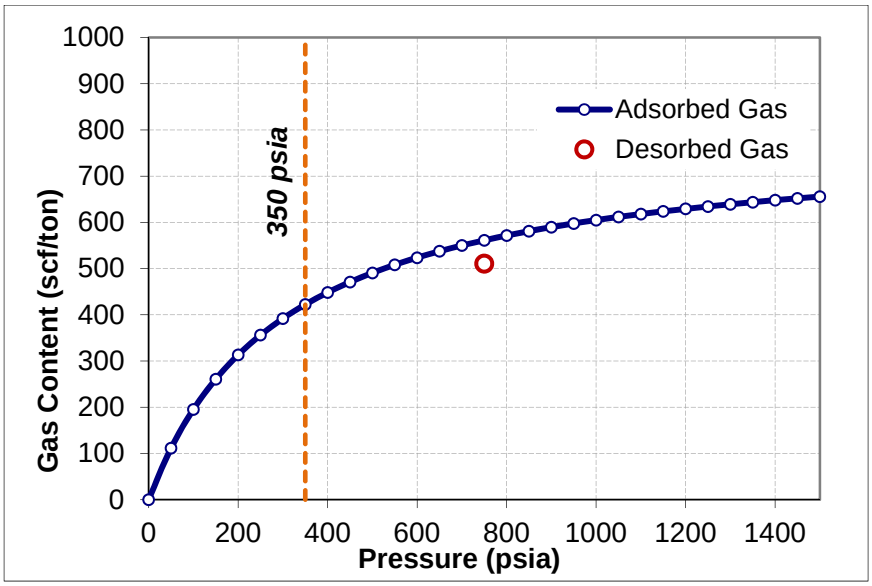

Figure 22: CH_4 Adsorption Isotherm (DMMF) Pocahontas #7 seam (depth 1,744'). Calculated Saturation = 90.8%[87].

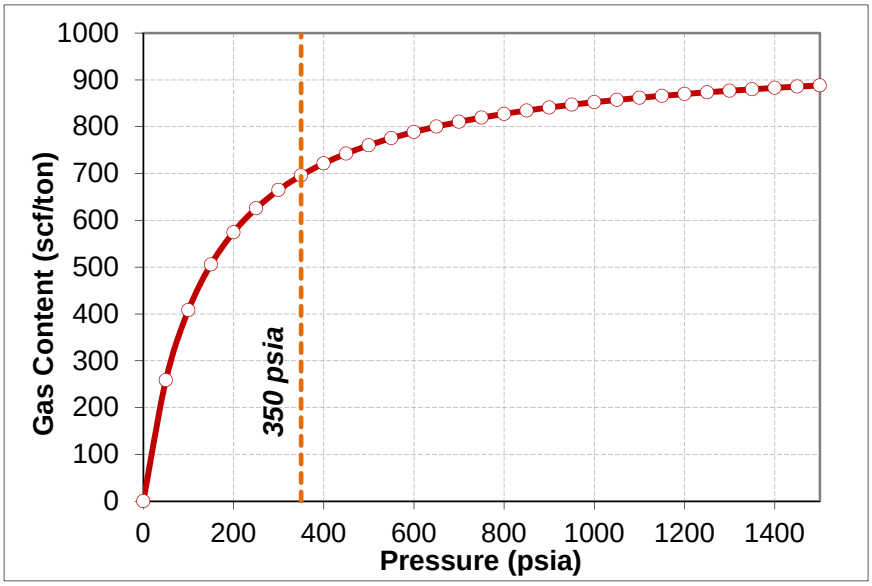

Figure 23: CO_2 adsorption isotherm (DMMF) for Pocahontas #7 seam [87].

3.3.1.6 Porosity and Permeability

Porosity measurements were performed under the low pressure conditions where (confining pressure = pore pressure = 101.5 psi). Obtained porosity values were in the range from 0.9% to 1.5%, which is typical for porosities of Eastern bituminous coals.

Vertical permeability was measured under simulated underground conditions (confining pressure = 1,450 psi, pore pressure = 650 psi). The average value for the permeability was in the range from 200 to 250 μD (microdarcies) [87].

3.3.1.7 Injection Test Results

Injection Rate:

As part of this characterization and field validation study, 1,000 tons of CO_2 was successfully injected into targeted injection zone. As shown in Figures 24 and 25, the average injection rate over a 30-day injection period was 45.2 tons/day.

CO_2 injection process started with the injection fall-off test, which was performed in order to measure the effective permeability of the targeted formation. After an initial slug of 45 tons of CO_2 was injected, formation was allowed to stabilize for three days. During this period, down-hole pressure at injection well was measured, as well as pressures at the monitoring wells M1 and M2 (Figure 26).

After fall-off test was completed, injection process resumed at an injection rate of 30 tons/day. The temperature of the injected CO_2 and injection pressure were maintained close to 100°F, and below 1,000 psia (the maximum injection pressure allowed by the Underground Injection Control (UIC) permit), respectively [86, 87]. As shown in Figure 24, after three days of injection, the injection rate was slowly increased from initial 30 tons/day to 50 tons/day. At the same time the pressure at the injection well increased from 660 psia to 915 psia, since the formation fracture network was saturated with CO_2 and the CO_2 migrated into the coal matrix [86, 87].

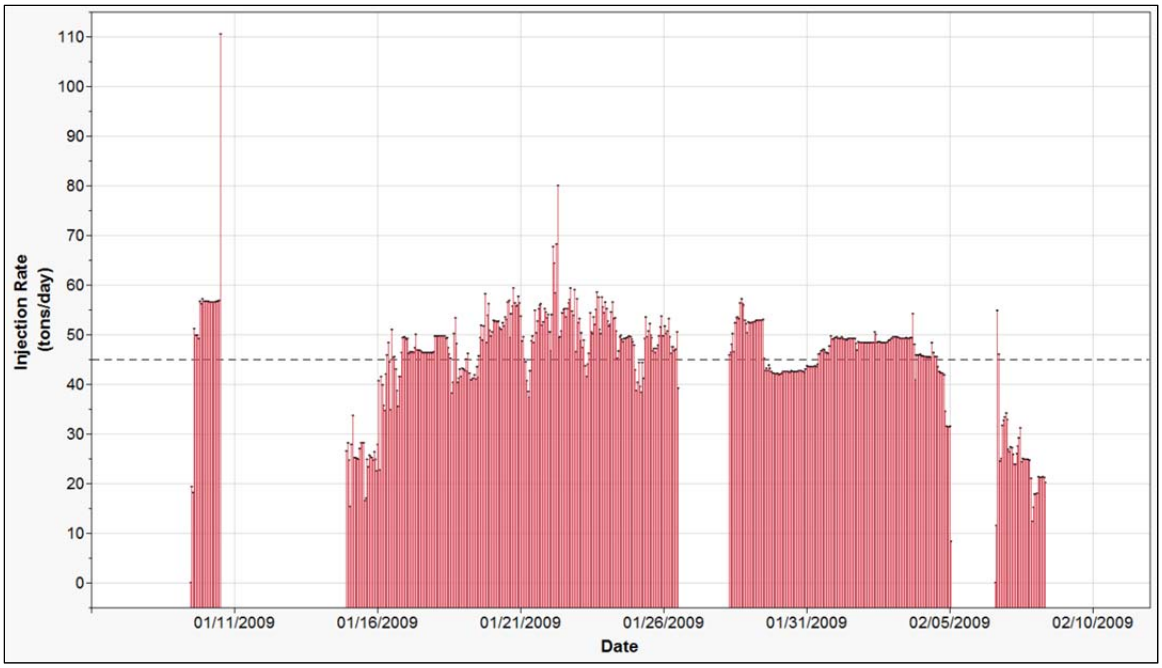

Figure 24: CO_2 injection rate.

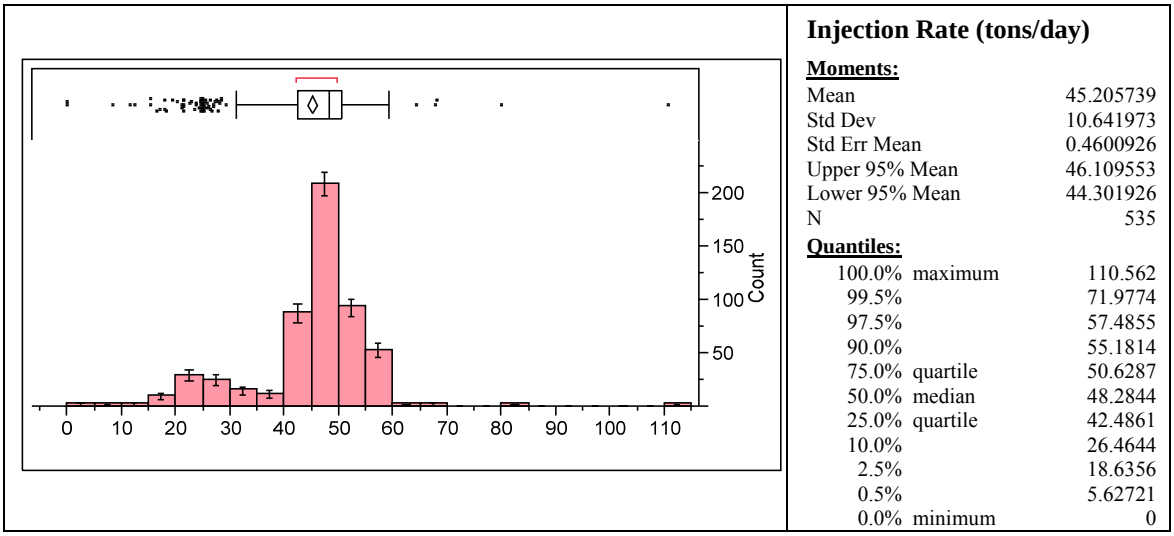

Figure 25: Frequency distribution of the injection rate.

Injection rate was maintained in the range of 40 and 50 tons/day for the rest of the test with two interruptions caused by breaks for equipment maintenance and CO_2 delivery (Figure 24). After 30 days of injection, the injection rate declined to 17 tons/day. This decrease was attributed to the increase of formation pressure due to fill-up of the fracture

network and, and on the other hand, swelling of the coals due to adsorption of CO_2 [86, 87].

Pressure Response[*]*:*

As shown in Figure 26, the pressure at monitoring well M1 increased rapidly to 500 psia within first 30 minutes of the injection process. This observation verified assumption that the CBM field and coal seams chosen for this validation test are interconnected by an extensive hydraulic fracture network.

As can be seen from the Figure 34, the pressure profile at monitoring well M1 mirrored the pressure profile at the injection well during the first day of injection. Over the next 30 days of injection, the pressure profile at M1 continued follow a pressure trend recorded at the wellhead of the injection well.

Due to the malfunction of the pressure monitor, some of the pressure readings from monitoring well M2 were lost. After the pressure monitor was changed, it was observed that the pressure change at M2 follows the same trend as pressures at M1 and the injection well (Figure 26).

Figures 27, 28, and 29 present statistical summary of pressure data obtained from injection and monitoring wells. The average pressures recorded at injection, M1, and M2 wells, over the course of the injection process, were 800.9 psia, 633.2 psia, and 267.1, respectively.

[*] All pressure readings reported in this section are surface pressure readings.

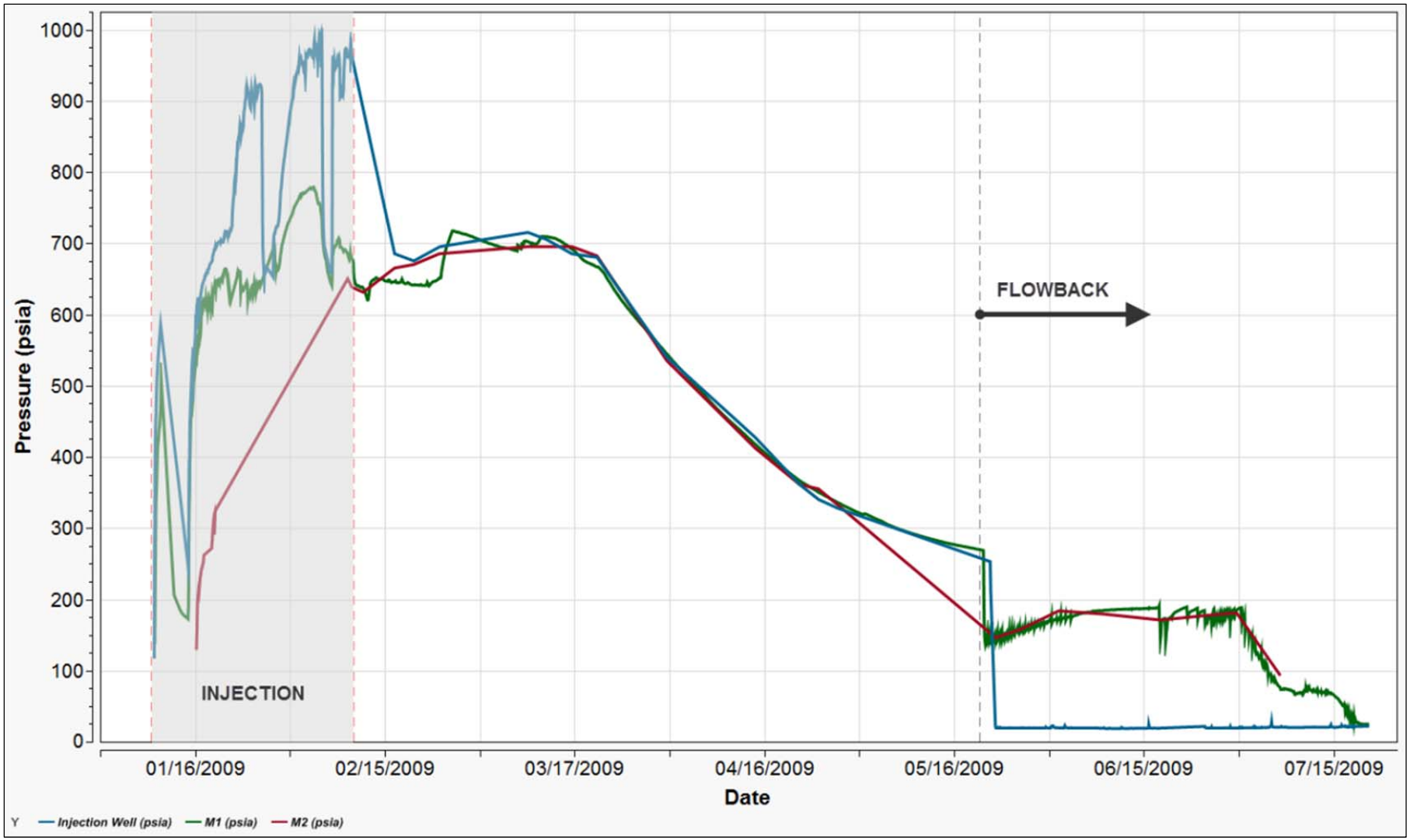

Figure 26: Pressures at injection and monitoring wells.

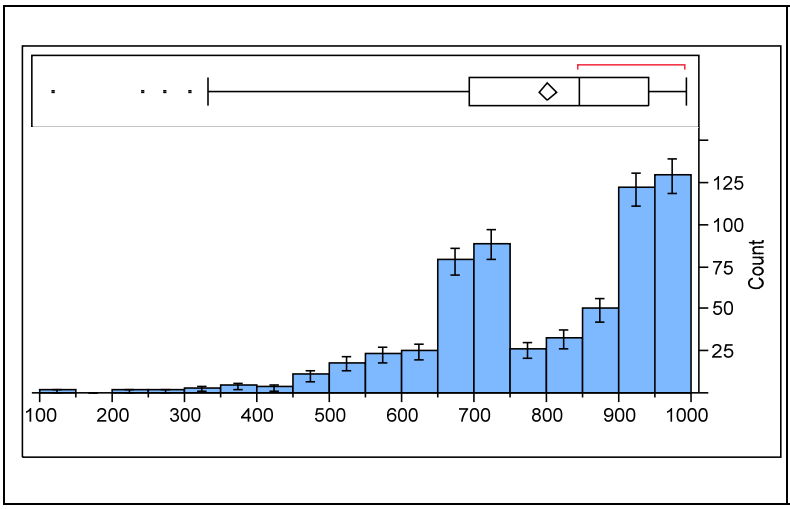

Injection Well (psia)

Moments:

Mean	800.93915
Std Dev	154.40726
Std Err Mean	6.2671972
Upper 95% Mean	813.24721
Lower 95% Mean	788.63109
N	607

Quantiles:

100.0%	maximum	992.995
99.5%		990.512
97.5%		979.477
90.0%		966.893
75.0%	quartile	940.705
50.0%	median	845.976
25.0%	quartile	694.06
10.0%		598.673
2.5%		463.506
0.5%		273.423
0.0%	minimum	117.725

Figure 27: Frequency distribution of the pressure at injection well.

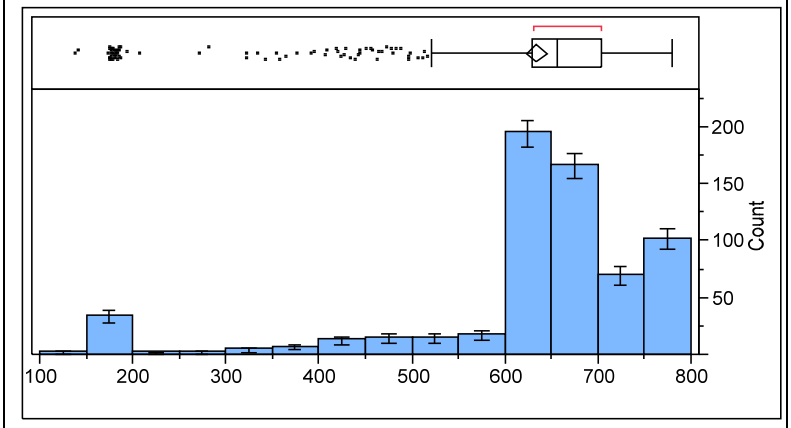

M1 (psia)

Moments:

Mean	633.23499
Std Dev	139.77826
Std Err Mean	5.5469311
Upper 95% Mean	644.12757
Lower 95% Mean	622.34241
N	635

Quantiles

100.0%	maximum	779.76
99.5%		779.61
97.5%		777.867
90.0%		767.35
75.0%	quartile	703.61
50.0%	median	656.38
25.0%	quartile	629.67
10.0%		459.532
2.5%		177.25
0.5%		173.078
0.0%	minimum	137.38

Figure 28: Frequency distribution of the pressure at monitoring well M1.

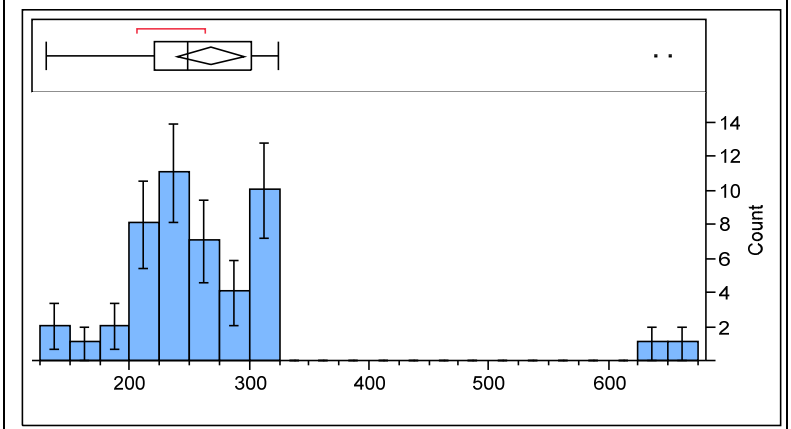

M2 (psia)

Moments:

Mean	267.08234
Std Dev	93.611233
Std Err Mean	13.654602
Upper 95% Mean	294.56763
Lower 95% Mean	239.59705
N	47

Quantiles:

100.0%	maximum	651
99.5%		651
97.5%		648.6
90.0%		322.468
75.0%	quartile	301.55
50.0%	median	247.99
25.0%	quartile	220.94
10.0%		192.51
2.5%		133.118
0.5%		129.74
0.0%	minimum	129.74

Figure 29: Frequency distribution of the pressure at monitoring well M2.

After injection process was completed, the formation was left to soak CO_2 for three months. As shown in Figure 26, pressures at all three wells started to rise three weeks after the end of injection operations. This change, or increase in pressure, can be attributed to CO_2 phase change and its vaporization from liquid to gas in the wellbore.

The flowback phase, when the injection well (BD114) was brought back on-line as a producing well, started after three months of soaking. It was observed that with the beginning of the flowback operations, the pressures dropped quickly at all three wells, and then slowly increased as the flow rate in BD114 decreased due to the influx of the formation water to wellbores of M1 and M2 [86, 87].

3.3.1.8 ECBM Recovery

The Central Appalachian Basin has abundant coal and CBM resources. It is estimated that unmineable coal seams in Central Appalachia hold approximately 5,000 billion cubic feet (Bcf) of CBM in place [96]. First commercial CBM operation in Central Appalachia started in 1988 and since that time over 5,000 CBM wells were drilled and completed in this region [97]. Many of these CBM wells and reservoirs are currently approaching maturity, thus providing a significant potential for carbon sequestration. It is estimated that CO_2 sequestration with CO_2-enhanced coal bed methane (CO_2-ECBM) recovery can help extract additional 0.9 trillion cubic feet (Tcf) of CBM in the Central Appalachian Basin [98].

For the purpose of this study, a daily CBM production data from the seven offset wells were monitored so that any change in production, caused by the CO_2 injection, could be detected. The data was recorded for a one-year period on an hourly basis, and included flow rate, differential pressure, and temperature. As can be seen from Figure 30,

a small increase in CBM production was observed at two offset wells, BD115 and BE114 during the CO_2 injection phase. This change was observed during the second week of the CO_2 injection.

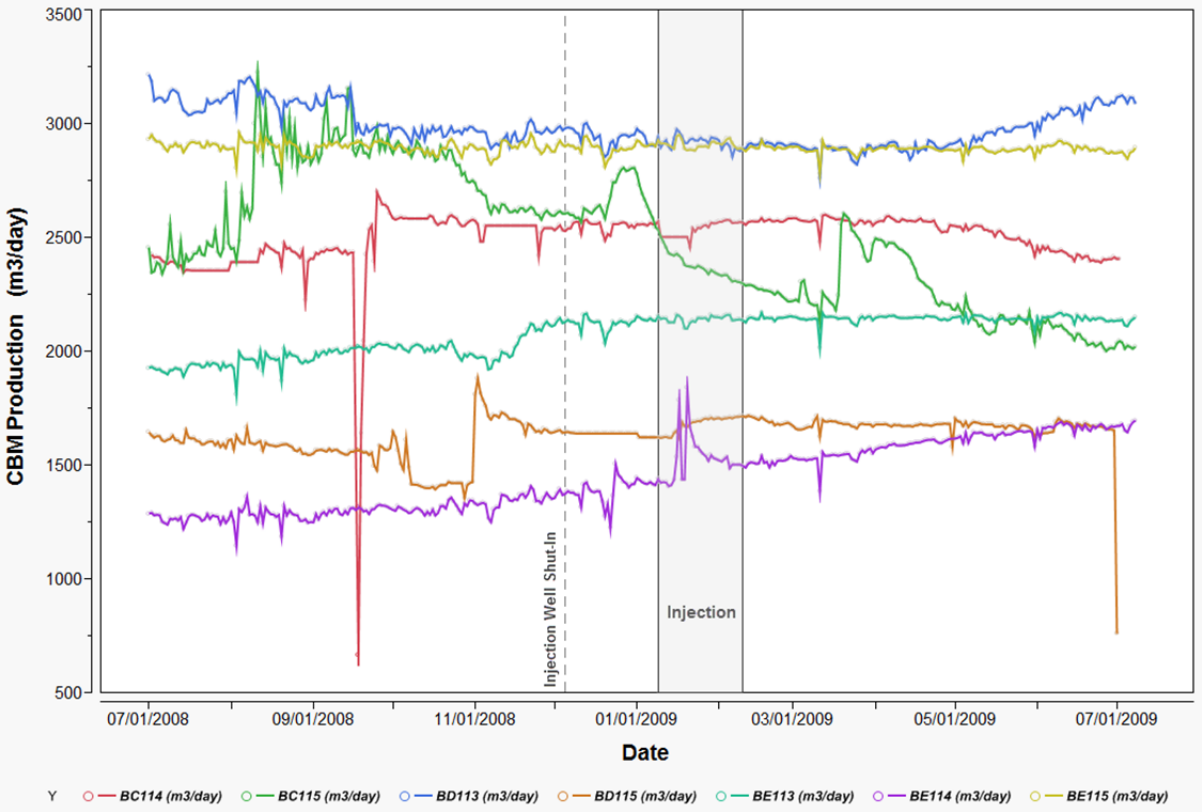

Figure 30: Production rates for seven offset producing wells.

The change in production trends at BD115 and BE114 was further examined by utilizing an auto regressive integrated moving average (ARIMA) method. This method allowed comparison of actual production data and values predicted based on CBM production before CO_2 injection. A time series graph (Figure 31) shows production data before and after injection and future production trends predicted based on a linear combination of past values and a series of errors, also known as random shocks or

innovations. A regression plots and summary of the fit parameters is given in Figures 32 and 33.

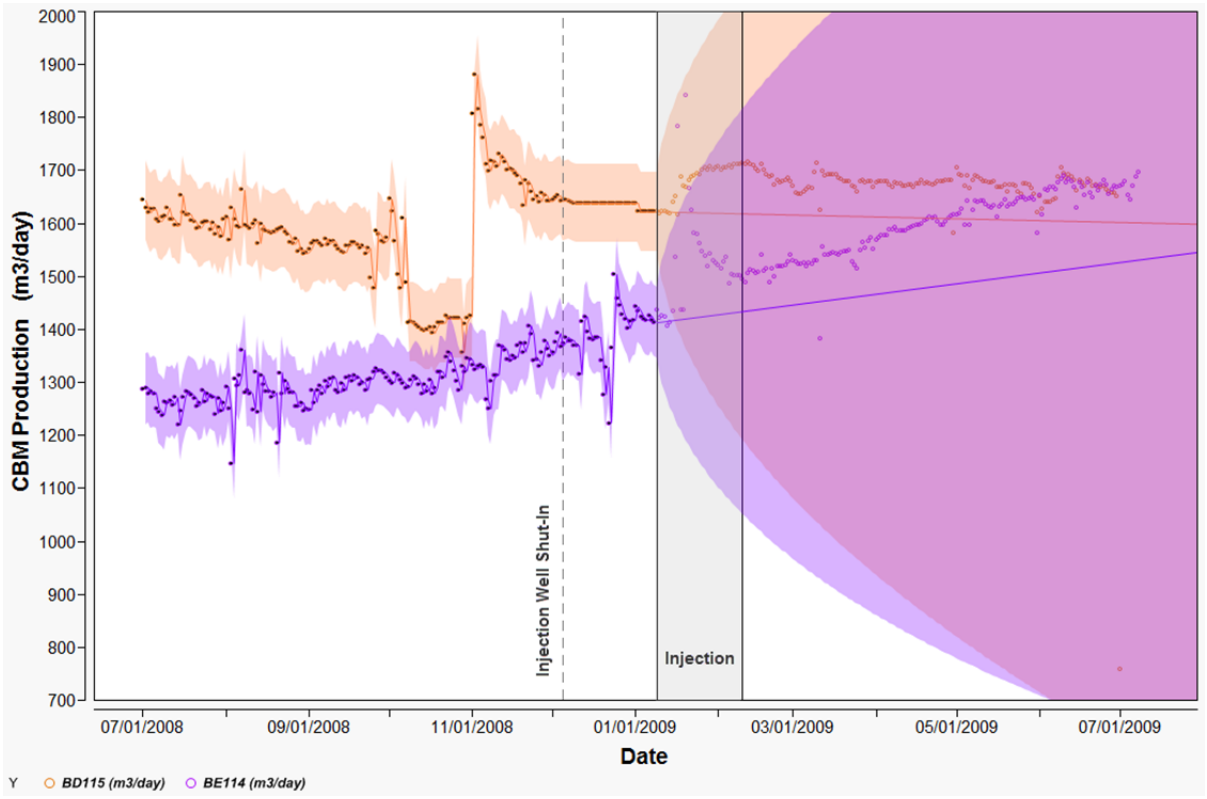

Figure 31: Actual and forecasted production rates at two offset wells.

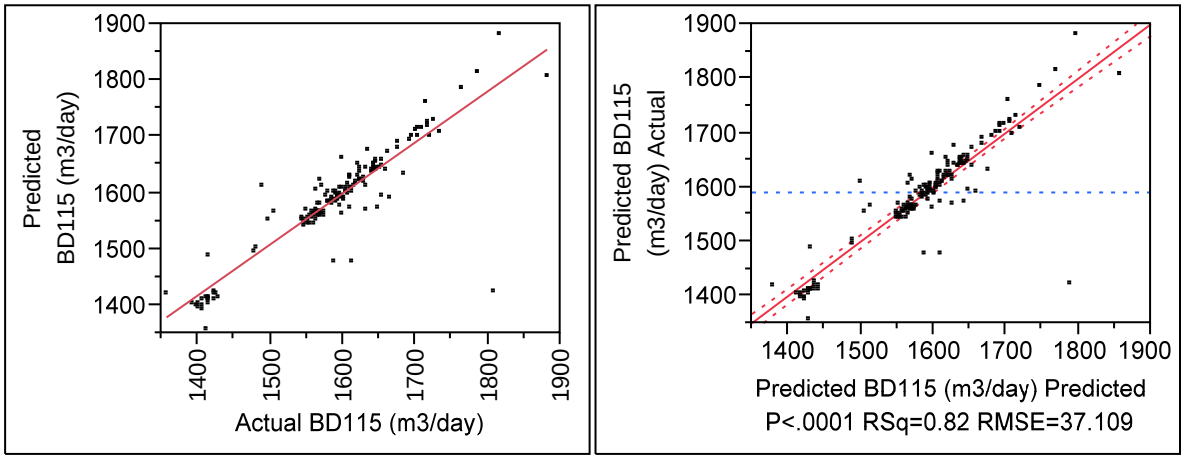

Figure 32: Regression and actual vs. predicted plots for BD115.

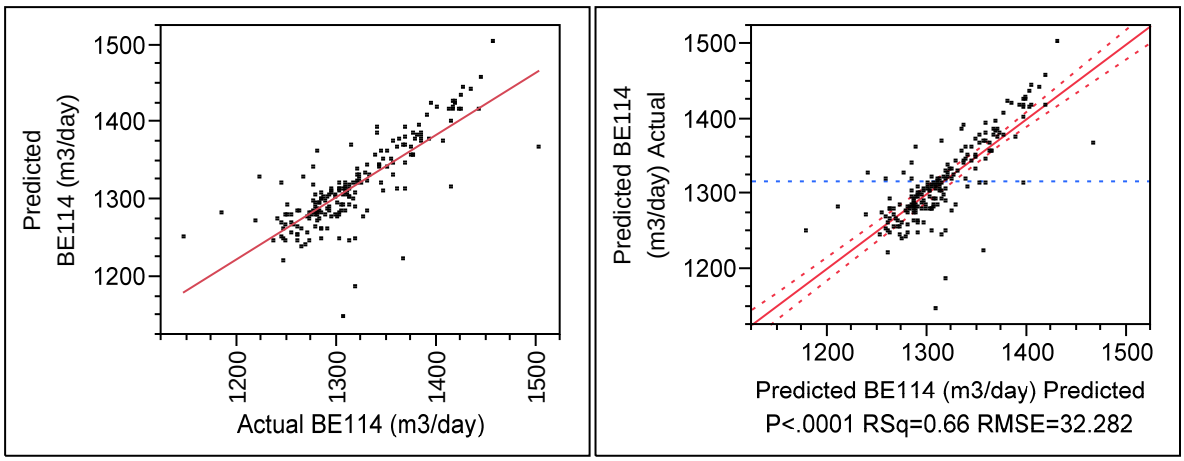

Figure 33: Regression and actual vs. predicted plots for BD115.

In order to estimate a percent change in CBM production, an average actual and predicted production rates were integrated over 155 days (Figures 33 and 43). As shown in Table 16, an average increase in production over this period was 4% and 7% at BD115 and BE114, respectively.

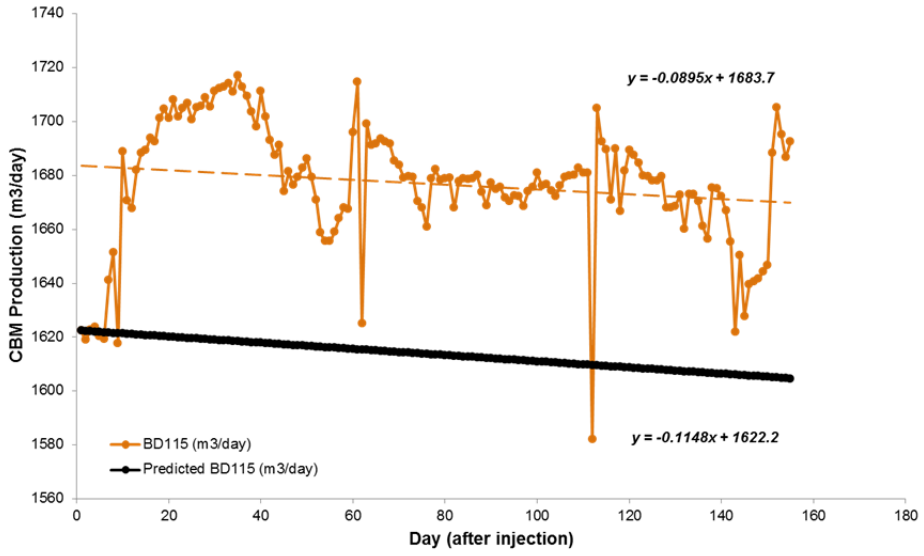

Figure 34: Actual vs. predicted CBM production at offset well BD115 (over period of 155 days after injection started).

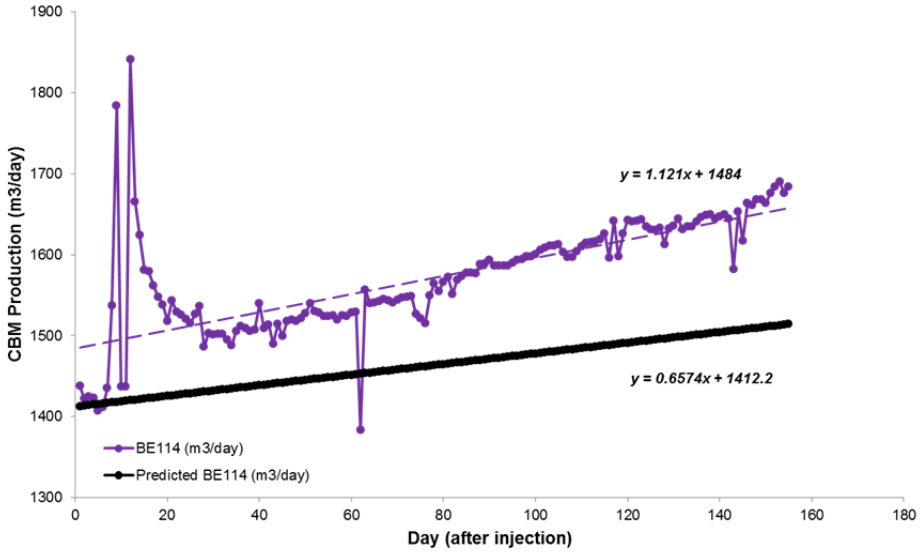

Figure 35: Actual vs. predicted CBM production at offset well BE114 (over period of 155 days after injection started).

Table 16: Enhanced CBM production at BD115 and BE114.

Well	Predicted CBM production (m^3/day)	Actual CBM production (m^3/day)	% increase
BD115	1613	1676	***4%***
BE114	1463	1571	***7%***

The increase in production rates at BD115 and BE114 can be correlated with pressures change (Figure 38) and changes in gas composition (Figures 36 and 37) observed at two producing wells during the injection phase. As shown in Figures 36 and 37, 3% decrease in the CH_4 and consequent 3% increase in CO_2 mole fractions were observed at both offset producing wells.

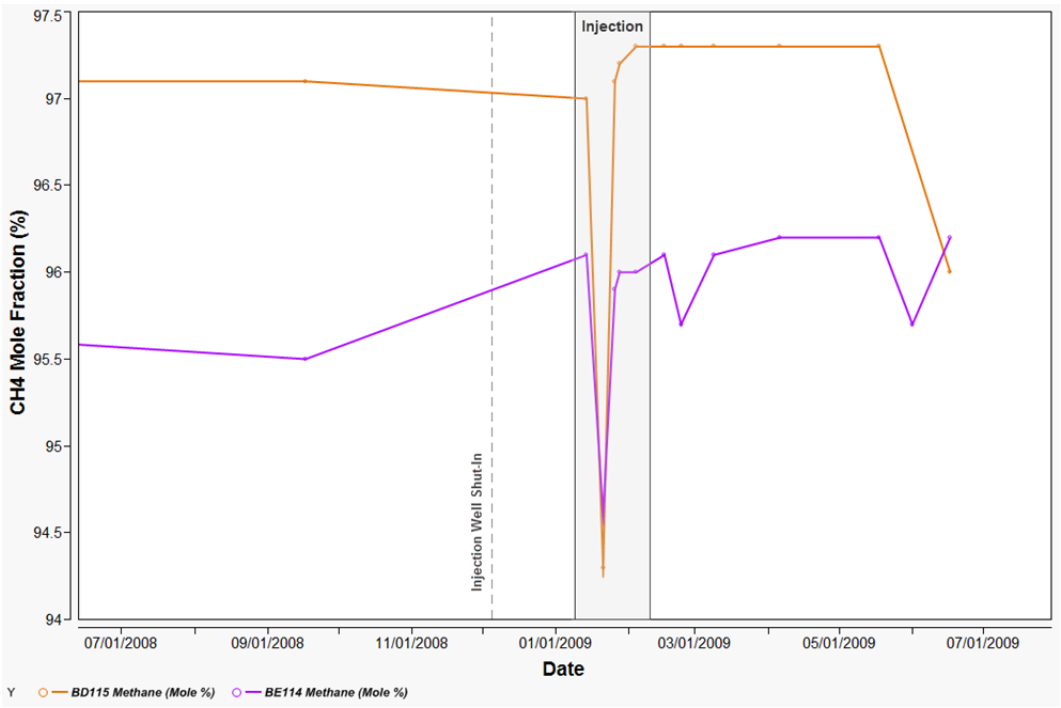

Figure 36: CH_4 mole fraction at offset producing well BD115 and BE114.

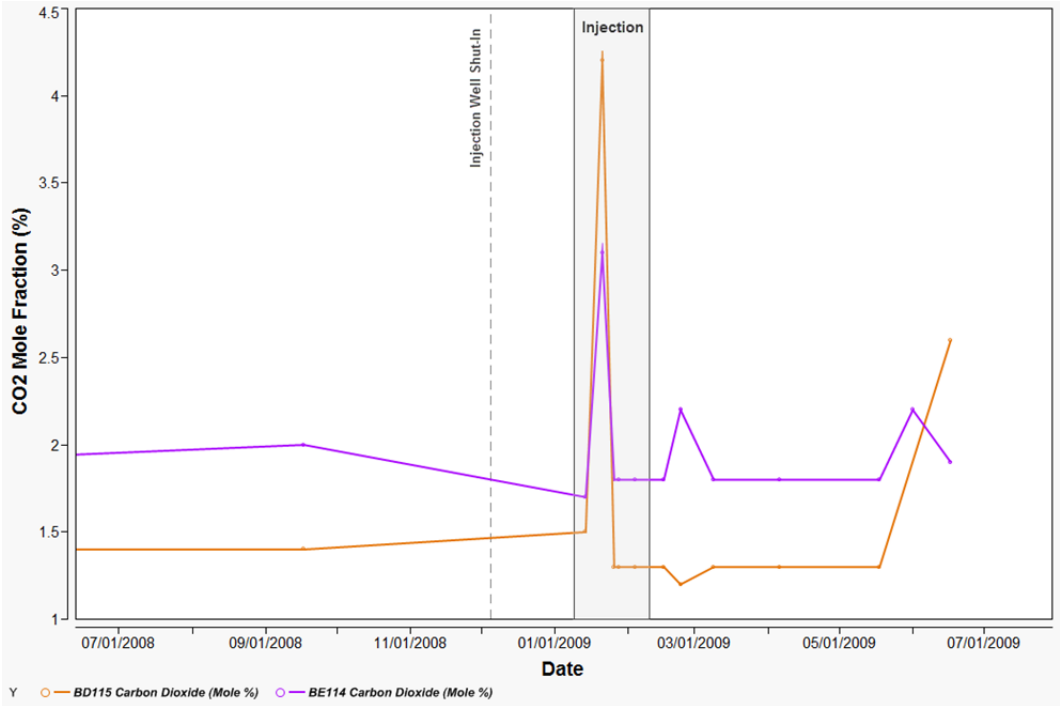

Figure 37: CO_2 mole fraction at offset producing well BD115 and BE114.

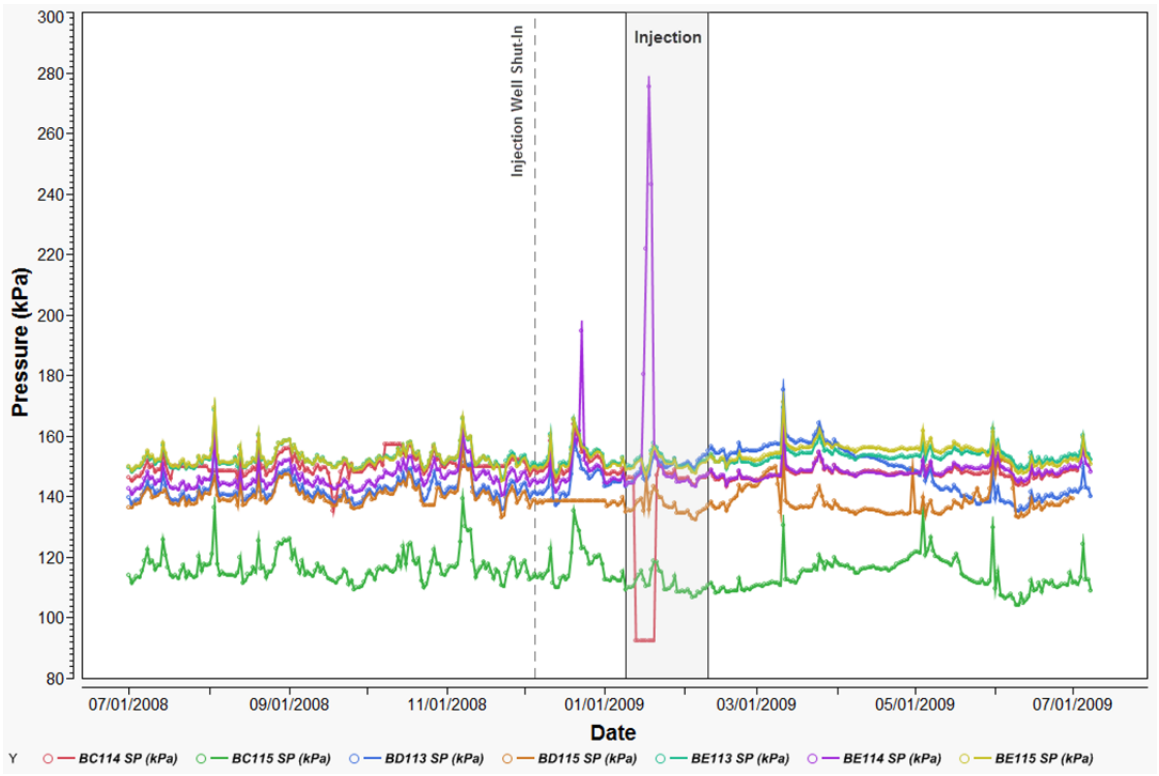

Figure 38: Pressures at seven offset producing wells.

Increase in production, as well as the amount of CO_2 detected, at two offset wells confirms presence of hydraulic and/or natural fractures and connection between the injection and two offset wells.

3.4 CONTAINMENT

Containment potential of CO_2 storage site refers to the potential of the injection and confining formations (seal) to retain injected CO_2 within the subsurface. Containment primarily depends on the geometry and spatial distribution of rocks comprising the injection and confining formations, and on pressure conditions that limit fluid flow in the subsurface [36]. Ideally, confining formations should have a regional extent and uniform lithology.

In the real world, there are many variations of seal geometries that limit the movement of CO_2 in the subsurface, including lateral and vertical variations in the reservoir and complex geometries of the ultimate seal. This also includes flow barriers such as faults and naturally over-pressurized zones [24, 29, 31, 37, 38]. However, the presence of faults and fractures does not necessarily imply a leakage problem [33, 34]. For example, even if the subsurface extent of hydrocarbon reservoirs is limited by faults and fractures, reservoir fluids do not directly flow to the surface along the faults because faults are not unimpeded leakage pathways to the surface [39].

The main idea behind the CO_2 sequestration in deep geological formations is that injected CO_2 can be trapped as a gas or supercritical fluid under a low-permeability cap rock; or be adsorbed on the surface of the coal.

A number of different technologies and procedures are currently used to assess and verify effectiveness of the CO_2 containment within the storage reservoir. These technologies are classified as a Monitoring, Verification, and Accounting (MVA) technology. Well planned and executed MVA program can assure continued confinement of CO_2; verify storage site integrity over the life cycle of the project; and demonstrate that the storage is performing according to long range predictions.

MVA protocol development and implementation is an essential part of overall risk management strategy in all CCS projects. In order to provide an assurance that a selected sequestration site can be operated safely, both the storage and seal formations should be closely monitored.

An appropriate monitoring protocol can provide data about CO_2 behavior (flow, extent, and immobilization) within the storage reservoir and information about seal

performance, which will allow better risk control and mitigation (primarily risk of leakage), as well as maximization of the operational efficiency and minimization of the operational costs through the lifecycle of a CCS project.

Currently, a large and diverse portfolio of standard, "off-the-shelf" monitoring tools and technologies is available for monitoring CO2 storage sites. The challenge is to define and successfully integrate different monitoring tools into one optimized MVA system for a specific CO_2 storage site [50].

The next section summarizes MVA results from the SECARB's Phase 2 field validation study in the Central Appalachia.

3.4.1 CASE STUDY: FIELD VALIDATION OF THE CO_2 SEQUESTRATION POTENTIAL OF COAL SEAMS IN THE CENTRAL APPALACHIAN BASIN

The Monitoring, Verification, and Accounting (MVA) program implemented at the test site was designed to ensure maximal storage capacity and integrity of CO_2 reservoir, as well as to guarantee safety of on-site personnel, protection of surrounding ecosystems and settlements, more precise long-term predictions, and lower operational costs.

The MVA program was designed to monitor, collect, and report relevant data about the storage system, especially data about chemical and physical processes in the targeted coal seams and surrounding geological formations before, during, and after CO_2 injection. Besides the subsurface monitoring, this comprehensive MVA program also included near-surface and atmospheric monitoring, as well as protocol for real-time remote data collection and online data dissemination.

The main purpose of this comprehensive MVA program was to investigate and assess possible leakage and seepage mechanisms in order to enable early detection of storage failure. To achieve all MVA objectives, a research team deployed a broad portfolio of subsurface, near-surface, and atmospheric monitoring tools and techniques at the test site.

3.4.1.1 Geological Setting

The rocks comprising the injection and confining units for injection well include those of the Pocahontas and Lee Formations. The confining units are comprised of low permeability shale, siltstone, and sandstone. Regional stratigraphic cross sections and geologic mapping demonstrate that these fluvial-deltaic sediments are laterally extensive, covering large portions of Buchanan, Dickenson, Russell, Tazewell, and Wise Counties, Virginia [84-87, 98, 99]

Effectiveness and seal capacity, as well as CO_2 leakage potential, at the test site were assessed based on subsurface geophysical field data for regional Hensley Shale and other seals overlying the targeted coals.

The primary confining units include multiple layers of low permeability shale and siltstone beds that range in thickness from 5 to 55 feet in the vicinity of the injection well. Permeability for the shale and siltstone units is expected to range from 0.001 to 0.1 md, with low porosity. Results from geophysical analysis of the Hensley Shale data shows that this confining unit is an effective seal since it is thick (>50ft), laterally continuous (>741,316 acres), and homogenous [99].

Even the sandstone units are considered to provide confining beds due to the well cemented nature of these rocks. The Lee and Pocahontas Formation sandstones are known to have low permeability and porosity values, and do not produce natural gas in this area. The tight sandstone units range in thickness from 5 to 60 feet. The sandstone units are expected to have porosity values that range from 1.0 to 3.0 percent and permeability values ranging from 0.1 to 1.0 md. All lithologies will encounter some natural fractures; however, these fractures are likely to be cemented with quartz and calcite and are not expected to provide permeability pathways [84, 87, 98]. Taking into account that maximum seal capacities are far greater than storage reservoir thicknesses in the target area, danger of capillary failure was eliminated.

3.4.1.2 Soil and Terrain Characteristics

The surface of the injection site is mountainous terrain at 2,400' above sea level that was previously strip-mined. The injection well is located on the mountain south of Hess Creek, at an elevation of 2,523 feet. Its depth is 2,534 feet. The top of the shallowest proposed injection zone lies at an elevation of approximately 905 feet above sea level, 1,618 feet below the surface of the wellhead, or 945 feet vertically below the elevation of the expected deepest potential source of drinking water in the adjacent valley, approximately one-quarter mile to the north.

Soils in Russell County, VA are generally composed of a light-to-heavy-textured surface soil and heavier textured subsoil. In texture, the surface soil is prevailingly fine and consists of silt loam, silty clay loam, loam, very fine sandy loam, or fine sandy loam. No large areas of heavily intractable soil or large areas of deep, highly leached sandy soil have developed [100].

As shown in Figure 39, in the 60 acres surrounding the test site, 48.4% of the soils are Shelocta-Kaymine complex (50F), 55% to 85% slopes, very bouldery; 30.7% are Shelocta-Cedarcreek complex (48E), 35% to 55% slopes, very bouldery; 18.8 percent are Cedarcreek-Sewell-Rock outcrop complex (16C) , 0% to 15% slopes, very stony; and 2.2% are Kaymine-Fiveblock-Cedarcreek complex (34C), 0% to 15% slopes, extremely stony [101].

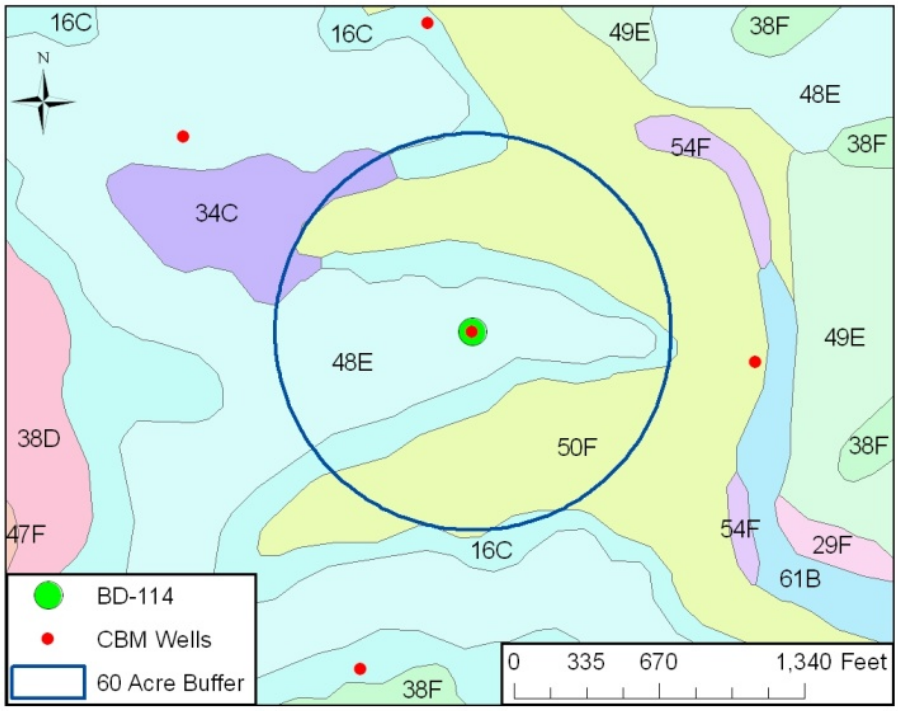

Figure 39: Soil survey map showing the location of the coal test site.

The test site is developed exclusively on the Shelocta-Cedarcreek complex, with the Shelocta and similar soils making up 70% of the complex and the Cedarcreek and similar soils comprising 25% [101]. No unique species are known in this soil or at the project site, and there have been no erosion problems observed at the test site. The Shelocta series consists of deep and very deep, well drained, moderately permeable soils formed in mixed colluvium from shale, siltstone, and sandstone or colluvium and

residuum [102]. The Shelocta soils are well drained with a moderately high to high capacity of the most limiting layer to transmit water (0.57 to 1.98 in/hr). A typical profile of the Shelocta soils are 0 to 4 inches: gravelly loam; 4 to 13 inches: loam; 13 to 15 inches: gravelly loam; and 50 to 86 inches: very gravelly loam.

The Cedarcreek series consists of very deep well-drained soils with moderate or moderately rapid permeability. These soils formed in acid regolith from the surface mining of coal. The regolith is a mixture of partially weathered fine earth and fragments of bedrock [103]. The Cedarcreek soils are typically found along ridges and spurs and are well drained with moderately high to high capacity of the most limiting layer to transmit water (0.57 to 5.95 in/hr). A typical profile of the Cedarcreek soils are 0 to 15 inches: very channery loam; and 15 to 65 inches: extremely channery loam.

3.4.1.3 Hydrologic Conditions

The principal underground source of drinking water in the area is the stress-relief fracture zone in rock strata underlying valley floors. That zone of enhanced fracture permeability is most permeable to depths of approximately 50 to 75 feet below the ground surface, typically, and grades less permeable downward. Below depths of about 200 to 300 feet, no distinguishable increase in permeability remains, and all rock strata exhibit very low permeability [104]. Outside the valley floor areas, some aquifer potential of secondary importance is afforded by several sandstone units and coal beds lying at depths of less than 300 feet. Below 300 feet, studies have shown transmissivity values of all strata to be very low.

The only known utilization of ground water in the vicinity of the injection well is from springs or wells situated along the floor of the valley of Hess Creek. The surface

elevation of the valley floor in that area is approximately 2,150 feet above sea level. The expected deepest occurrence of a potential underground source of drinking water is about 300 feet below that, or about 1,850 feet in elevation.

3.4.1.4 MVA Results

This section will review only results related to near-surface and atmospheric monitoring (leakage detection), since all results related to subsurface monitoring are reported in other parts of this dissertation.

Monitoring Network Design:

It is well recognized that success of any experimental study highly depends on quantity and quality of collected data. When collecting data, the decision about the type and quantity will depend in large on how the data will be used and what are the overall scientific goals of the study. The data type, quantity, and sampling procedures, constrain the choice of data analysis technique. In the case of poor quality or undesirably low quantity data, the analysis will lead to vague results.

Taking into account these constraints, a new data collection and dissemination protocol was developed and implemented at the test site. This data management protocol was designed to enable a continuous, online, multi-parametric monitoring and online data analysis and dissemination. This approach required the exploitation of existing data management resources, as well as the implementation of ad-hoc configurations and data exchange methodologies capable of meeting demanding scientific requirements during this project. Requirements for near-real-time communications have been derived from the quantity and quality of observational and modeling tasks planned during pre-operational

activities. As an initial step, three major "information domains" were identified, corresponding to logical areas where information was produced and processed (Figure 40). The first domain was assigned to the test site. This domain provided capability for data collection and conditioning, and data transfer and execution of internal and external commands, including sensor management. The second domain was associated with the Virginia Center for Coal and Energy Research (VCCER), which acted as a central gateway for the execution of all data protocols, with focus on data storage and dissemination. The third domain referred to experiment contributors connected over the Internet.

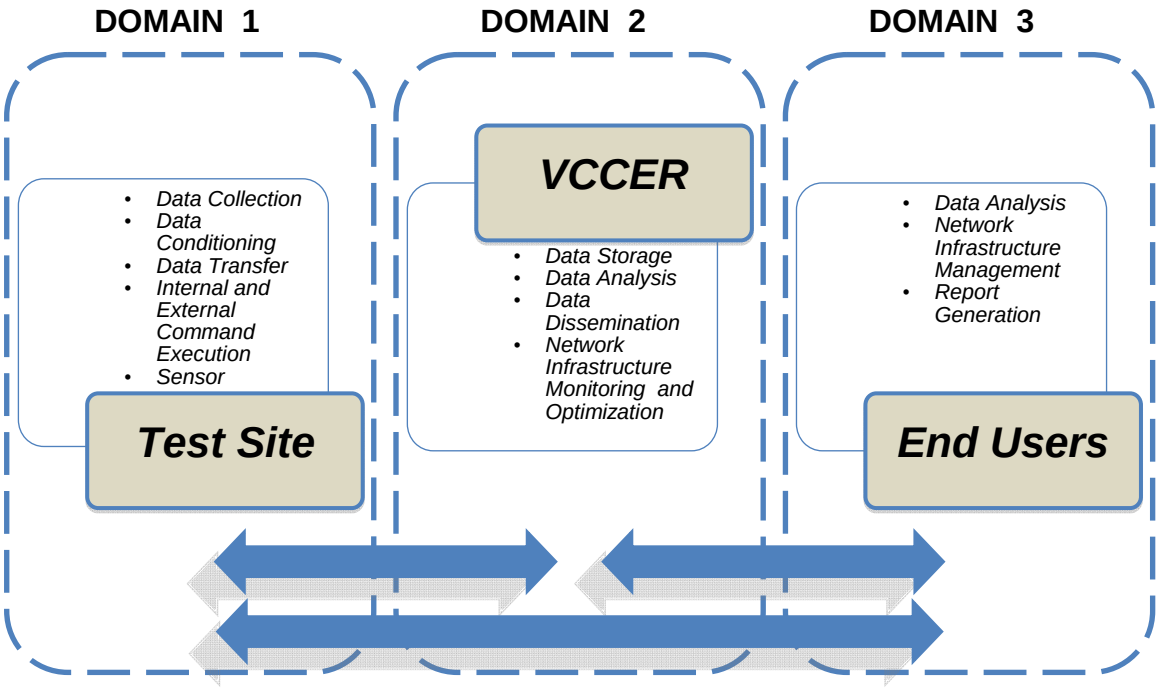

Figure 40: Soil survey map showing the location of the coal test site.

Throughout the lifecycle of this project, data was generated by a variety of sensors deployed at the test site. To accommodate an infrastructure for continuous, online, multi-parametric monitoring and online data analysis and dissemination, a new

50-foot monitoring tower with a control unit was built and installed at the test site (Figure 41). Each sensor was capable of data collection and had varying amounts of data storage. Some sensors were already available to the research team and were not purchased for this specific project. As a result, a universal data acquisition system was not available. Instead, the research team installed a laptop and communication network to each device by the device's communication means.

Additionally, each sensor had specific data collection software provided by the vendors that was not interoperable between the sensors. For each sensor, automated data collection software was developed. These programs had variable complexity based on the sensor software characteristics. In all cases, the automation program produced a text comma separated file with the sensor data. This data was input into the local computer's database server, filtering out replicated data. In designing the system, bandwidth limitations had to be taken into account.

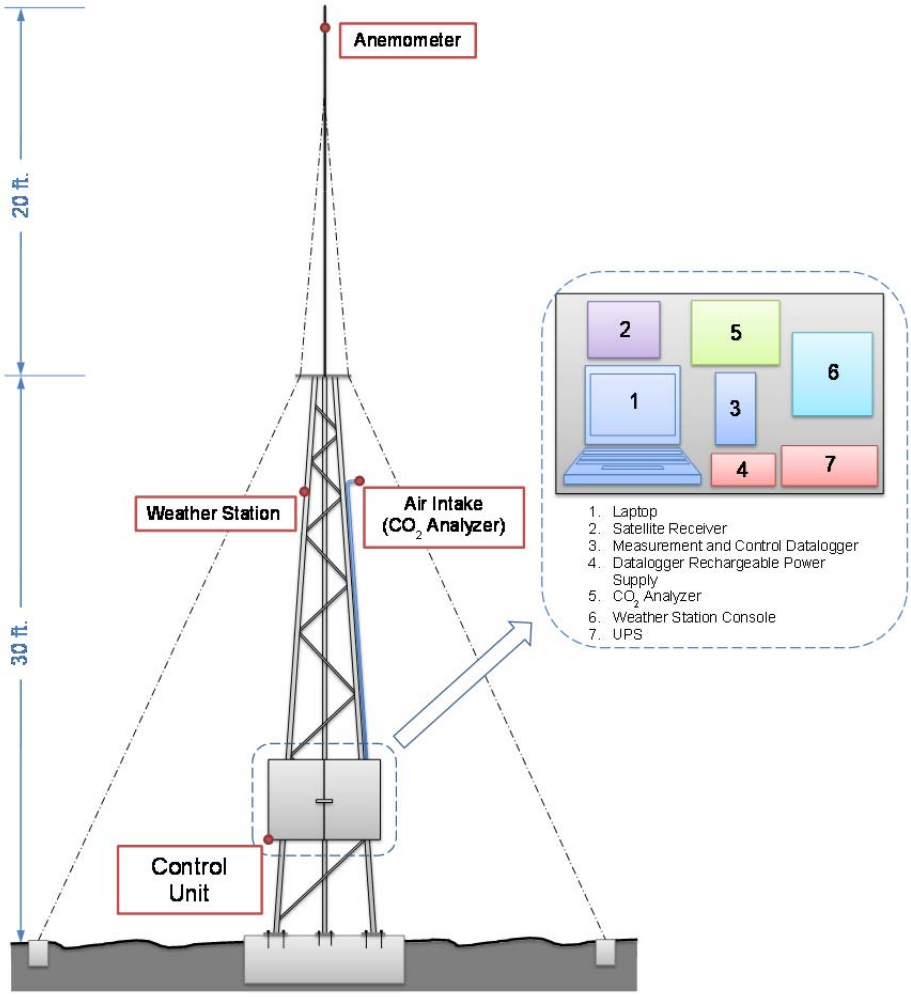

Figure 41: Monitoring tower.

Because of these bandwidth limitations, each data file was compressed before being transmitted via File Transfer Protocol (FTP) to the VCCER FTP Server. The software collection automation software was set up on the remote computer to run at pre-determined intervals. The web interface at the remote computer was capable of triggering a data collection activity. This was useful for updating the data during an activity at the remote site, without requiring a computer user to be in direct contact with the computer.

The web interface was also mirrored on the VCCER website, allowing a user to trigger an action from either web server. The data files were stored in specific directories

that indicated their source sensor. A software program that monitored these folders was developed. When the new file was received at the server, a program would decompress the file and input the data into the main and backup databases. The input routine was designed to filter out repeat data. The VCCER website had an area dedicated to displaying and graphing this data in real-time by a variety of means.

This integrated data management system enabled three desirable outcomes: 1) remote control and remote monitoring of equipment deployed in the field; 2) collection and storage of large data sets; and 3) communication links between the monitoring site and other research locations (Figure 42).

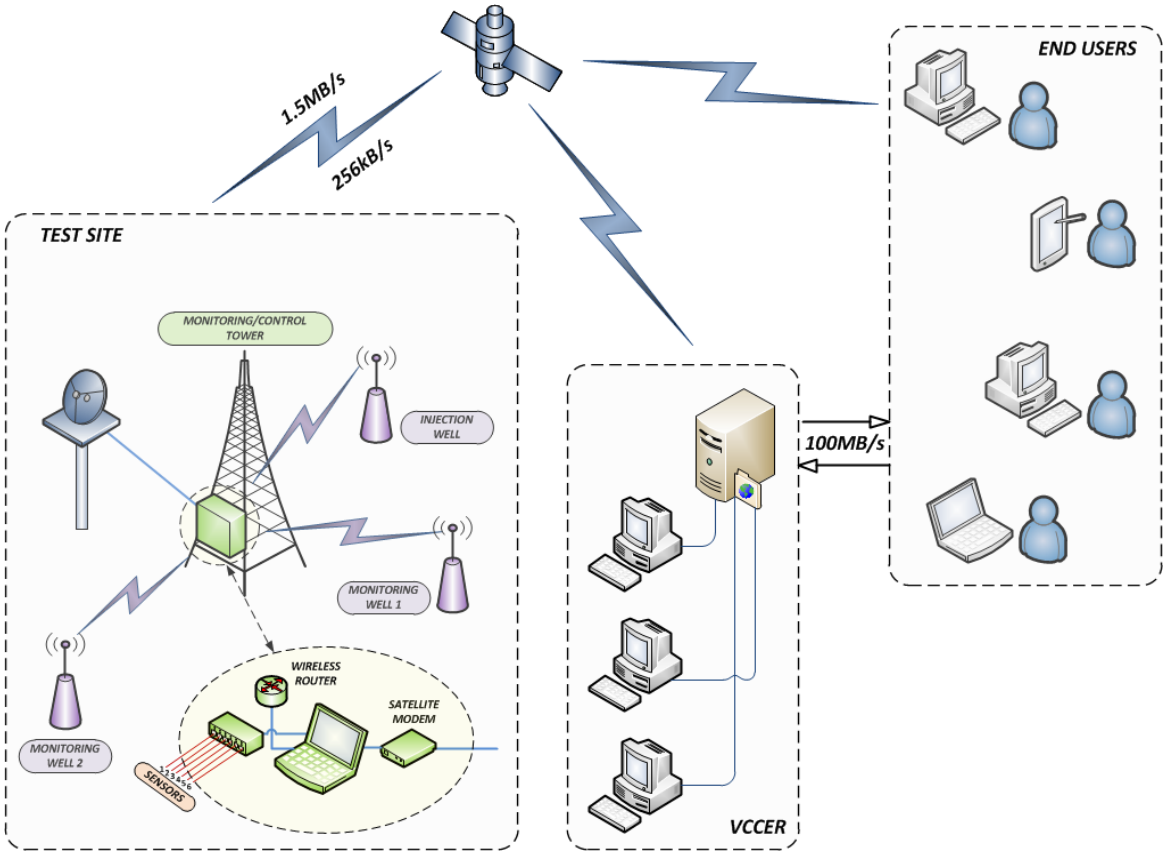

Figure 42: Remote control and data acquisition system diagram.

The optimal selection of sampling sites (monitoring points) and sampling frequencies were major considerations in designing an information-effective monitoring network that could provide sufficient but not redundant information about monitoring variables.

The initial monitoring network at the test site (e.g., grid spacing, network extent around the injection well, and monitoring equipment selection) was designed using results obtained in the initial reservoir modeling study taking into account site-specific characteristics that could affect implementation and efficiency of the monitoring program in the field.

A list of all site-specific characteristics that were considered to have a significant impact on the implementation and long-term operation of the MVA program is given in Table 17.

Table 17: Site-specific characteristics.

SUBSURFACE	**NEAR-SURFACE AND ATMOSPHERIC**
Geological setting at the test site	Monitoring area topography
Depth of the targeted coal seam	Hydrologic conditions Surface
Subsurface hydrological conditions	Land cover
Coalbed methane composition	Soil characteristics
Hydrologic fracture orientation and extent at the injection well	Natural fluctuations in CO_2 concentrations due to biogenic sources
Presence of the CO_2 in storage formations	Weather conditions
Type and size of the injection well	Proximity of settlements

The monitoring network designed for this project incorporated eighteen locations for surface monitoring, two monitoring wells for deep well monitoring, a weather and air quality monitoring tower, and a data acquisition and control system. The network also

included six surface water sampling points (locations of previous underground coal mining) and seven offset CBM wells used for gas and formation water sampling.

The surface monitoring grid for soil gas and soil CO_2 flux monitoring was initially designed as three concentric circles with the center on the injection well, as shown in Figures 43 and 44. Diameters of circles were 300, 600, and 900 feet, giving a total monitoring area of 14.6 acres around the injection well. The circular design was chosen based on the expected CO_2 plume footprint and locations/directions (hot spots) with higher leakage probability.

The size and the shape of the CO_2 plume footprint were defined during the initial reservoir and CO_2 injection modeling study. Based on the modeling results, the CO_2 plume footprint was expected to have a diamond shape and to cover approximately 14 acres around the injection well (Figure 43).

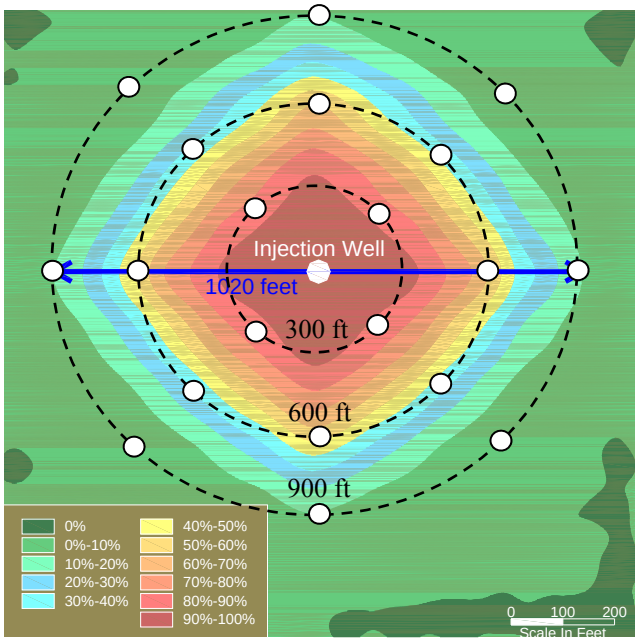

Figure 43: Anticipated CO_2 Plume Footprint and Applied Monitoring Grid.

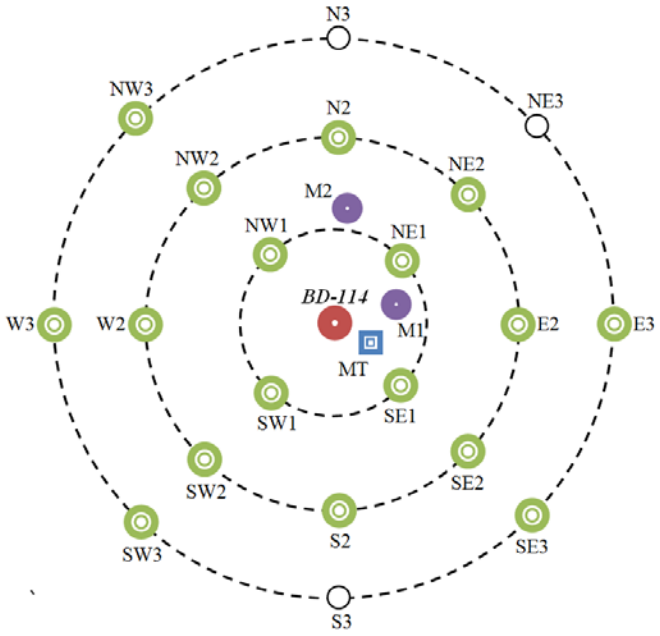

Figure 44: Surface monitoring grid layout showing the injection well (BD114), two monitoring wells (M1 and M2), a monitoring tower (MT), and twenty surface monitoring locations (N, NE, E, S, SW, W, and NW).

All surface monitoring locations were defined with consideration of site-specific conditions and equipment requirements. As shown in Figure 44, the innermost monitoring circle included four monitoring points: SW1, SE1, NW1, and NE1. The second circle included eight monitoring points: N2, S2, W2, E2, SW2, SE2, NW2, and NE2. Excluding points N3, S3, and NE3 due to inaccessible topography, the third circle included only five monitoring points: W3, E3, SW3, SE3, and NW3. Thus, there were 17 total monitoring points.

Soil CO_2 Flux Monitoring:

Pre-operational CO_2 soil flux monitoring started in the spring of 2008 by developing a soil CO_2 flux baseline. It is known that CO_2 concentration in soil can increase and decrease over time, and varies from point to point across the land surface

and with depth. These changes depend on different biogenic and anthropogenic processes. For these reasons, it is important to establish a baseline for all abiotic and biotic parameters in and around the injection site. Baseline data, such as seasonal variations in CO_2 flux, are very important to separate changes related to carbon storage activities from natural variations.

The first soil CO_2 flux measurement was performed on April 25, 2008, at the proposed injection site. Soil CO_2 flux was measured once a week at measurement points SW1, NW1, and NE1, and biweekly at SE1, N2, S2, W2, E2, SW2, SE2, NW2, NE2, N3, W3, E3, SW3, SE3, and NW3. For point measurements of soil CO_2 flux, a survey system was comprised of the LI-8100 analyzer control unit with an 8100-103 survey chamber. To ensure a tight seal of the survey chamber, permanent PVC collars, with a height of 11.25cm (4.5 inches) and a diameter of 20cm (8 inches), were inserted into the soil at each measurement point. The collars were installed one week before the first CO_2 flux measurement. After nine months of pre-operational/baseline measurements, maximum (8.77 $\mu mol/m^2/s$) and minimum (1.85 $\mu mol/m^2/s$) CO_2 flux rates were observed at E2 and NE1 measurement points, respectively.

As shown in Figure 45, the highest average CO_2 flux rates (4.69 $\mu mol/m^2/s$) in the pre-operational phase were detected at NW1 during the second quarter of 2008 (April-June 2008). On the other hand, minimum average CO_2 flux rates (0.47 $\mu mol/m^2/s$) were measured at NW2 during the fourth quarter of 2008 (October-December 2008).

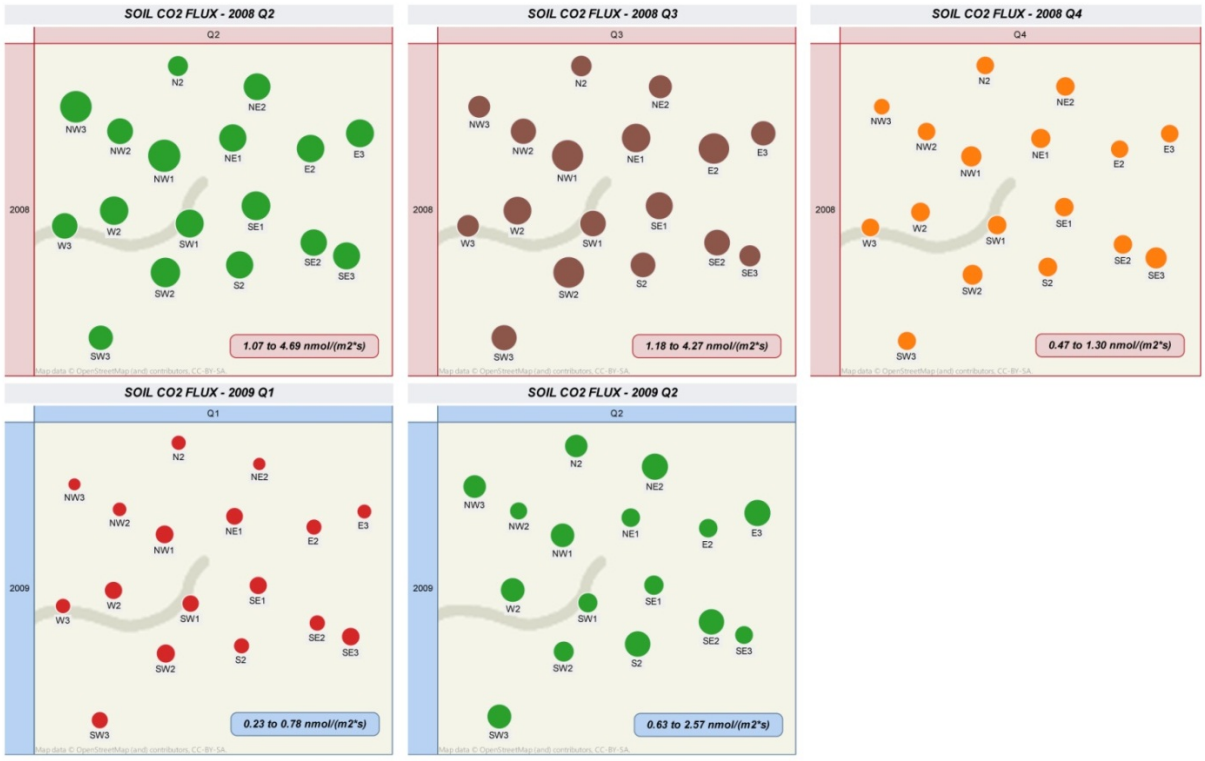

Figure 45: Average soil CO_2 flux rates per quarter.

During the operational/injection phase of this project, maximum (0.51 µmol/m^2/s) and minimum (0.1 µmol/m^2/s) CO_2 flux rates were observed at SW3 and NE2, respectively. The highest average CO_2 flux rates (0.45 µmol/m^2/s) in this phase (January-February 2009) were detected at SW3. Addtionally, minimum average CO_2 flux rates (0.15 µmol/m^2/s) were measured at NW3.

In the post-injection phase the highest average CO_2 flux rates (2.47 µmol/m^2/s) were detected at E3 during the second quarter of 2009. The lowest average CO_2 flux rates (0.23 µmol/m^2/s) were detected at NW3 during the first quarter of 2009. The maximum CO_2 flux rate (2.65 µmol/m^2/s) was observed at E3 on April 27, 2009, and the minimum (0.17 µmol/m^2/s) at N2 on February 23, 2009.

As shown in Figure 46, the direction and change in magnitude of CO_2 fluxes correlates positively with change in soil and ambient air temperature. Still, the relationship between CO_2 flux rate and air temperature varied between measurement points. These variations suggest that CO_2 flux rates depend on properties particular to specific areas within the larger site, such as soil composition, root respiration, or microbial activity.

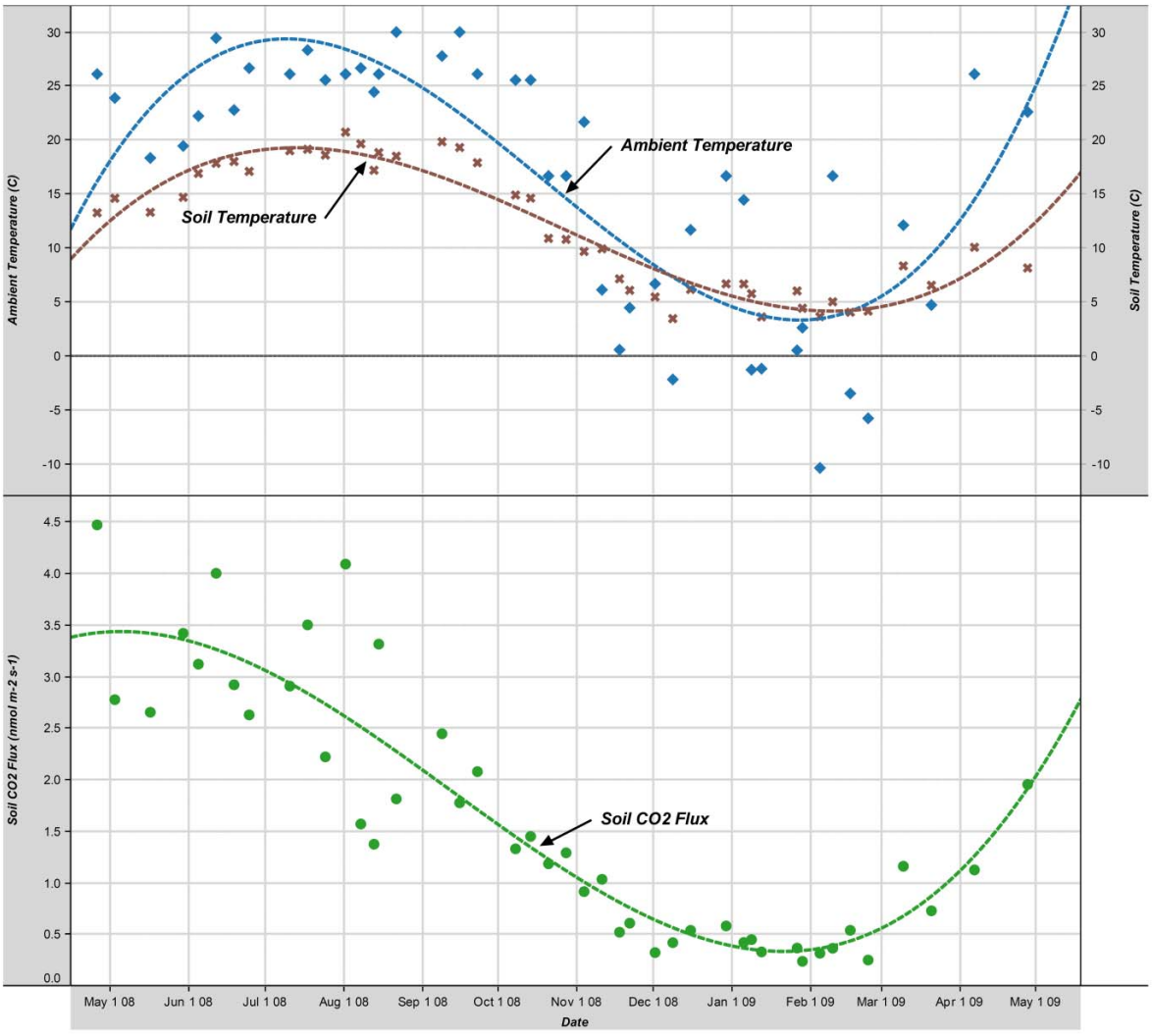

Figure 46: Relationship between average CO_2 flux rates and soil and ambient air temperatures.

Ambient CO_2 Concentration:

Carbon dioxide leakage from a storage reservoir may create an atmospheric surface layer with a concentration high enough to be distinguished from background CO_2 levels. In order to detect possible leakage at the test site, near-surface CO_2 concentration measurements were conducted simultaneously with soil CO_2 flux measurements. A portable infrared gas analyzer (IRGA) was placed 0.5m above the surface and CO_2 concentration was measured for 30 minutes at each measurement location. The magnitude of near-surface atmospheric CO_2 concentrations is shown in Figure 47. An average CO_2 concentration at the test site ranged from 372 ppm in the second quarter of 2008 at NW3, to 462 ppm in the first quarter of 2009 at W3.

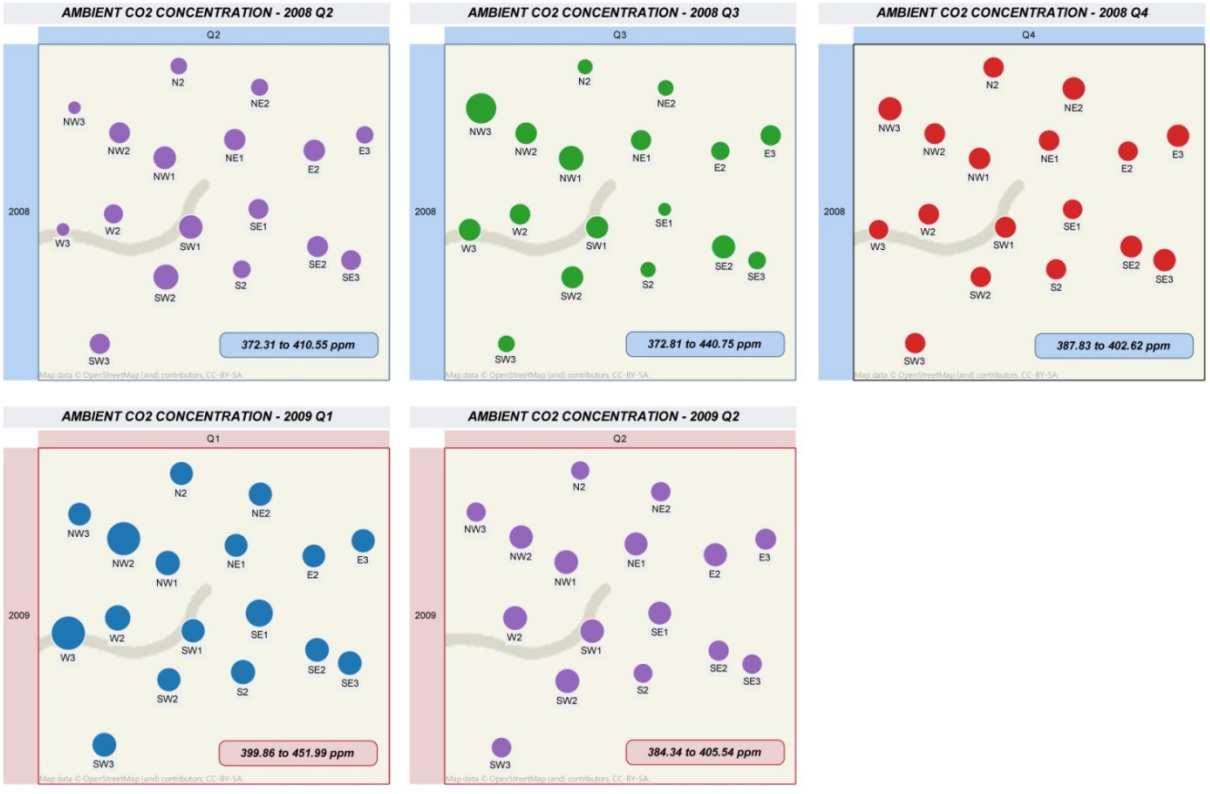

Figure 47: Average near-surface CO_2 concentration measured 0.5m above surface using portable infrared gas analyzer.

Maximum CO_2 concentration (647 ppm) was recorded at NW2 on January 31, 2009, during the operational/injection phase. Taking into account a variety of factors such as the CO_2 injection process, wind direction and speed, and density-driven atmospheric dispersion, the high concentration at NW2 is attributed to injection phase activities at the test site (e.g., CO_2 transport and exchange, and injection losses).

Secondly, an IRGA was mounted at the injection site, inside the control unit, in order to collect ambient CO_2 level data around the injection well during the operational/injection phase of this project. As shown in Figure 48, Detail 1, a maximum CO_2 concentration of 6,331 ppm was detected on January 31, 2009, at 11:11 AM. The onsite IRGA also recorded 20 similar events with CO_2 concentrations ranging from 600 ppm to 5,269 ppm.

These extremely high CO_2 concentrations were a direct result of CO_2 manipulation at the injection site; more specifically, all events with high concentration were recorded when tubing used for pumping CO_2 from delivery trucks to the onsite CO_2 tank was disconnected and purged with CO_2.

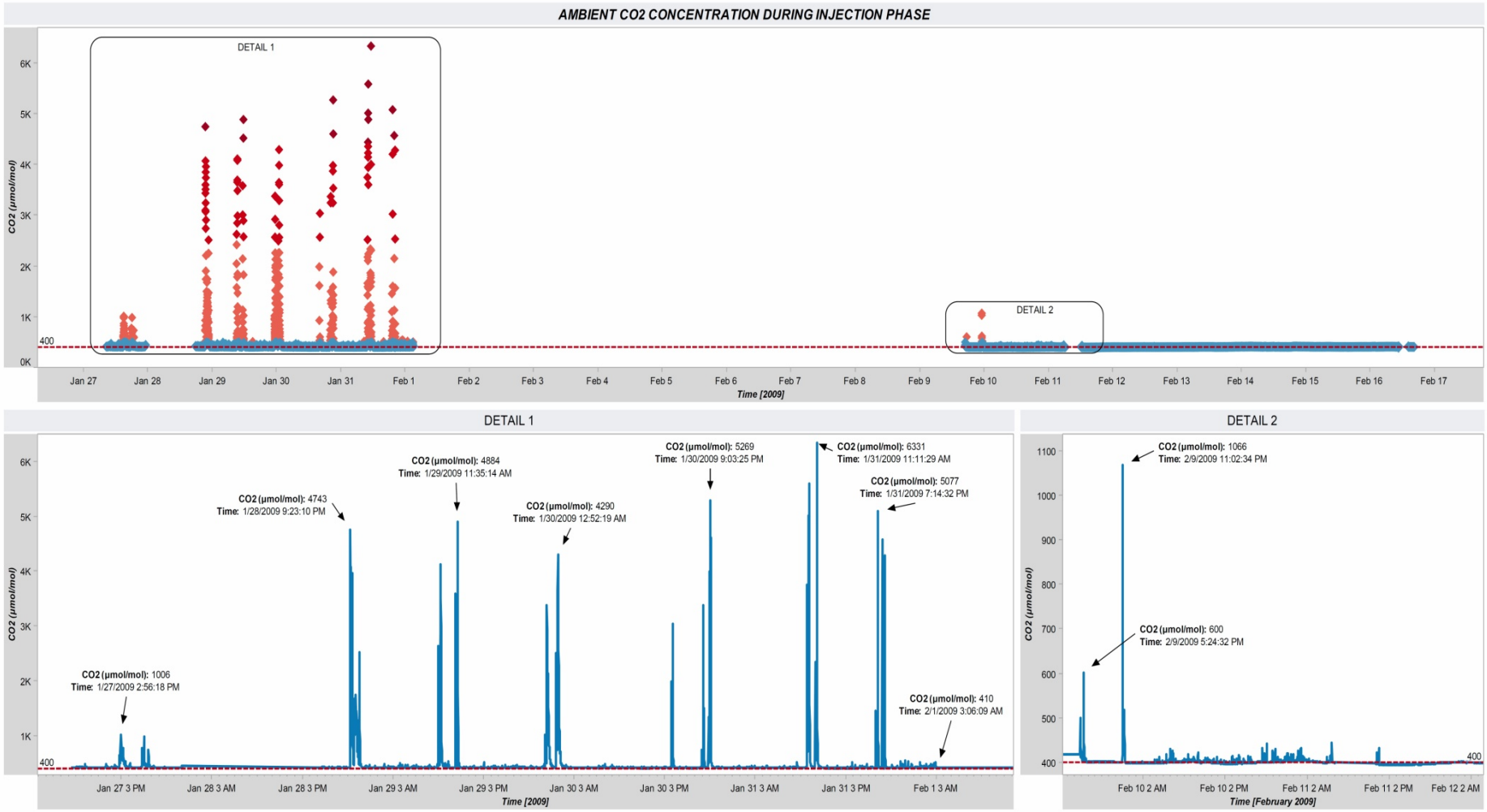

Figure 48 Ambient CO_2 concentration during operational/injection phase at the injection site.

Water Quality:

It is widely acknowledged that leakage through faults and fractures, as well as active and preexisting wells, are the most likely pathways for CO_2 release from a storage formation. It is expected that slow and continuous leakage from the reservoir can gradually alter surrounding aquifers. Release of CO_2 or brine into underground sources of drinking water (USDWs) could be accompanied by measurable alteration in pH, major ions, and mobilization of hazardous inorganics.

In order to detect and measure potential changes in water quality, caused by CO_2 injection, a pre-injection baseline was established for eight CBM wells, seven offset producing and one injection well. In addition to formation water sampling, this water quality monitoring program included six surface water locations for sampling both surface and ground water discharge from nearby abandoned mines.

As shown in Figure 49, pH values for all seven offset CBM wells dropped as injection process commenced. While these pH levels are not alarming and cannot be directly correlated with CO_2 leakage, this rate of change is not characteristic for the natural systems. Also, it was observed that the rate of change decreases as the distance between sampling location and injection well increases.

Furthermore, post-injection sampling results showed an increase in iron (Fe), manganese (Mn), and free CO_2. As shown in Figure 50, the Fe, Mn, and free CO_2 concentrations at the injection well were two to four times higher than average concentrations measured at seven offset wells.

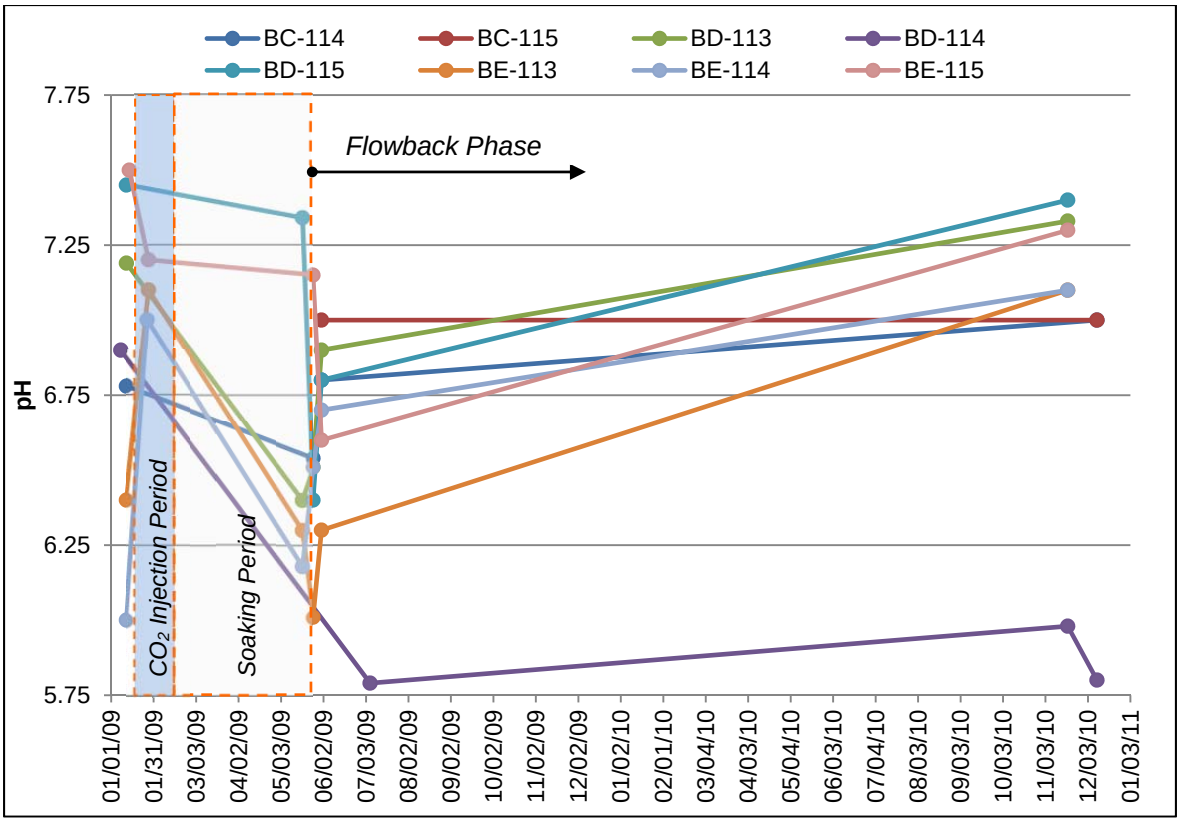

Figure 49: pH values at BD-114 and surrounding CBM wells.

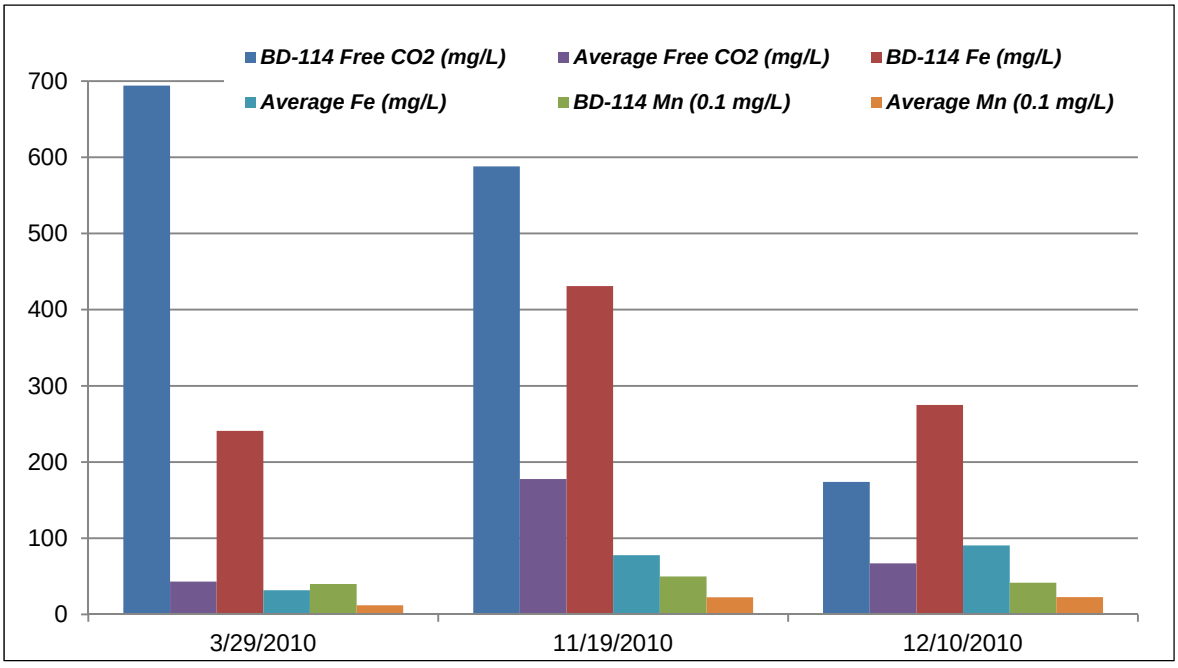

Figure 50: BD-114 water results vs. the average values at surrounding well.

Tracer Monitoring Results:

In order to help detection of potential CO_2 leakage pathways and map the fracture network, the PTMCH tracer, perfluoro-trimethyl-cylclohexane, was injected at the injection well. Tracer samples were taken periodically from all seven offset production wells. Tracer map presented in Figure 51 shows the minimum, maximum, and average tracer concentration at all sampling locations.

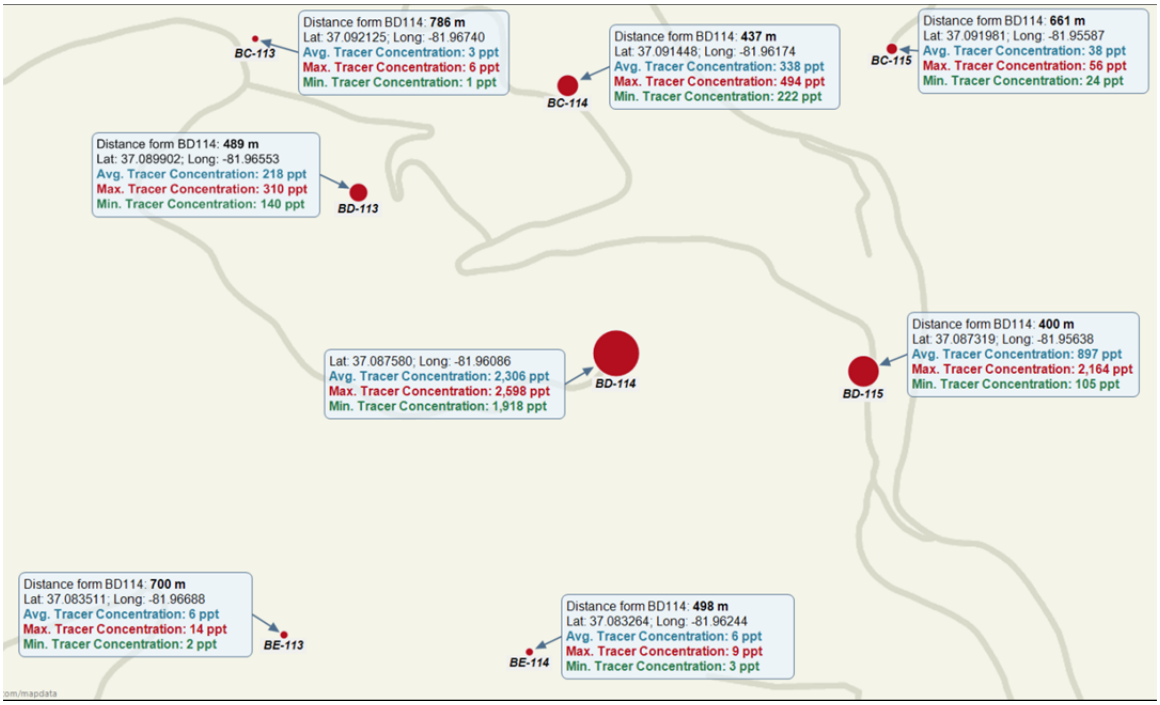

Figure 51: Tracer map.

In general, detection of tracer molecules in gas samples from all seven offset wells and three wells in the next ring, 3,700 feet from the injection well, indicate migration of the tracer and CO_2 plume in all directions from the injection well. These results are consistent with the pressure observations, and present another proof that targeted coal seams at the injection site are interconnected via extensive fracture network.

Chapter 4.
ECONOMIC ASSESSMENT

This segment of the research uses a real options analysis (ROA) as a method to evaluate the impact of major sources of uncertainty on the total cost of developing and operating a CCS project in a regulatory environment that expects implementation of carbon taxes, but with uncertainty about the timing of this penalty. ROA valuation allowed creation of a quantitative framework that explicitly accounts for uncertainties and also represents complex dynamics of CCS project.

Over the last few decades, it was suggested that energy companies, in evaluation of their decisions about their asset dynamics, should take into account the multi-dimensional structure and the time evolution of the uncertainty in the determinants of asset cash-flows; and how asset structure, including the flexibility that asset managers have to change that structure, influences the effect of underlying uncertainties on asset value [59].

Traditional way to evaluate such decision was to determine the net NPV of the investment by computing the sum of the anticipated costs and revenues, and discounting them to the present year. At the end of the process, decision maker would decide to invest only if the NPV value is positive [60]. However, when not faced with the choice between immediate investment and forfeiture, computing the NPV only in the current period may not result in the best choice [61]. The NPV calculation may not provide an optimal result,

because calculating the NPV for the present ignores any possible value of the option to delay investment. On the other hand, a ROA is a valuation method that is particularly useful in defining an optimal timing for investment decisions under uncertainty.

4.1 GOVERNING EQUATIONS

The following chapter is focused on development of real options modeling methodology that will allow analysis of the investment decision to sequester CO_2 in deep unmineable coal seams, under certain market and legislative conditions. Under assumption that stored CO_2 will not be released and used as a commercial product over the life time of the storage system, this study significantly differs from other approaches used for modeling storage facilities (e.g., natural gas storage).

The equations derived in this chapter are unique since they incorporate both technical and economic parameters relevant to CO_2 sequestration in unmineable coal seams.

The first step in the analysis is assessment of available storage capacity. The capacity of any storage facility can be described as:

$$dG = - v_f \cdot G_{max} dt \qquad \textbf{(Equation 11)}$$

where:

- G – Mass estimate of available storage capacity;
- v_f – Velocity of filling; and
- G_{max} – Initial or maximum storage capacity.

In the case of CO_2 storage in coal seams, G_{max} is a function of regional extent of the targeted coals, coal thickness, adsorption capacity, storage efficiency, and CO_2 density, as described by Equation 1 in Chapter 3:

$$G_{CO_2max} = A \cdot h_g \cdot C_{s,max} \cdot \rho_{CO_2std} \cdot E_{coal}$$

Based on assumption that the CO_2 properties are constant and that pressure profile is uniform through the storage formation, velocity of filling can be defined as [105, 106]:

$$v_f = \frac{(P_i - P_{inf}) \cdot 4 \cdot k \cdot h_g}{[ln(t_d) + 0.80907] \cdot \mu_c} \quad \textbf{(Equation 12)}$$

where:

- P_i – Pressure at the injector wellbore;
- P_{inf} – Far-field reservoir pressure;
- k – Average reservoir permeability;
- h_g – Coal thickness;
- μ_c – Viscosity of the CO_2; and
- t_d Dimensionless time.

Dimensionless time presented in Equation 12 is given by [106]:

$$t_d = \frac{k \cdot t}{\varphi \cdot \mu_c \cdot c \cdot r_i^2} \quad \textbf{(Equation 13)}$$

where:

- t – Time;
- φ – Porosity;
- c – CO_2 compressibility; and
- r_i^2 Injector well bore radius.

Combining of Equations 1, 11, and 12 yields expression that can be used to predict the change in the reservoir holding capacity over the lifetime of the CO_2 sequestration project:

$$dG_{CO_2} = - \frac{4 \cdot h_g^2 \cdot (P_i - P_{inf}) \cdot A \cdot C_{s,max} \cdot \rho_{CO_2 std} \cdot E_{coal}}{[ln(t_d) + 0.80907] \cdot \mu_c} dt \qquad \textbf{(Equation 14)}$$

Under assumption that after implementation of climate change bills in the U.S. a person or company that invests in and owns a CO_2 storage facility will receive income gained by CO_2 sequestration. In the case of coal and CO_2 sequestration in the CBM fields, storage operations will receive additional earnings through CO_2-ECBM production. Furthermore, owners of the CO_2 storage and ECBM operations have a significant potential for future discounted earnings, coming from holding a storage capacity and utilizing ECBM potential. Following equation represents both types of earnings, expected from CO_2 operations, in continuous time:

$$E_{CO_2} dt = v_f \cdot G_{co_2} \cdot \pi_{CO_2} dt + d(G_{CO_2} \cdot V_{CO_2}) \qquad \textbf{(Equation 15)}$$

where:

E_{CO_2} – Total earnings from CO_2 sequestration in coal seams;

π_{CO_2} – Profit (after taxes) from storing one ton of CO_2;

V_{CO_2} – Market value of one unit of the stored CO_2;

$v_f \cdot G_{CO_2} \cdot \pi_{CO_2}$ – CO_2 sequestration earnings; and

$G_{CO_2} \cdot V_{CO_2}$ – Future discounted earnings.

Final equation that describes expected earnings from CO_2 operations can be written, with respect to Equation 15, as:

$$E_{CO_2}dt = v_f \cdot G_{co_2} \cdot \pi_{CO_2}dt + G_{CO_2}dV_{CO_2} - V_{CO_2} \cdot v_f \cdot G_{CO_2}dt \qquad \textbf{(Equation 16)}$$

Difference between CBM production before and amount of CBM produced during CO_2 injection can be calculated based on the displacement potential (d_p), which is derived from CO_2/CH_4 exchange ratio. Based on average CO_2/CH_4 exchange ratio of 2:1, it is expected that one tone of injected CO_2 will displace 0.72 tons of CH_4. Displacement potential is used in Equation 13 to correlate two processes (CO_2 sequestration and ECBM production) and to allow calculation of potential earnings for CO_2-ECBM production*. Similarly to Equation 15, next expression can be used to estimate earnings related to CO_2-ECBM production:

$$E_{ECBM}dt = d_p \cdot \left[v_f \cdot G_{co_2} \cdot \pi_{CH_4}dt + d\left(G_{CO_2} \cdot V_{CH_4}\right)\right] \qquad \textbf{(Equation 17)}$$

where:

E_{ECBM} – Total earnings from CO_2 enhanced CBM production;

d_p – Displacement potential;

π_{CH_4} – Profit (after taxes) from CO_2-CBM production;

V_{CH_4} – Market value of one ton CH_4 unit;

$d_p \cdot \left(v_f \cdot G_{CH_4} \cdot \pi_{CO_2}\right)$ – Earnings from CO_2-ECBM production; and

$d_p \cdot \left(G_{CO_2} \cdot V_{CH_4}\right)$ – Future discounted earnings from CO_2-ECBM production.

Displacement potential presented in Equation 17 is given by:

$$\mathbf{d_p = e_r \cdot \frac{M_{CH_4}}{M_{CO_2}} \cdot m_{CO_2}} \qquad \textbf{(Equation 18)}$$

where:

e_r – CO_2/CH_4 exchange ratio;

* Fraction of CBM production induced by CO_2 injection.

M_{CH_4} – Molecular weight of CH_4;

M_{CO_2} – Molecular weight of CO_2; and

m_{CO_2} – Mass of injected CO_2.

Similarly to Equation 16, final expression that describes expected earnings from potential CO_2-ECBM production is:

$$E_{ECBM}dt = d_p \cdot \left[v_f \cdot G_{co_2} \cdot \pi_{CH_4} dt + G_{CO_2} dV_{CH_4} - V_{CH_4} \cdot v_f \cdot G_{CO_2} dt\right] \qquad \textbf{(Equation 19)}$$

With respect to Equations 16 and 19, the total earnings from CO_2 sequestration in coal seams and related CO_2-ECBM production are:

$$E_{total} = E_{CO_2} + E_{ECBM} \qquad \textbf{(Equation 20)}$$

The rate of return for CO_2 storage and CO_2-ECBM production can be calculated as ratio of earnings and potential turnovers (Equations 21 and 22) . The possible turnover can be calculated by multiplying storage capacity and ECBM potential with corresponding market prices (V). After adding earnings-related uncertainties, a value process for the stored CO_2 can be formulated as arithmetic Brownian motion (ABM) [60, 61]:

$$\frac{E_{CO_2} d}{G_{CO_2} \cdot V_{CO_2}} = \mu_{V_{CO_2}} dt + \sigma_{V_{CO_2}} dz \qquad \textbf{(Equation 21)}$$

where:

$\mu_{V_{CO_2}}$ – Drift for V_{CO2};

$\sigma_{V_{CO_2}}$ – Volatility of the CO_2 price process; and

z – Standard Wiener process.

For the CO_2-ECBM production this process can be expressed as:

$$\frac{E_{ECBM}d}{d_p \cdot G_{CO_2} \cdot V_{CH_4}} = \mu_{V_{CH_4}} dt + \sigma_{V_{CH_4}} dz \qquad \textbf{(Equation 22)}$$

where:

$\mu_{V_{CH_4}}$ – Drift for V_{CH4};

$\sigma_{V_{CH_4}}$ – Volatility of the CH_4 price process; and

The drift terms in Equations 21 and 22 are time variables and they depend on evolution of market values of stored CO_2 and produced CBM, respectively. Drifts can take positive or negative values and they reflect the expected development in prices as well as long- and short-term trends in price evolution [60].

Under assumption that potential investor will be faced with uncertain and asymmetric profit and loss restrictions due to GHG regulation; following equation, which defines the market value of stored CO_2, incorporates investor's option to delay investment decision [60, 107, 108]:

$$dV_{CO_2} = \left(\mu_{V_{CO_2}} - \delta_{CO_2}\right) \cdot V_{CO_2} dt + \sigma_{V_{CO_2}} \cdot V_{CO_2} dz \qquad \textbf{(Equation 23)}$$

where:

$$\delta_{CO_2} = \frac{E_{CO_2}d}{d_p \cdot G_{CO_2} \cdot V_{CH_4}} = \mu_{V_{CO_2}} dt + \sigma_{V_{CO_2}} dz \qquad \textbf{(Equation 24)}$$

Term δ represents an opportunity cost of delaying investments or "rate of foregone earnings". In the context of the storage evaluation, and assessment of CO_2 sequestration, this term is known as convenience yield or expected dividend of the storage project [60, 109]. In the case of CO_2 sequestration, the convenience yield is defined as the value that can be gained from holding potential CO_2 storage capacity. This

value is negatively correlated with inventories (i.e., the higher the level of stored goods the lower the value that can be gained from storing an additional unit). Consequently, the value of the marginal convenience yield declines as the cumulative inventory increases Finally, in order to determine the market value of available sequestration capacity in the continuous time, it is assumed that the value of stored CO_2 follows similar dynamics as the market price of the carbon credits. The dynamics of the market price for carbon credits, or emission certificates, can be expressed as:

$$dp_{CO_2} = \left(\mu_{p_{CO_2}} - \delta_{CO_2}\right) \cdot pdt + \sigma_{p_{CO_2}} \cdot p_{CO_2} dz \qquad \textbf{(Equation 25)}$$

4.2 ROA MODEL

Model presented in this section is based on previously published data and assumes that the opportunity costs of delaying CCS investment can be described as time-dependent linear functions. This implies that the market value of stored CO_2 and related profit after taxes are linear functions [110, 111].

All modeling parameters used in this study are listed in Tables 19 and 20.

Table 18: Emission certificate dynamics from the literature [60, 112-114].

Market	Price Mean		Price Volatility	
	Maximum	Minimum	Maximum	Minimum
Nordpool, Powernext	-0.0032	-0.0039	0.8105	0.7379
EEX(EUA)	0.069		0.4683	
EEX(EUA)	0.1298	-0.1528	0.0319	

Table 19: Modeling parameters and variation limits [115-120]**.**

Parameter	Description	Base Case	Min.	Max.	Variation steps
D	Total Cost	$53	$27	$108	$27
r_f	Risk Free Rate	5%	3%	10%	1%
δ	Fixed convenience yield	10%	1%	10%	1%
σ_δ	Convenience yield volatility	1%	1%	20%	5%

Goal of this linear model is to maximize the value of the investment opportunity. This was achieved by using the contingent claims analysis procedure and setting up a risk less portfolio [61]. The value of the portfolio can be expressed as:

$$\Phi = F - F'(p)p \qquad \textbf{(Equation 26)}$$

where:

F – Value of the investment opportunity; and

p – Emission certificate price.

The total return of the portfolio can be derived from the following partial differential equation:

$$\frac{1}{2} \cdot \sigma_p^2 \cdot p^2 \cdot \frac{\partial^2 \cdot F(p,t)}{\partial_p^2} + (r_f - \delta) \cdot p \cdot \frac{\partial F(p,t)}{\partial_p} - r_f \cdot F(p,t) + \frac{\partial F(p,t)}{\partial_t} = 0 \qquad \textbf{(Equation 27)}$$

It is expected that the holder the option will benefit only in case that project has positive NPV. NPV in this case can be calculated as:

$$NPV(p,t^*) = p \sum_{t^*}^{n} e^{-\delta \cdot t} - D \sum_{t^*}^{n} e^{-r \cdot t^*} - I_0 \qquad \textbf{(Equation 28)}$$

where:

D – Discounted costs for storing 1 ton of CO_2;

I_0 – The investment costs per unit (t=0); and

t^* Final date.

With respect to this assumption, a partial equation is solved numerically, using following boundary conditions:

$$F(0,t) = 0 \qquad \textbf{(Equation 29)}$$

$$F(p^*,t) = p^* - D - I_0 \qquad \textbf{(Equation 30)}$$

$$\frac{\partial F(p_t,t)}{\partial p^*} = 1 \qquad \textbf{(Equation 31)}$$

4.2.1 RESULTS

The numerical results for linear convenience yield model are plotted in Figures 52-56. It is important to note that all scenarios with negative NPV are excluded from this section since negative values automatically imply rejection of the investment. Figures 52 and 53 illustrate the response of the option value and the NPV on change in the risk free rate. It is observed that variations in the risk free rate have negligible effect on both NPV and option value.

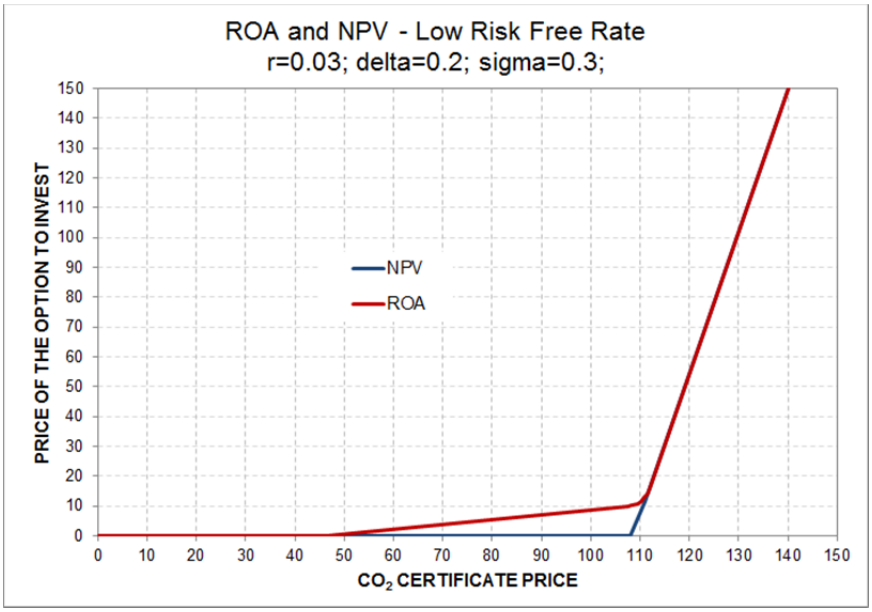

Figure 52: Impact of low risk free rate on NPV and option value.

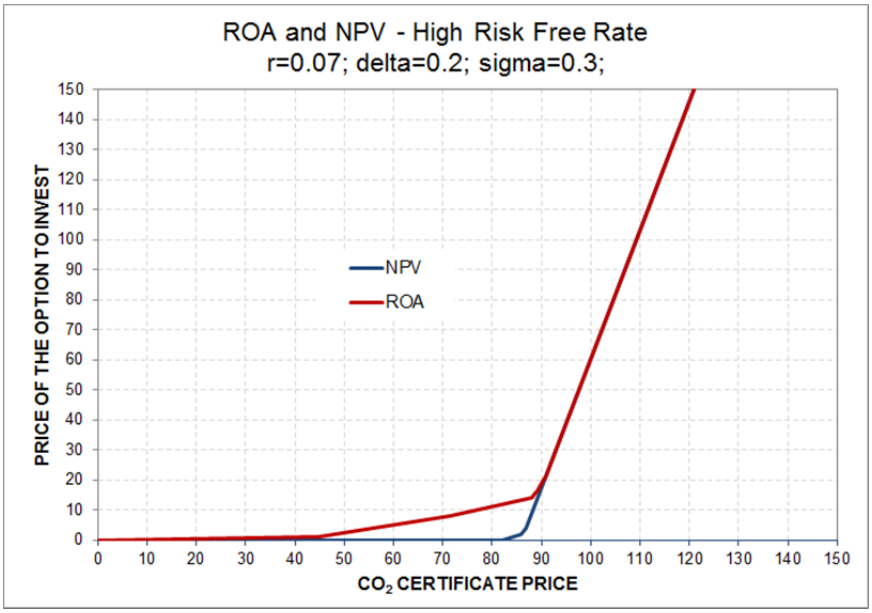

Figure 53: Impact of high risk free rate on NPV and option value.

The impact of the CO_2 price volatility on the value of the option is shown in Figures 54 and 55. Low volatility values directly imply lower NPV and option values. As expected, with the increase of CO_2 price volatility is followed by the gradual increase in NPV and option values. This can be explained by the fact that risk and uncertainty reduction inevitably lead to decrease in option value (high risk/uncertainty – high option value) [61].

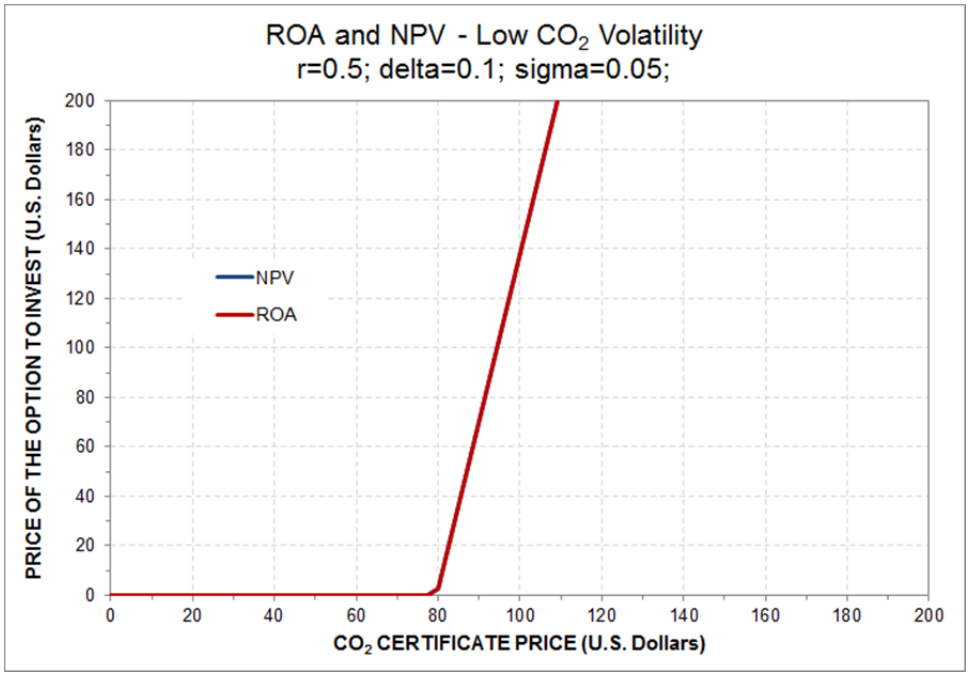

Figure 54: Impact of low CO_2 price volatility on NPV and option value.

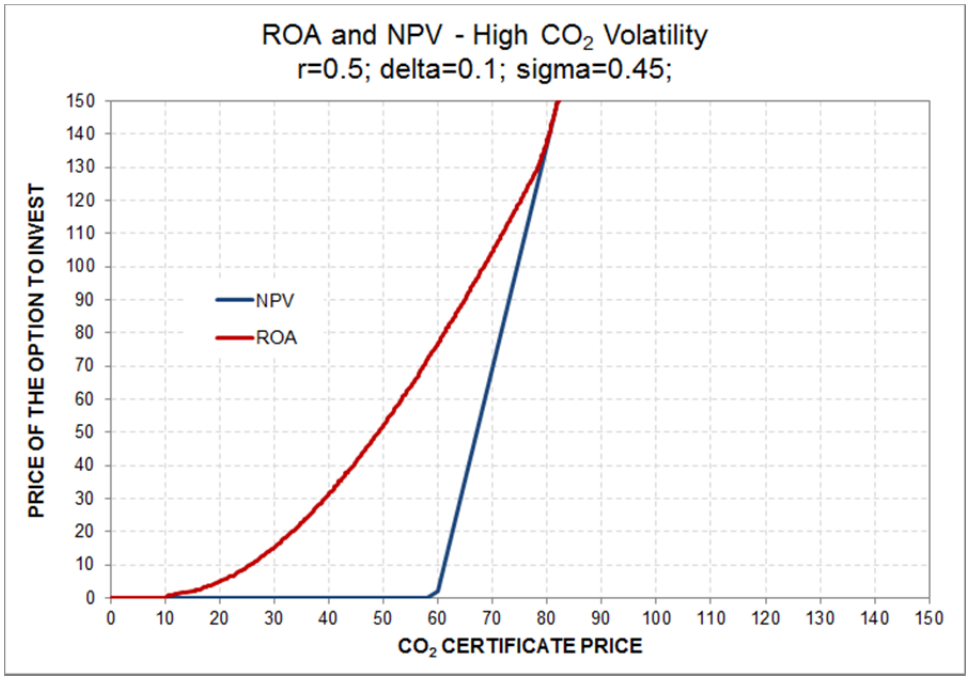

Figure 55: Impact of high CO_2 price volatility on NPV and option value.

The impact of low and high convenience yields on NPV and option value is illustrated in Figures 56 and 57, respectively. It is obvious that NPV and option value decrease as convenience yield increases, and vice versa. This reverse process adds additional level of financial security to the project by providing additional assets that can be used to cover future liabilities (e.g., dividends, royalties, etc.).

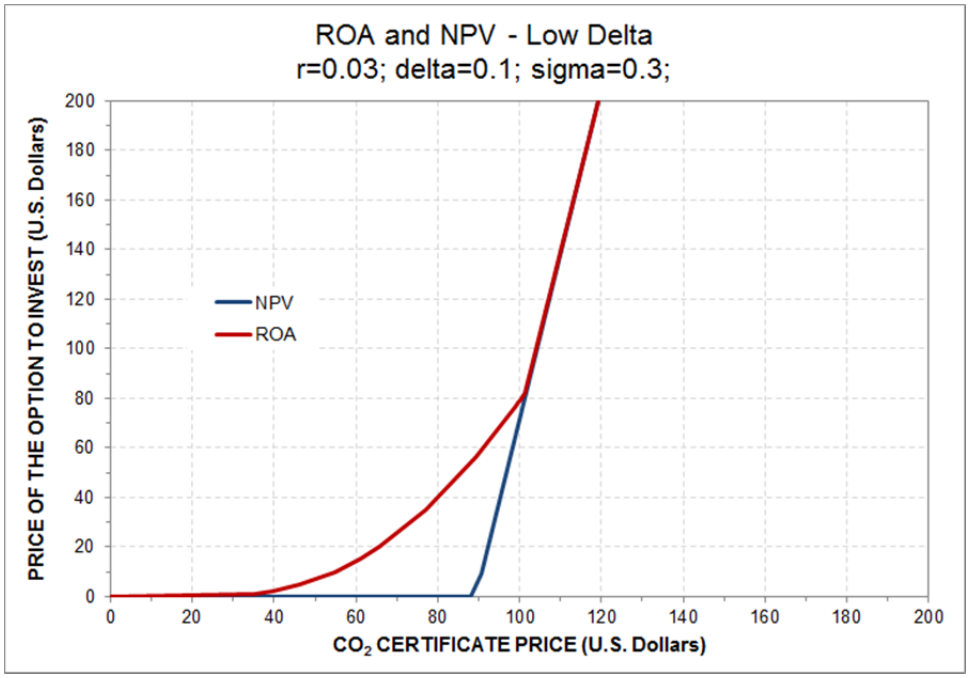

Figure 56: Impact of low convenience yield on NPV and option value.

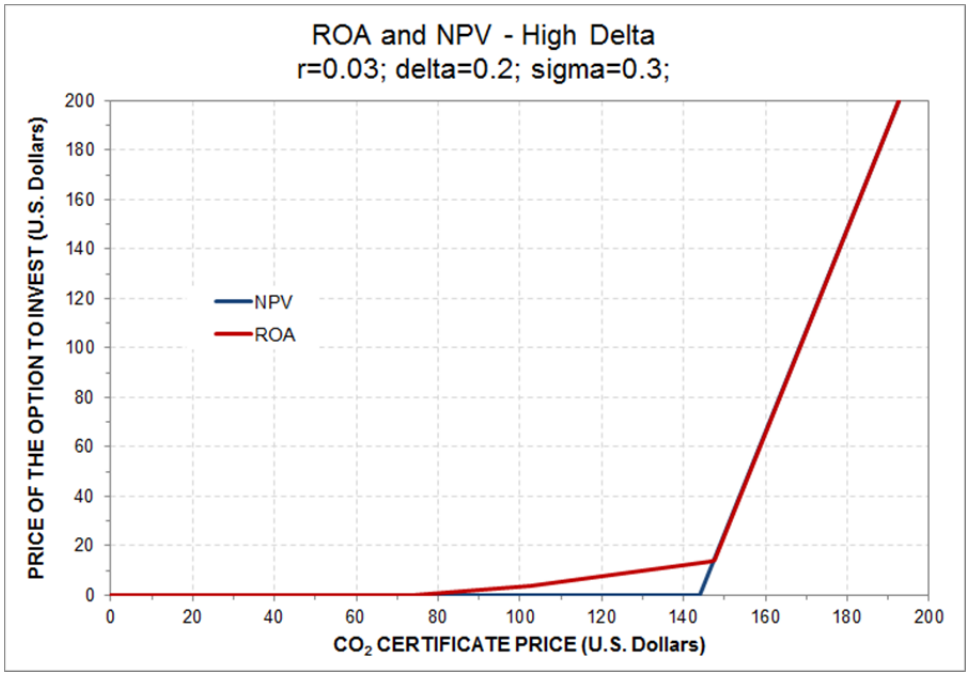

Figure 57: Impact of high convenience yield on NPV and option value.

Based on results from this numerical study, it was found that, under current policy framework, investment risk for CCS technology is very high. Of all uncertainties, the climate policy and carbon price have the most significant impact on CCS investment. Even with additional value added by ECBM recovery, commercial-scale implementation of CCS would yield losses. On the other hand, decreasing the costs of CO_2 capture, which accounts for more than 90% of total CCS costs, would probably lead to a profitability of CCS investment.

Chapter 5.
DECISION MAKING FRAMEWORK

Because of complex and multiple interactions between different components in the CCS chain, there is a need for a systematic decision support framework that can help project designers, policymakers, and other parties involved in CCS process to evaluate all available data and make knowledgeable decisions. With this in mind, this chapter focuses on the creation of a cohesive decision making framework that integrates technical and economic aspects of geologic CO_2 sequestration into decision making process. The long-term goal of this research is to create a comprehensive system of indicators that can provide quantitative and qualitative information about various performance characteristics of each component in the chain.

Although this decision making framework does not provide a decision rule or a "right" solution to a set of complex problems expected in commercial operations, it can help provide a view of the different perspectives, facilitating an examination of the necessary trade-offs and leading to responsible decisions.

By aligning research findings and knowledge gained through pilot-scale studies with short- and long-term business objectives, this framework will provide user with capability to address complex problems in a more systematic way and to analyze the most efficient way to utilize available resources.

5.1 FRAMEWORK STRUCTURE

The decision making process described in this section takes into account four general decision categories: initial actions; assessment procedures; selection of technical concepts; and basic decision options and initial project implementation. Figure 58 illustrates general structure and examples of decision making elements that can be used for the development of the decision making process for geological CO_2 storage. Each step in Figure 58 is characterized by a number of possible decision elements that should be taken into account when designing CO_2 storage. It is important to note that decision making process may yield different conclusions by incorporating some of the elements, but not including other. For that reason, the framework should be re-assessed regularly as new technical data or regulatory information become available. This allows revision and "calibration" of previously made conclusions and decisions.

Following sections will show structure of the decision making methodology and describe assessment procedures for geological CO_2 sequestration in unmineable coal seams. This particular framework was developed based on a general methodology shown in Figure 58, but it has slightly different structure due to the specifics related to sequestration in unmineable coal seams.

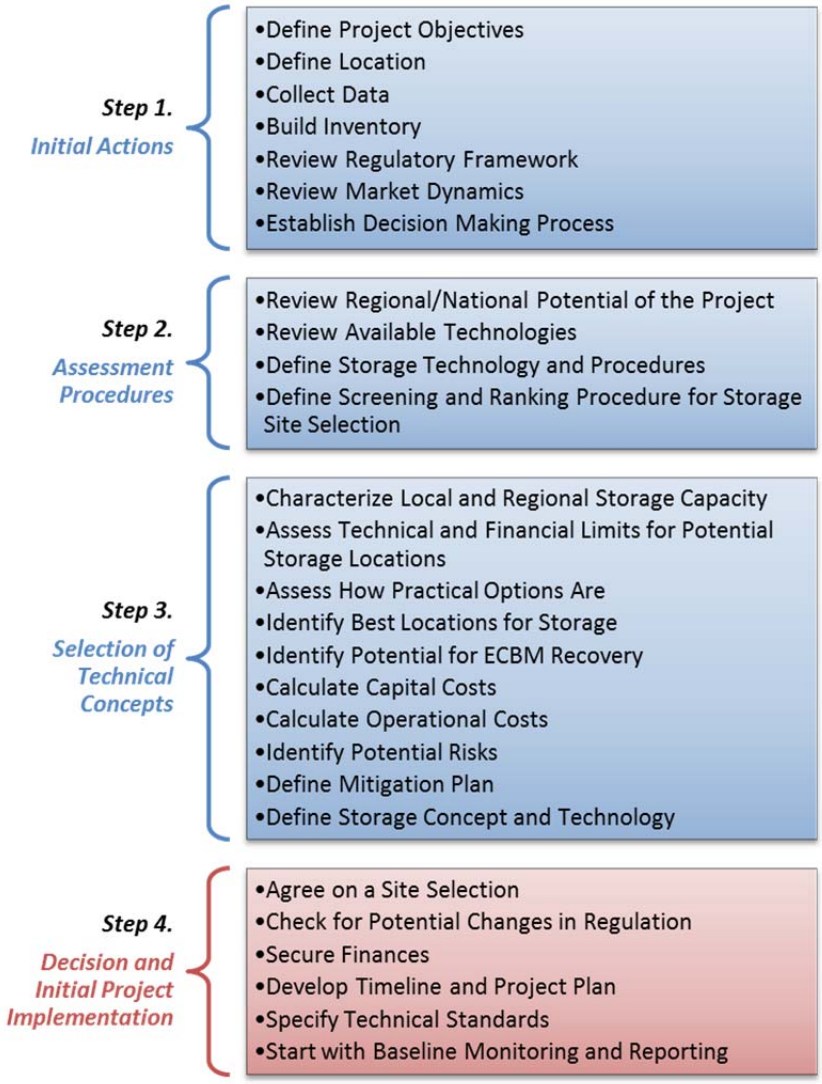

Figure 58: General structure of the decision making framework.

5.1.1 DECISION MAKING FRAMEWORK FOR GEOLOGICAL CO_2 SEQUESTRATION

The structure of the newly developed framework is illustrated in Figure 59. As it can be seen, framework consists of four distinct stages that allow incorporation of different qualitative and quantitative information into decision making process. Each stage allows multiple transformations of data so that outputs from one algorithm can be used as inputs to other algorithms.

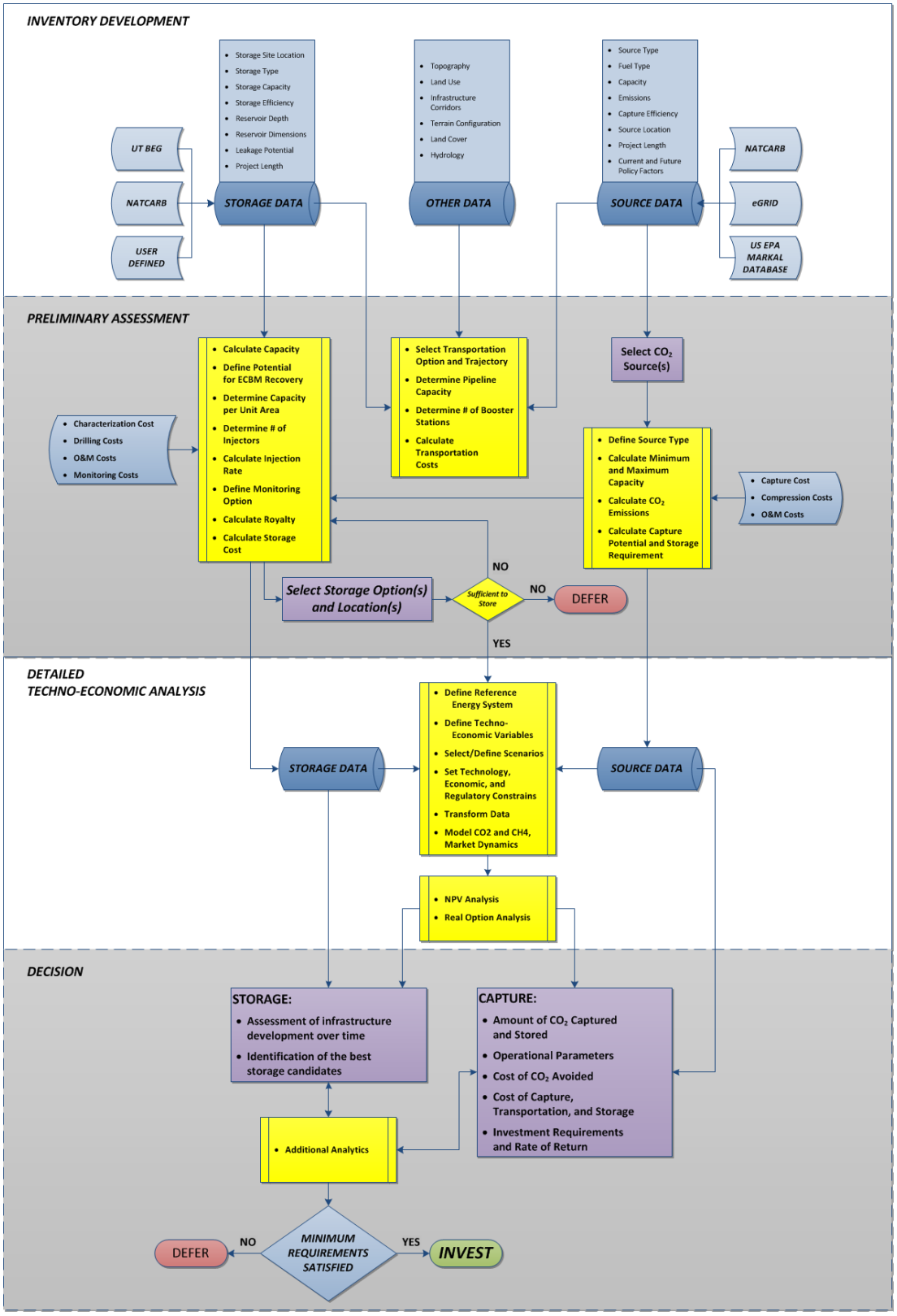

Figure 59: Structure of new decision making framework for geological CO_2 sequestration.

This decision making framework is developed by considering three main concerns:

1. Necessary inputs;
2. Assessment procedures; and
3. The structure of the output.

The input was determined by identifying the critical design parameters necessary for successful implementation of CO_2 storage in unmineable coal seams. Parameters were identified and categorized based on experience gained through characterization and pilot-scale field validation studies, as well as on empirical and theoretical data obtained from relevant scientific literature.

The initial assessment procedures link the input parameters and inventory with the intermediate modeling processes, which provide the foundation for comparative analysis and final conclusions.

Since the data generated through the decision making process must be understandable for its intended users, the type and format of the final output information must be carefully considered.

5.1.1.1 Inputs and Initial Inventory

The first step in the proposed decision making process is identification of the project location and collection of preliminary data about potential storage system, as well as data about CO_2 sources, potential transportation corridors, and other data necessary for preliminary and detailed assessments (Figure 59). This work has been already

undertaken, at least in part, by federal agencies and natural resource-based industries (e.g., mining and oil and gas industry).

As shown in Figure 61, there are a number of external databasses that can be used as a source for developing an initial inventory (U.S. DOE National Carbon Sequestration Database and Geographic Information System – NATCARB; IEA FEP Database; U.S. EPA MARKAL Database; U.S. EPA eGRID Database; University of Texas - Bureau of Economic Geology Database, etc.)

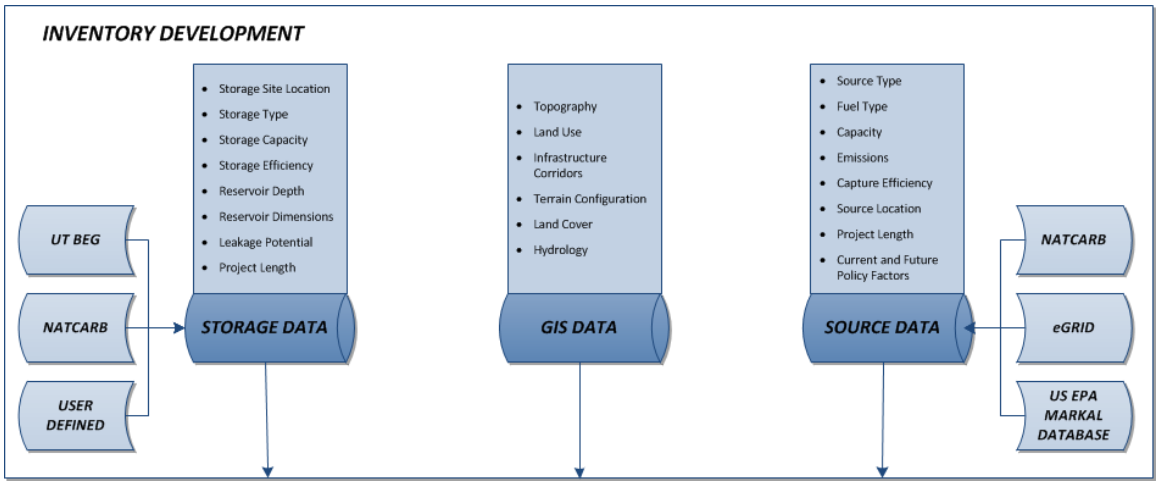

Figure 60: Inventory module.

All quantitative and qualitative factors critical in decision making process were identified in the first two stages of this research (Table 20). They can be divided into four major groups: source-related; sink- or storage-related, economic, and other variables (i.e., transportation, risk, and MVA).

Table 20: Decision variables associated with CO_2 sequestration in unmineable coal seams.

Group	*Parameter:*
SOURCE	Type of the CO_2 source
	Age of the CO_2 source
	Source capacity
	Fuel type
	Emissions
	Capture efficiency
STORAGE	Area of the coal basin
	Coal thickness
	Coal depth
	Formation pressure
	Permeability
	Porosity
	Adsorption capacity
	Dry coal bulk density
	CO_2 storage efficiency
	Pressure at the injector
	Ash weight fraction
	Viscosity of the CO_2
	Coal seam temperature
	Injection rate
	CO_2 compressibility
	Injector well bore radius
	Gas in place
	Reservoir depletion
	CBM production
	Water production
	Gas composition
	Displacement potential

Group	*Parameter:*
ECONOMICS	Project timeframe
	Market value of 1 ton of stored CO_2
	Profit from storing one ton of CO_2
	Market value of one ton CH_4
	Profit from ECBM production
	Royalty
	Drift for CO_2
	Volatility of the CO_2 price
	Drift for CH_4
	Volatility of the CH_4 price
	Rate of foregone earnings
	Carbon credit price
	CH_4 price
	Characterization cost
	Drilling costs
	O&M costs
	Monitoring costs
	Capture cost
	Compression costs
	Transportation cost
	Leakage cost
OTHER	Hydrology factor
	Land use factor
	Active monitoring area
	Leakage potential
	Transportation trajectory
	Pipeline capacity
	Number of booster stations

As mentioned, variables listed in Table 20 are used to define major performance attributes or constraints for developing CO_2 storage project. These performance factors may be categorized as: those associated with the user's goals and objectives; those associated with the project design; those associated with site and technology selection,

and the relative level of importance for each performance mandate, representing how user weighs and ranks the importance of each framework module.

Typically, all performance factors may not have equal importance in decision making process. For that reason, the relative rank for each of the performance attributes (storage capacity, seismicity risk, seal capacity, earnings from the CO_2-ECBM recovery, etc.) must be defined by the user and used as part of the assessment process.

Inputs to from framework algorithms and their outputs, depending on desired information or data format, may be reported or stored as:

- *Binary (Yes or No):* For example, storage capacity estimation assessment yields information whether the storage system has sufficient capacity or not (Figure 67).
- *Scalar:* For example, assessment of potential earnings from CO2-ECBM recovery can rate the estimated profit as low, medium or high, or in a numeric scale, such as 1(very low) to 10 (very high).
- *Categorical:* This is the case when assessment procedure yields categorized results (e.g., ranking of alternative transportation options or categorized design suggestions).

5.1.1.2 Assessment Procedures

The proposed decision methodology has two assessment stages: preliminary assessment and detailed techno-economic analysis. The first evaluates the project as a stationary system and provides suggestions whether the storage system has anticipated techno-economic potential or not. In the case that all techno-economic requirements and

constrains are met, results from this stage are used as inputs into detailed analysis algorithm. This algorithm further evaluates project and potential investment decision by taking into account multi-dimensional nature and time evolution of all uncertainties related to performance factors defined by the user.

Figure 61 illustrates preliminary assessment process. All procedures necessary for the preliminary assessment of potential storage site are presented in Chapter 3. However, this work is focused only on evaluation of CO_2 storage and does not include description of methods used for assessment of CO_2 sources nor transportation.

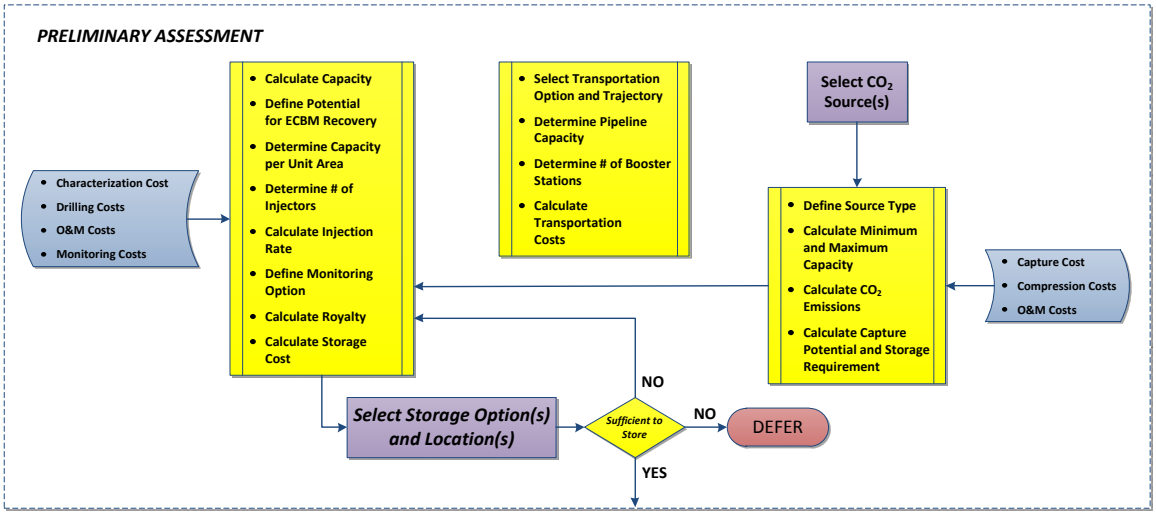

Figure 61: Preliminary assessment algorithm.

The main goal of the detailed techno-economic analysis is, based on the energy supply and demand trends, to model and project storage infrastructure needs under certain market and legislative conditions, over a specified time horizon (Figure 62). Furthermore, this stage allows projection of asset cash-flows, as described in Chapter 4.

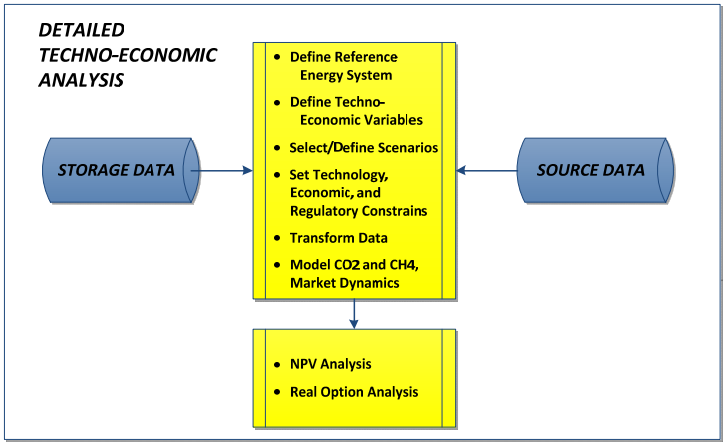

Figure 62: Detailed techno-economic analysis algorithm.

As shown in Figure 63, a number of analytical tools and software packages can be used in conjunction with this framework. For example, IEA's TIMES is software that enables a user to represent a complex energy system - national, regional, local, or sectorial- as a linear system. It generates a matrix with all techno-economic coefficients that specify the economic equilibrium model of the energy system as a mathematical programing problem. TIMES model generator provides a menu of technologies for energy extraction, transport, conversion, and utilization, as well as for related by-products such as CO_2 emissions. These technologies can be defined either as an existing or those expected to be available within the time horizon of the model. The model chooses the best combination of technologies (existing and/or investments in new technologies) to satisfy the project goals and techno-economic constrains.

Further analysis and optimization of analytical results can be performed using Monte Carlo simulation software packages such as GoldSim. Also, due to the fact that the system-wide analysis can include thousands of variables and constrains, it is

recommended that linear or stochastic solver is used, depending on the type of the model. An example of detailed techno-economic analytical procedure is given in Figure 69.

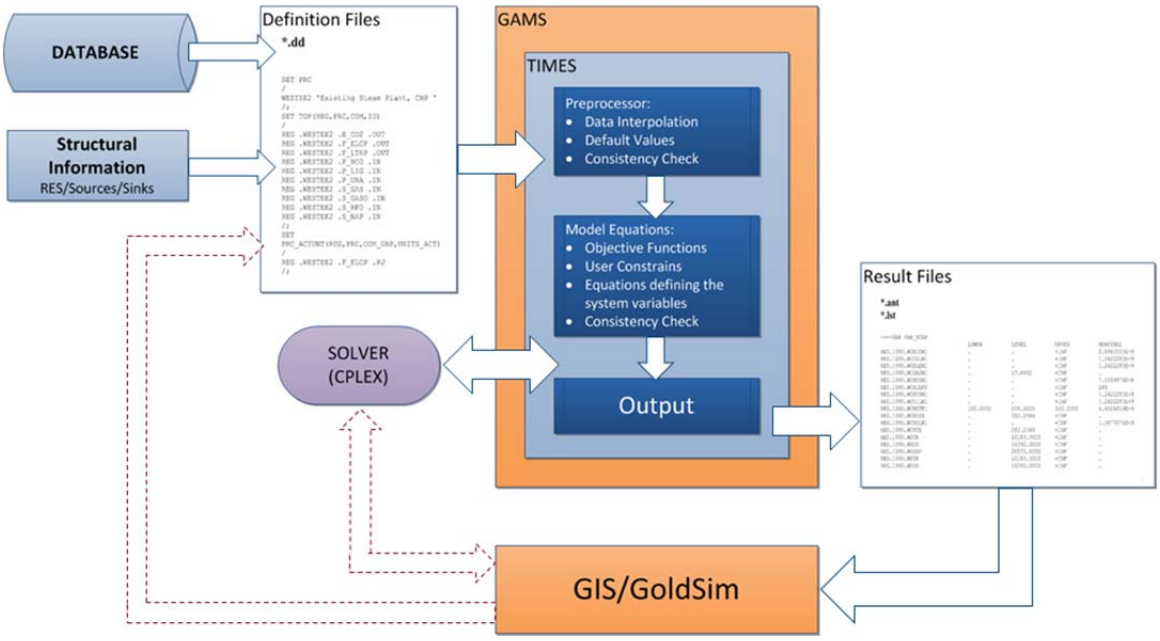

Figure 63: Example of the detailed techno-economic analytical procedure.

5.1.1.3 Decision

Once the preliminary and detailed assessments are concluded, information from multiple levels of analysis are collected and synthesized at final level of the framework. As illustrated in Figure 64, if minimum requirements are met, the user can select an option to invest and proceed with the implementation of the project. In the case that minimum requirements are not met, user should revisit the assessment algorithms and redefine performance mandates and constrains, if possible. If not, decision maker should defer investment decision and proceed with the assessment of secondary options.

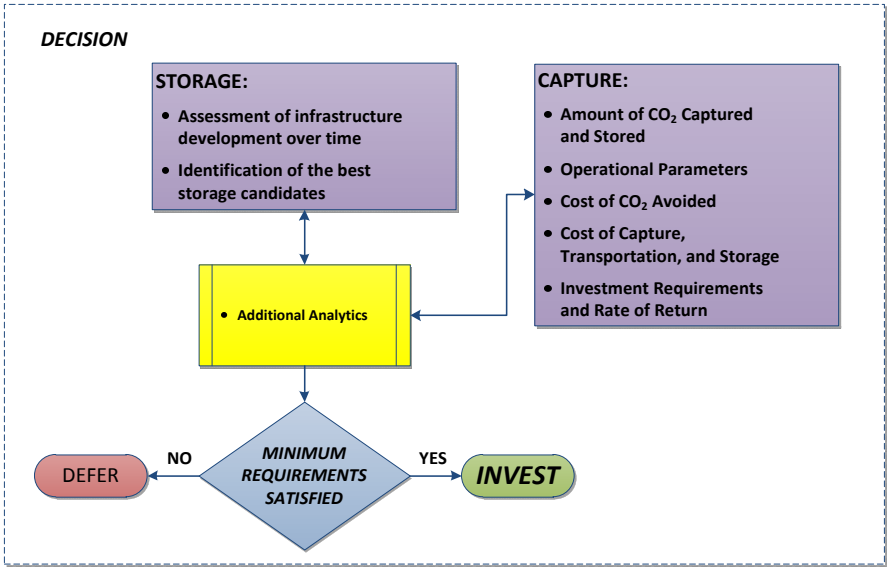

Figure 64: Decision algorithm.

Once the decision to invest is made, the decision maker should make a list of potential short- and long-term technical and management options. This process should be transparent and involve all stakeholders.

5.2 CASE STUDY: PRELIMINARY ASSESSMENT OF POTENTIAL SITES FOR A LARGE-VOLUME CARBON SEQUESTRATION TEST IN CENTRAL APPALACHIA

The following section describes development of a screening and evaluation framework used for preliminary assessment of the three most promising locations for large-scale storage in Central Appalachia (Figure 68). The Central Appalachian Basin offers a range of geologic options that can be utilized for large-scale CO_2 storage (i.e., unmineable coal seams, organic-rich shales, depleted oil and gas reservoirs, and deep saline aquifers).

As mentioned earlier, CO_2 storage site selection requires an individual assessment of different technical and non-technical performance parameters. In this case,

development of a preliminary evaluation procedure was complicated by the fact that data quantity and quality were very different for each storage site. For that reason a simplified ranking procedure has been developed and applied. This procedure was developed based on three basic performance categories:

1. Site-specific requirements:
    a. Capacity and storage availability
    b. Size of the monitoring area
    c. Site topography and land cover
    d. Available infrastructure at the site - ease of access
2. Techno-economic parameters:
    a. Injectivity
    b. ECBM-EGR potential
    c. Proximity to CO_2 sources
    d. Costs of MVA program
3. Risk parameters:
    a. Probability of seismic events
    b. Spatial distribution of completed/abandoned wells around storage site
    c. Cap rock/sealing properties

5.2.1 SITE-SPECIFIC PARAMETERS

5.2.1.1 Capacity and storage availability

The first step in this evaluation process was assessment of the storage capacity for all available storage options. In order to provide a coherent comparison between potential storage sites, the storage capacity potential was assessed and reported per unit area. Table 21 summarizes low and high capacity estimates for all fields included in this assessment.

Table 21: Field capacities (source: MM&A, 2011) [85].

Field	High Capacity (tonnes)	Low Capacity (tonnes)	Area (acres)
Frying Pan	----	3,352,965	7,200
Lick Creek	----	21,737,117	31,020
Sourwood	----	5,198,184	11,220
South Oakwood	----	30,281,915	38,400
Loup Creek	----	4,454,290	29,915
Bradshaw	18,164,812	----	7,500
Roaring Fork	27,715,011	----	447,709
Ashland-Clark Gap-Eckman	28,982,620	----	202,779
Rock Creek	310,681	----	15,377
Granny Creek	149,478	----	3,890
Kentucky EOR-Big Lime	6,356,315	144,125	13,556
Tuscarora Saline Reservoir	422,184,093	105,546,023	7,640,516

Estimated low and high storage capacities, expressed as mass estimate per unit area, and available geological options for all three storage locations are given in Table 22.

Table 22: Estimated CO_2 storage capacities available storage options for three potential storage locations.

Performance Category	Site 1 Dickenson County, Virginia	Site 2 Wyoming County, West Virginia	Site 3 Clay County, West Virginia
Storage Capacity (tonnes/acre)	582 - 864	260 - 352	55 - 217
Storage Reservoir Availability	Coal Seam - Partial Depleted Gas - Partial Devonian Shale - Future	Coal Seam - Partial Depleted Gas - Partial Tuscarora - Available	Saline Reservoirs - Available
Rank	**1**	**2**	**3**

5.2.1.2 Size of the Monitoring Area

Data regarding reservoir properties and extent of the CO_2 plume, obtained in the reservoir modeling study, were used as a baseline for estimating the size of the affected surface area, or active monitoring area (*AMA*), at the potential test sites. The AMA ranges from 281 acres to 640 acres (Table 23) for three most promising storage locations:

- Site I: Aily/Nora, Dickenson County, VA
- Site II: Saulsville, Wyoming County, WV

- Site III: Nebo/Ivydale, Clay County, WV

As shown in Table 23, the largest AMA, with 640 acres footprint, is expected at the Site I, followed by Site II with 465 acres, and then Site III, 281 acres. Since the size of the monitoring area dictates costs and efficiency of the MVA program, the ranking system in Table 23 was based on the assumption that MVA program deployed at smaller AMA is always less expensive and more efficient.

Table 23: Sizes of active monitoring areas.

Location	Sink Option	AMA (acres)	Rank
Site I	ECBM - Weir	640	**3**
Site II	ECBM –Weir, Tuscarora	465	**2**
Site III	Depleted O&G, Saline Oriskany and Tuscarora	281	**1**

5.2.1.3 Monitoring area topography and land cover

One of the most important factors to consider in ranking three potential sites on the basis of MVA requirements is terrain configuration. Figures 65, 66, and 67 show terrain configuration at potential storage sites I, II, and III, respectively. All three sites are representative of Central Appalachian topography, having heterogeneous and complex terrain configuration. The AMAs at Sites I and III are predominantly rural areas densely covered with the mixed forest.

The AMA at the Site II is semi-rural area with small-scale mining and agricultural activities nearby. Major factors in this category are terrain complexity (flat vs. heterogeneous/mountainous terrain), land cover, land use, hydrological conditions, and proximity to settlements. Table 24 shows qualitative rank in this category.

Table 24: Monitoring area topography and land cover summary.

Location	Site Description	Proximity to Nearby Settlements	Elevation (ft)	Site-Specific Features	Rank
Site I	Rural area / Complex Terrain / Dense Forest / Number of surface water bodies	2.5 miles to Aily, VA	1,900–2,300		**3**
Site II	Semi-rural area / Complex Terrain	1.0 mile to Saulsville, WV	2,000–2,400	Mining Operations Agricultural Land Twin Falls State Park	**1**
Site III	Rural area / Complex Terrain / Dense Forest	1.0 mile to Ivydale, WV	1,000–1,300	River Elk	**2**

Figure 65: Aerial view of Site I, located in Dickenson County, Virginia. (Source: Google Inc. (2011). Google Earth (Version 6.1.0.5001))

Figure 66: Aerial view of Site II, located in Wyoming County, West Virginia. (Source: Google Inc. (2011). Google Earth (Version 6.1.0.5001))

Figure 67: Aerial view of Site III, located in Clay County, West Virginia. (Source: Google Inc. (2011). Google Earth (Version 6.1.0.5001))

5.2.1.4 Available Infrastructure - Ease of Access

As shown in Figures 65-67, the best infrastructure (access roads, electricity, etc.), is present at the Site II. The other two sites are less developed and additional construction work will be required in order to provide access and power at the injection site and AMA.

5.2.2 TECHNO-ECONOMIC PARAMETERS

5.2.2.1 Injectivity

A summary of minimum and maximum injection rates is given in Table 25. The values presented in the table are based on CO_2 injection profiles determined through initial reservoir modeling study. Results from this study reflect the combination of three major injectivity factors: high permeability-thickness; high reservoir depletion; and high injection pressure.

Table 25: Minimum and maximum injection rates determined through initial reservoir modeling study.

Performance Category	Site 1 Dickenson County, Virginia	Site 2 Wyoming County, West Virginia	Site 3 Clay County, West Virginia
Modeled Injectivity (tonnes/day)	260 - 566	70 - >330	70 - 210
Rank	**1**	**2**	**3**

5.2.2.2 Proximity to CO_2 Source

Figure 69 shows three potential storage sites and spatial distribution of all CO_2 sources in Virginia and West Virginia. A distance from storage site to CO_2 source is one of the most important parameters to consider in the design phase of any CCS project. CO_2 transportation is a factor that significantly influences overall costs of CCS project and the extent of the project footprint (passive monitoring area). As shown in Figure 68, Site I should have the best qualitative score in this category since it is located closest to the potential CO_2 source. On the other hand, Site II is most remote in terms of proximity to CO_2 source.

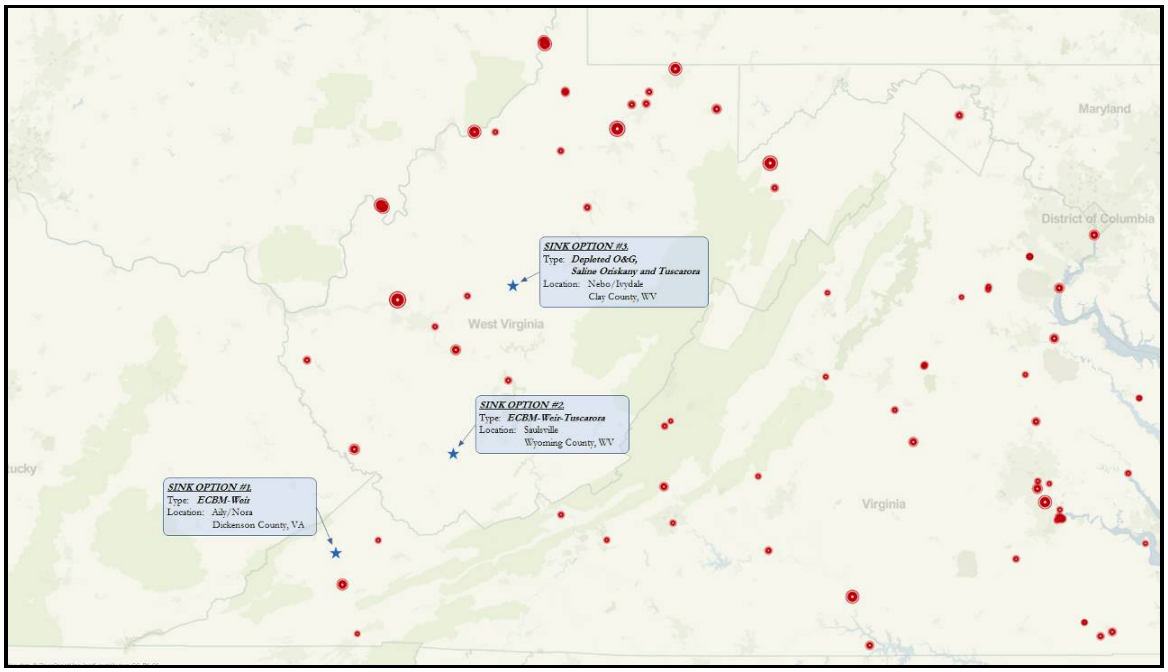

Figure 68: Sink and source map.

Figures 69 through 72 show buffer zones around the sites with all the major CO_2 sources included. Tables 26, 28, and 30 list the major CO_2 sources and emissions near each site. Tables 27, 29 and 31 show the summaries of CO_2 emissions per buffer zone for each site.

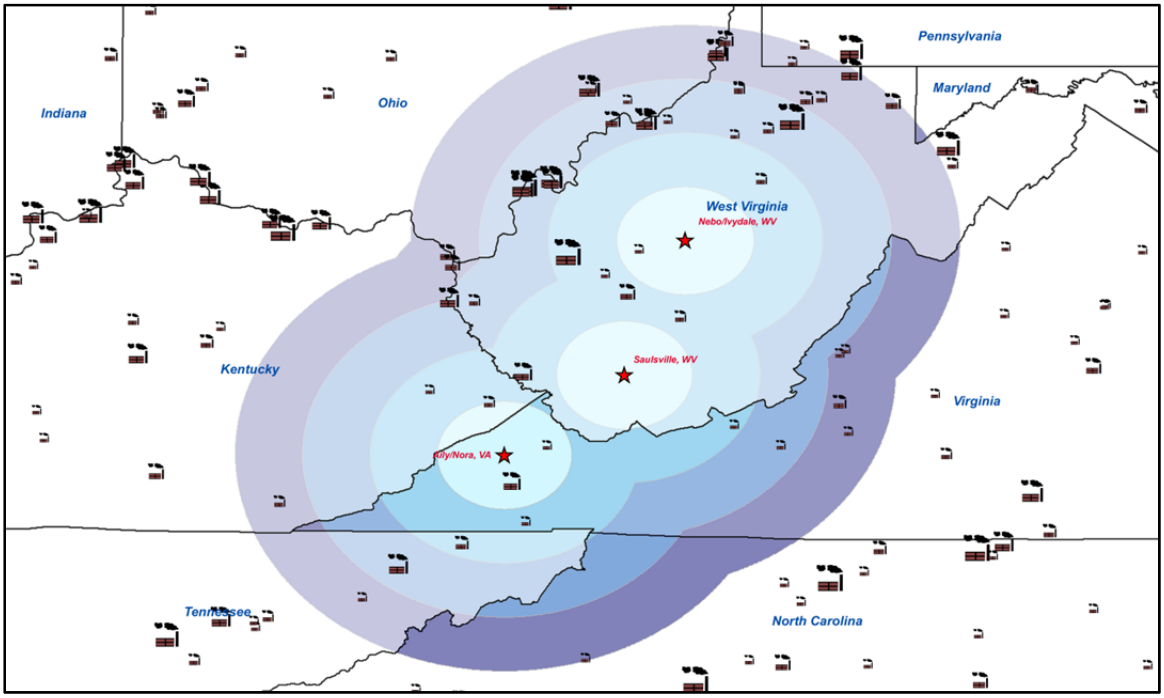

Figure 69: Four buffer zones (25 miles, 50 miles, 75 miles, and 100 miles) around three potential storage sites with major CO_2 sources.

Table 26: Major CO_2 sources and CO_2 emissions near Site I, Aily/Nora, Dickenson County, Virginia.

Source Site	Source Name	State	Source Type	Buffer Zone (miles)	CO_2 Emissions (tonnes/year)
I	Boldman	KY	Gas processing	0-25	222,840
I	Clinch River	VA	Power (Coal)	0-25	3,764,565
I	Buchanan County Generating Facility	VA	Power (Gas)	0-25	20,474
I	Maytown	KY	Gas processing	25-50	198,530
I	Wolf Hills Energy LLC	VA	Power (Gas)	25-50	614
I	Mingo County CBM	WV	Gas processing	25-50	2,836,420
I	Tennessee Eastman Operations	TN	Power (Coal)	25-50	754,512
I	Big Sandy	KY	Power (Coal)	50-75	6,048,400
I	Kenova	WV	Gas processing	50-75	498,350
I	John Sevier	TN	Power (Coal)	50-75	5,334,486

I	Ashland Plant	KY	Iron & Steel	75-100	2,261,640
I	Pineville	KY	Power (Coal)	75-100	208,520
I	Marathon Ashland Petroleum	KY	Refineries	75-100	2,138,530
I	Cinergy Solutions of Narrows	VA	Power (Coal)	75-100	133,496
I	Alloy Steam Station	WV	Power (Coal)	75-100	297,990
I	Kanawha River	WV	Power (Coal)	75-100	2,338,270
I	Cobb	WV	Gas processing	75-100	101,290
I	John E. Amos	WV	Power (Coal)	75-100	15,231,230
I	Lowland	TN	Power (Coal)	75-100	84,299
I	Water Filter Plant #2	NC	Power (Oil)	75-100	159

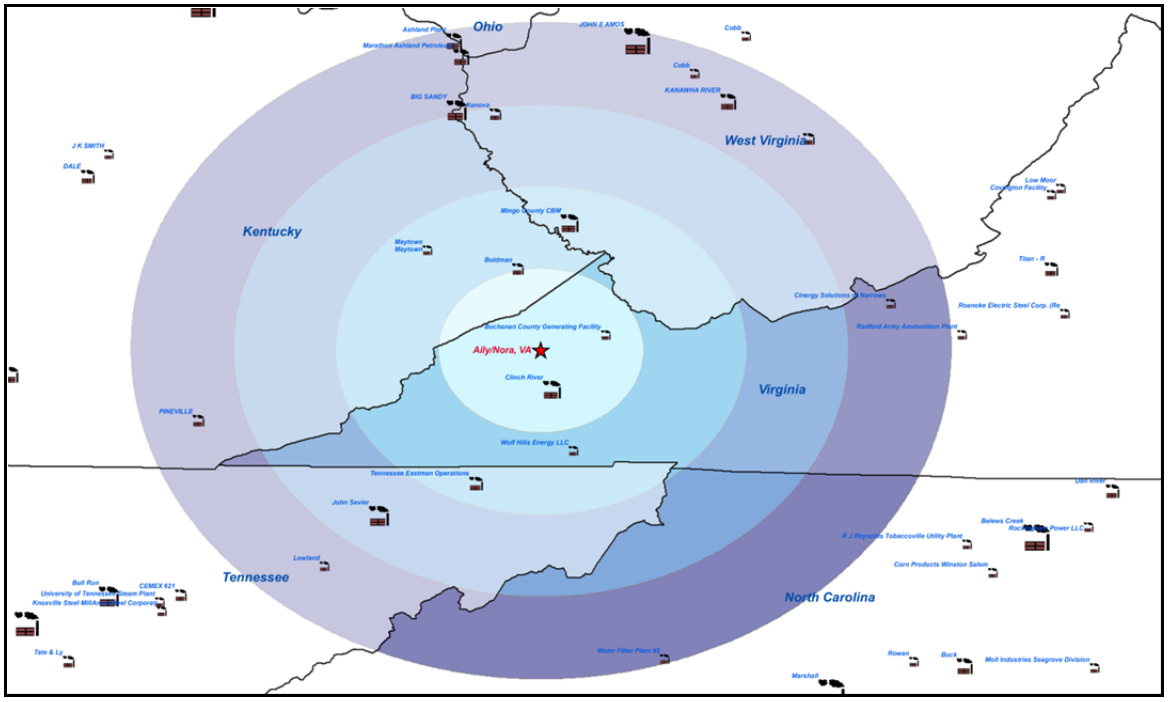

Figure 70: Buffer zones (25 miles, 50 miles, 75 miles, and 100 miles) around Site I with major CO_2 sources in Virginia, West Virginia, Kentucky, Tennessee, Ohio, and North Carolina.

Table 27: CO_2 emissions per buffer zone for Site I.

CO_2 Emissions per Buffer Zone (tonnes/year)				
Zone 1 0-25 miles	**Zone 2** 25-30 miles	**Zone 3** 50-75 miles	**Zone 4** 75-100 miles	**Total CO_2 Emissions**
4,007,879	3,790,076	11,881,236	22,795,424	**42,474,615**

Table 28: Major CO_2 sources and CO_2 emissions near Site II, Saulsville, Wyoming County, West Virginia.

Source Site	**Source Name**	**State**	**Source Type**	**Buffer Zone (miles)**	**CO_2 Emissions (tonnes/year)**
II	Kenova	WV	Gas processing	25-50	498,350
II	Kanawha River	WV	Power (Coal)	25-50	2,338,270

II	Alloy Steam Station	WV	Power (Coal)	25-50	297,990
II	Cinergy Solutions of Narrows	VA	Power (Coal)	25-50	133,496
II	Maytown	KY	Gas processing	50-75	198,530
II	Boldman	KY	Gas processing	50-75	222,840
II	Big sandy	KY	Power (Coal)	50-75	6,048,400
II	Cobb	WV	Gas processing	50-75	101,290
II	John E. Amos	WV	Power (Coal)	50-75	15,231,230
II	Radford Army Ammunition Plant	VA	Power (Coal)	50-75	40,828
II	Tennessee Eastman Operations	TN	Power (Coal)	75-100	754,512
II	Wolf Hills Energy LLC	VA	Power (Gas)	75-100	614
II	Ashland Plant	KY	Iron & Steel	75-100	2,261,640
II	Marathon Ashland Petroleum	KY	Refineries	75-100	2,138,530
II	Roanoke Electric Steel Corp.	VA	Iron & Steel	75-100	85,079
II	Titan - R	VA	Cement	75-100	1,120,580
II	Low Moor	VA	Power (Oil)	75-100	162
II	Covington Facility	VA	Power (Coal)	75-100	194,423
II	Mountaineer (1301)	WV	Power (Coal)	75-100	7,663,480
II	Phil Sporn	WV	Power (Coal)	75-100	5,383,580
II	Kyger Creek	OH	Power (Coal)	75-100	6,603,140
II	Gen. J.M. Gavin	OH	Power (Coal)	75-100	16,838,850

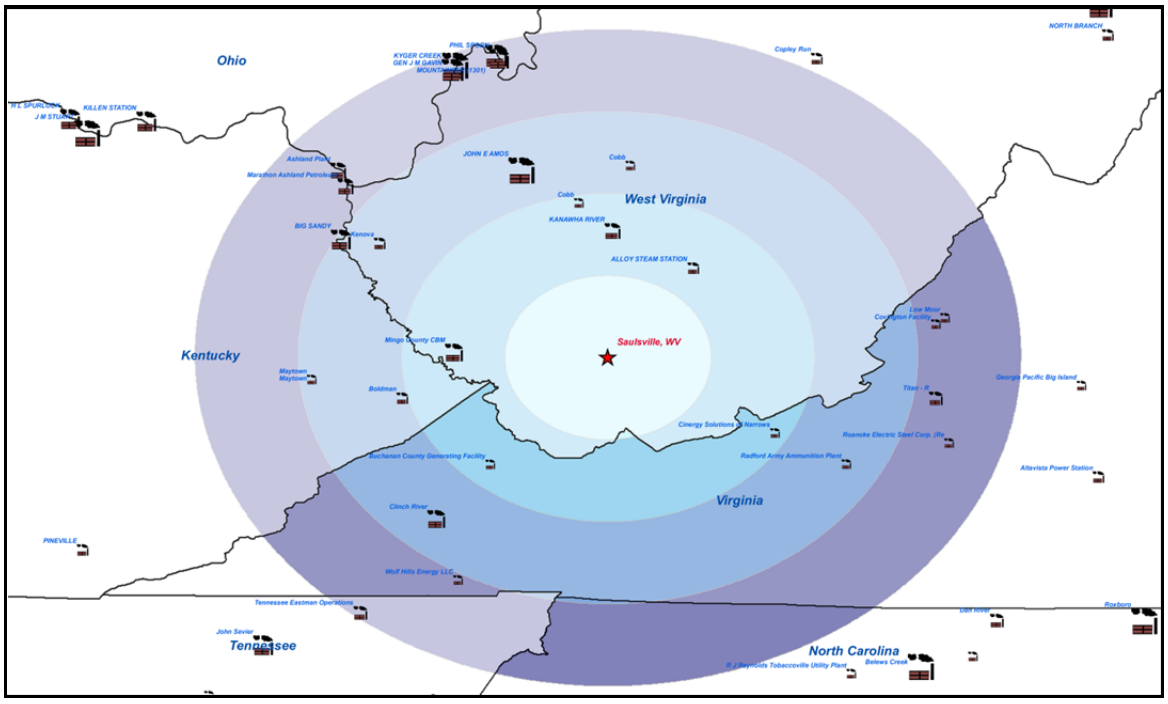

Figure 71: Buffer zones (25 miles, 50 miles, 75 miles, and 100 miles) around Site II with major CO_2 sources in Virginia, West Virginia, Kentucky, Tennessee, and Ohio.

Table 29: CO_2 emissions per buffer zone for Site II.

CO_2 Emissions per Buffer Zone (tonnes/year)				
Zone 1 0-25 miles	**Zone 2** 25-30 miles	**Zone 3** 50-75 miles	**Zone 4** 75-100 miles	**Total CO_2 Emissions**
0	3,268,106	21,843,118	43,044,590	**68,155,814**

Table 30: Major CO_2 sources and CO_2 emissions near Site III, Nebo/Ivydale, Clay County, West Virginia.

Source Site	**Source Name**	**State**	**Source Type**	**Buffer Zone (miles)**	**CO_2 Emissions (tonnes/year)**
III	Cobb	WV	Gas processing	25-50	101,290
III	John E. Amos	WV	Power (Coal)	25-50	15,231,230
III	Kanawha River	WV	Power (Coal)	25-50	2,338,270
III	Alloy Steam Station	WV	Power (Coal)	25-50	297,990
III	Copley Run	WV	Gas processing	25-50	491,278
III	Mountaineer (1301)	WV	Power (Coal)	50-75	7,663,480
III	Phil Sporn	WV	Power (Coal)	50-75	5,383,580
III	Kyger Creek	OH	Power (Coal)	50-75	6,603,140
III	Gen. J.M. Gavin	OH	Power (Coal)	50-75	16,838,850
III	Churchtown	OH	Gas processing	50-75	111,653
III	Richard Gorsuch	OH	Power (Coal)	50-75	1,616,710
III	Pleasants	WV	Power (Coal)	50-75	7,224,740
III	Willow Island	WV	Power (Coal)	50-75	1,367,590
III	Schultz	WV	Gas processing	50-75	111,653
III	West Union	WV	Gas processing	50-75	200,973
III	Natrium Plant	WV	Power (Coal)	50-75	593,320
III	Hastings	WV	Gas processing	50-75	486,190
III	Morgantown Energy Facility	WV	Power (Coal)	50-75	448,840
III	Harrison	WV	Power (Coal)	50-75	12,862,820
III	Big Sandy	KY	Power (Coal)	75-100	6,048,400
III	Ashland Plant	KY	Iron & Steel	75-100	2,261,640
III	Marathon Ashland Petroleum	KY	Refineries	75-100	2,138,530
III	Kenova	WV	Gas processing	75-100	498,350
III	Mingo County CBM	WV	Gas processing	75-100	2,836,420
III	Cinergy Solutions Of Narrows	VA	Power (Coal)	75-100	133,496
III	Titan - R	VA	Cement	75-100	1,120,580
III	Covington Facility	VA	Power (Coal)	75-100	194,423
III	Muskingum River	OH	Power (Coal)	75-100	7,275,020
III	Washington Energy Facility	OH	Power (Gas)	75-100	266,420
III	R.E. Burger	OH	Power (Coal)	75-100	1,941,190
III	Kammer	WV	Power (Coal)	75-100	3,449,410
III	Mitchell	WV	Power (Coal)	75-100	7,973,820
III	Rivesville	WV	Power (Coal)	75-100	608,430
III	Grant Town Power Plant	WV	Power (Coal)	75-100	790,850
III	Albright	WV	Power (Coal)	75-100	1,760,340
III	Fort Martin	WV	Power (Coal)	75-100	6,895,640
III	Greene County CBM	PA	Gas processing	75-100	141,820
III	Waynesburg	PA	Gas processing	75-100	187,580

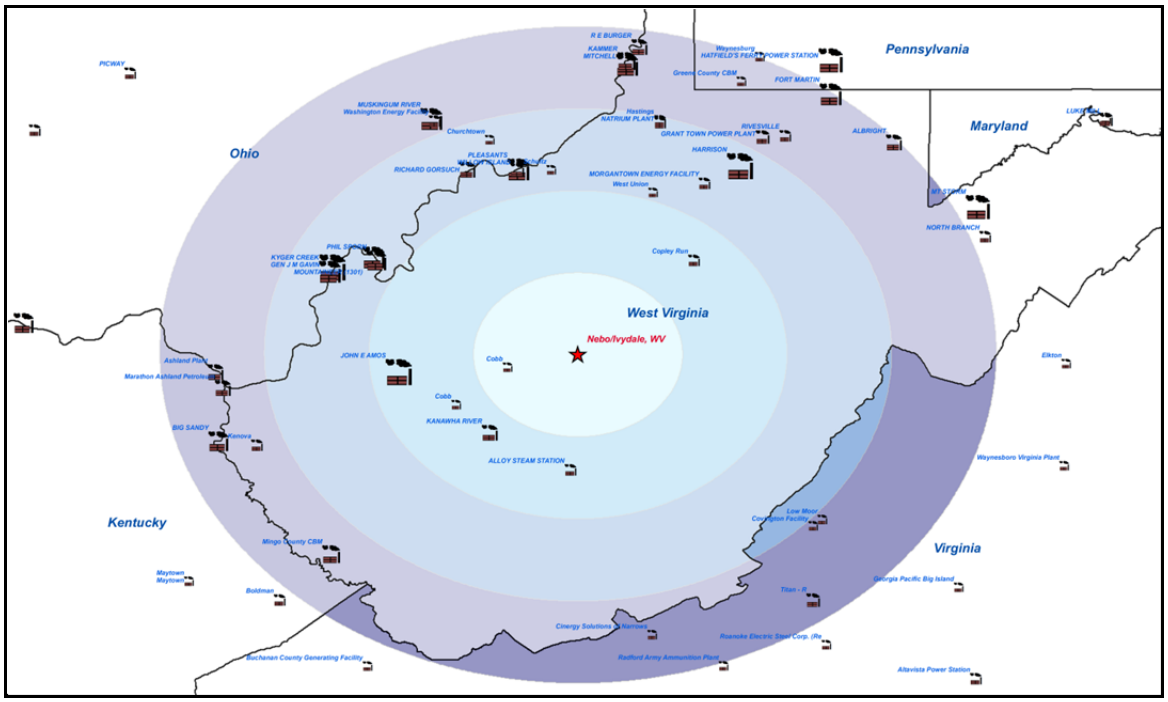

Figure 72: Buffer zones (25 miles, 50 miles, 75 miles, and 100 miles) around Site III with major CO_2 Sources in Virginia, West Virginia, Kentucky, Ohio, and Pennsylvania.

Table 31: CO_2 emissions per buffer zone for Site III.

CO_2 Emissions per Buffer Zone (tonnes/year)				
Zone 1 0-25 miles	**Zone 2** 25-30 miles	**Zone 3** 50-75 miles	**Zone 4** 75-100 miles	**Total CO_2 Emissions**
0	18,460,058	61,513,539	46,522,521	**126,496,118**

5.2.2.3 Cost of Monitoring Technology

In order to estimate an average cost of monitoring per acre of AMA, a monitoring unit cost scheme developed by the U.S. Environmental Protection Agency (2009) was used [121]. The cost of monitoring is directly influenced by type of storage reservoir, depth of the reservoir, and all surface site-specific parameters. In this category, a significant element of uncertainty is associated with potential changes/advancements in technology through time. For this reason, figures presented in Table 32 (for saline

reservoirs) and Table 33 (for unmineable coal seams) are just rough estimates of potential monitoring costs.

Table 32: Estimated costs of monitoring for saline reservoirs over 2 years of injection (based on EPA 2009).

		Cost Algorithm			
Unit Cost Heading	**Cost Item**	**Price $/unit**	**Unit**	**Qty**	**Total Price**
Site Selection and Evaluation	Develop geochemical baseline for injection zone and confining zone	200	sample	72	$14,400.00
Site Selection and Evaluation	Develop a baseline of surface air CO_2 flux for leakage monitoring	50,000	station	2	$100,000.00
Site Selection and Evaluation	Conduct front-end engineering and design (monitoring wells)	25,000	monitoring well	8	$200,000.00
Land and Land Use Rights	Obtain rights-of-way for surface uses (monitoring wells)	10,000	monitoring well site	8	$80,000.00
Land and Land Use Rights	Obtain rights-of-way for surface uses (monitoring sites)	5,000	air monitoring station site	2	$10,000.00
Drilling and Equipping Injection Wells	Downhole safety shut-off valve	2	ft depth	8,000	$31,000.00
Drilling and Equipping Monitoring Wells	Standard monitoring well cost (above injection zone) (4 wells x 4500ft/well=18000ft)	130	foot	18,000	$2,340,000.00
Drilling and Equipping Monitoring Wells	Standard monitoring well cost (into injection zone) (4 wells x 8000ft/well=32000ft)	130	foot	32,000	$4,160,000.00
Downhole monitoring Equipment (for Monitoring Wells or Injection Wells)	Pressure and temperature gauges and related equipment for monitoring wells	10,000	well	9	$90,000.00
Downhole monitoring Equipment (for Monitoring Wells or Injection Wells)	Salinity, CO_2, tracer, etc. monitor equipment for wells (portion of equipment may be at surface such as for in-situ sampling using U-tubes)	10,000	well	9	$90,000.00
Surface or Near-Surface Monitoring Equipment	Develop plan and implement surface air and/or soil monitoring within current plume footprint	74,252	monitoring site	2	$148,504.00
Surface or Near-Surface Monitoring Equipment	Develop plan and implement surface air and/or soil monitoring within current plume footprint, at artificial	74,252	monitoring site	4	$297,008.00

	penetrations and sensitive locations (human occupancy)				
Surface or Near-Surface Monitoring Equipment	Surface microseismic detection equipment	50000	site	8	$400,000.00
Operating Costs	Monitoring well O&M	3	ft	50,000	$175,000.00
Operating Costs	Annual cost of air and soil surveys & equipment	10,000	station	8	$80,000.00
Operating Costs	Annual cost of passive seismic equipment	10,000	station	8	$80,000.00
Operating Costs	Periodic 3D seismic surveys	75,000	survey	6	$450,000.00
Operating Costs	Complex modeling of fluid flows and migration (reservoir simulations) every five years	10,918	injection well	1	$10,918.00
Operating Costs	Annual reports to regulators	1,070	report	2	$2,140.00
Operating Costs	Quarterly reports to regulators	803	report	8	$6,424.00
Operating Costs	Monthly reports to regulators	428	report	24	$10,272.00
TOTAL COST					**$8,775,666.00**

Table 33: Estimated costs of monitoring for unmineable coal seams over 1 year of injection (based on EPA 2009).

		Cost Algorithm			
Unit Cost Heading	**Cost Item**	**Price $/unit**	**Unit**	**Qty**	**Total Price**
Site Selection and Evaluation	Develop geochemical baseline for injection zone and confining zone	200	sample	72	$14,400.00
Site Selection and Evaluation	Develop a baseline of surface air CO_2 flux for leakage monitoring	50,000	station	3	$150,000.00
Site Selection and Evaluation	Conduct front-end engineering and design (monitoring wells)	25,000	monitoring well	4	$100,000.00
Land and Land Use Rights	Obtain rights-of-way for surface uses (monitoring wells)	10,000	monitoring well site	4	$40,000.00
Land and Land Use Rights	Obtain rights-of-way for surface uses (monitoring sites)	5,000	air monitoring station site	3	$15,000.00
Drilling and Equipping Injection Wells	Downhole safety shut-off valve	2	ft depth	3,000	$21,000.00

Drilling and Equipping Monitoring Wells	Standard monitoring well cost (above injection zone) (2 wells x 1500ft/well=3000ft)	130	foot	3,000	$390,000.00
Drilling and Equipping Monitoring Wells	Standard monitoring well cost (into injection zone) (2 wells x 3000ft/well=6000ft)	130	foot	6,000	$780,000.00
Downhole monitoring Equipment (for Monitoring Wells or Injection Wells)	Pressure and temperature gauges and related equipment for monitoring wells	10,000	well	5	$50,000.00
Downhole monitoring Equipment (for Monitoring Wells or Injection Wells)	Salinity, CO_2, tracer, etc. monitor equipment for wells (portion of equipment may be at surface such as for in-situ sampling using U-tubes)	10,000	well	5	$50,000.00
Surface or Near-Surface Monitoring Equipment	Develop plan and implement surface air and/or soil monitoring within current plume footprint	74,252	monitoring site	3	$222,756.00
Surface or Near-Surface Monitoring Equipment	Develop plan and implement surface air and/or soil monitoring within current plume footprint, at artificial penetrations and sensitive locations (human occupancy)	74,252	monitoring site	6	$445,512.00
Surface or Near-Surface Monitoring Equipment	Surface microseismic detection equipment	50,000	site	4	$200,000.00
Operating Costs	Monitoring well O&M	3	ft	9,000	$52,000.00
Operating Costs	Annual cost of air and soil surveys & equipment	10,000	station	9	$90,000.00
Operating Costs	Annual cost of passive seismic equipment	10,000	station	4	$40,000.00
Operating Costs	Periodic 3D seismic surveys	75,000	survey	6	$450,000.00
Operating Costs	Complex modeling of fluid flows and migration (reservoir simulations) every five years	10,918	injection well	1	$10,918.00
Operating Costs	Annual reports to regulators	1,070	report	1	$1,070.00
Operating Costs	Quarterly reports to regulators	803	report	4	$3,212.00
Operating Costs	Monthly reports to regulators	428	report	12	$5,136.00
TOTAL COST					**$3,131,004.00**

5.2.3 RISK PARAMETERS

5.2.3.1 Probability of Seismic Events

Figures 73, 74, and 75 show probability of earthquakes with magnitude M≥ 4.75 within 50 years and 31 miles (50 kilometers) around potential storage sites. The earthquake probabilities were computed from the source model of the 2008 USGS-National Seismic Hazard Mapping Project (NSHMP) update. Earthquake probability values for sites I and II are very similar and they range from 0.06 to 0.08 for Site I and 0.05-0.06 for Site II. The lowest probability range, 0.01-0.015, was calculated for Site III.

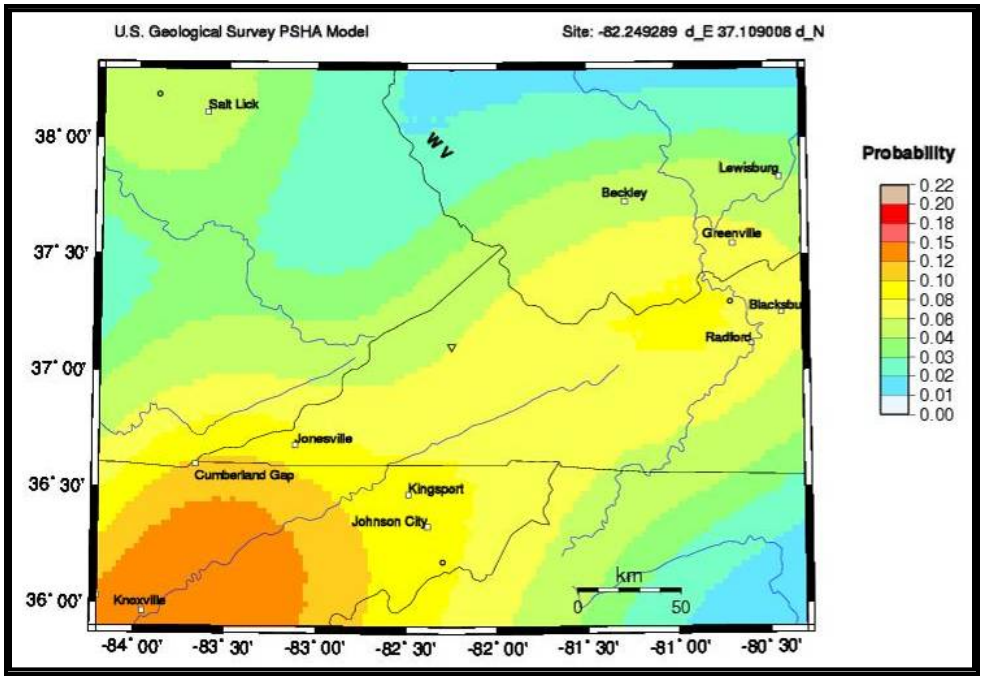

Figure 73: Probability of earthquake with M≥4.75 within 50 years and 50km from Site I in Dickenson County, Virginia.

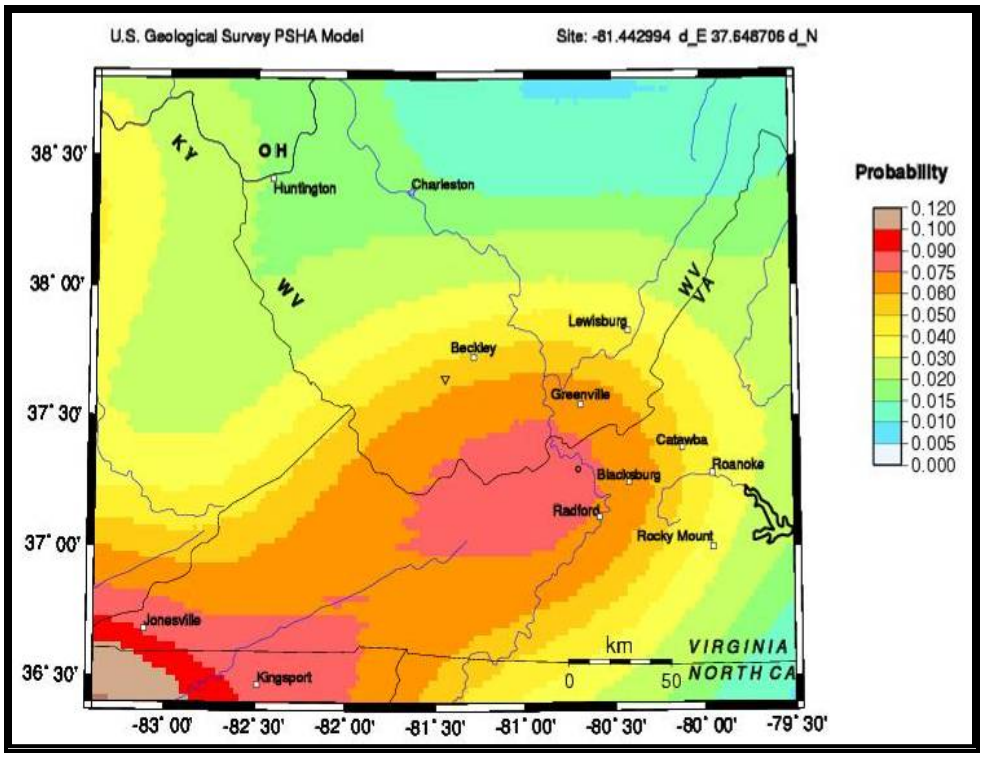

Figure 74: Probability of earthquake with M≥4.75 within 50 years and 50km from Site II in Wyoming County, West Virginia.

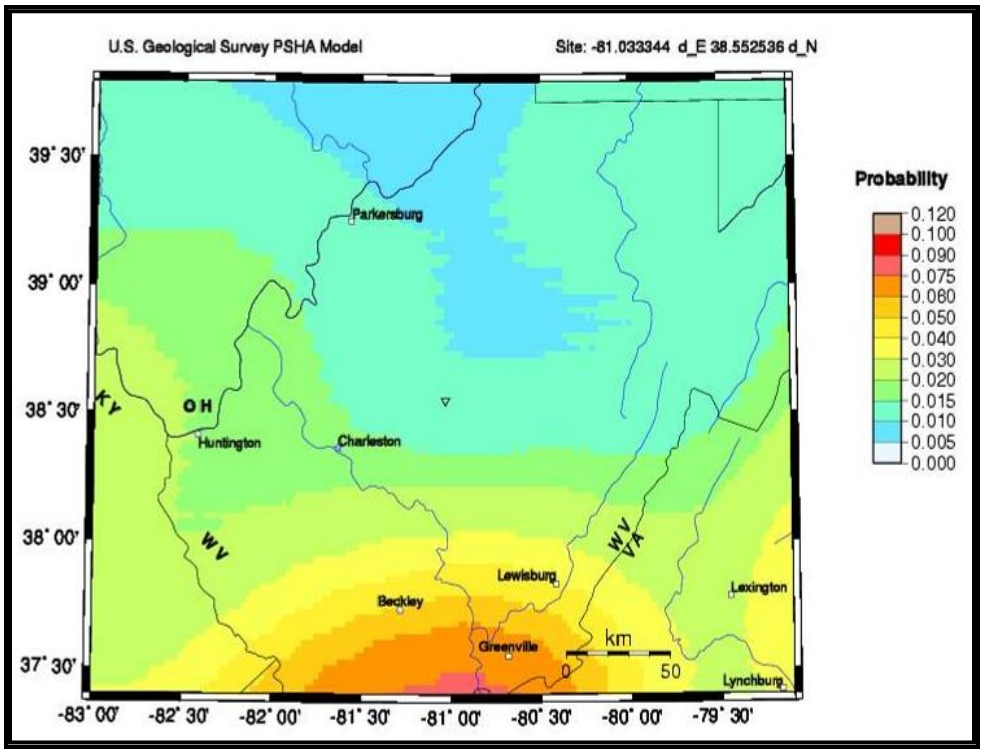

Figure 75: Probability of earthquake with M≥4.75 within 50 years and 50km from Site III in Clay County, West Virginia.

5.2.3.2 Preexisting (Completed/Abandoned) Wells

Preexisting oil and gas (*O&G*) wells and well bores, which penetrate through targeted storage formations, are high-permeability pathways for leakage and as such present zones of increased risk. Although today's well closure and abandonment practices, extensively used in the O&G industry, appear to be sufficient to contain injected CO_2 in the reservoir, some preexisting wells may gradually lose their integrity.

All three potential storage areas have a long history of O&G exploration and production and therefore there are many completed or abandoned wells in proximity to potential injection sites, potentially penetrating into the injection formation. As shown in Figure 76, a number of completed or abandoned wells surrounding potential injection sites ranges from hundreds at Site I, to thousands around Site II. Most of these wells are 30-50 years old and have been abandoned. Since their hydraulic properties are unknown, they pose the largest risk to implementation of CCS in those areas. Given the number of preexisting wells present in the area, Site III has the lowest leakage potential. The highest leakage risk is present at the Site II. Maps presented in Figure 76 are generated using data from the West Virginia Geological & Economic Survey's "Pipeline-Plus" System and the Virginia Department of Mines, Minerals, and Energy's Division of Gas and Oil Data Information System.

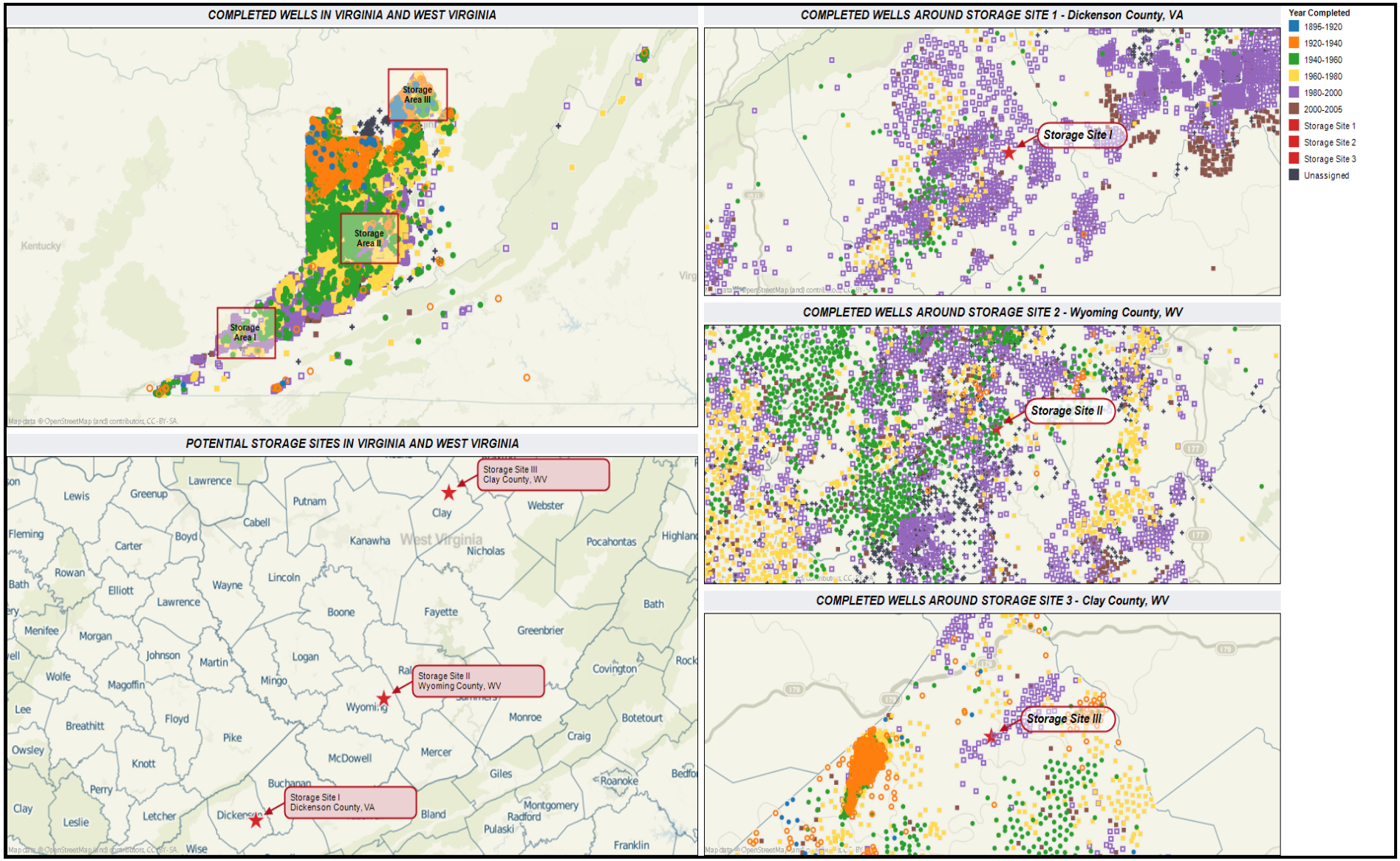

Figure 76: Preexisting wells near potential CO_2 storage sites in Virginia and West Virginia.

5.2.4 DISCUSSION AND RANKING

The screening and ranking procedure described in this chapter was used to identify the best candidate for the large-scale CO_2 storage project. As shown earlier, each of three potential storage sites has specific advantages and limitations. The list of all performance parameters used in this preliminary assessment study is given in Table 34.

Table 34: Summary of performance parameters for three potential CO_2 storage sites in Central Appalachia.

Performance Category	**Site 1 Dickenson County, Virginia**	**Site 2 Wyoming County, West Virginia**	**Site 3 Clay County, West Virginia**
Storage Capacity (tonnes/acre)	582 - 864	260 - 352	55 - 217
Modeled Injectivity (tonnes/day)	260 - 566	70 - >330	70 - 210
Confinement Characteristics	Multiple Carboniferous shale seals	Multiple Carboniferous, Devonian, and Rose Hill shale seals	Multiple Rose Hill and Devonian shale seals
Storage Reservoir Availability	Coal Seam - Partial Depleted Gas - Partial Devonian Shale - Future	Coal Seam - Partial Depleted Gas - Partial Tuscarora - Available	Saline Reservoirs - Available
ECBM or EGR Potential	ECBM, EGR	ECBM, EGR	None
Storage Risks	Faults, abandoned wells	Faults, numerous abandoned wells	Faults
MVA Challenges	Large monitoring area, complex terrain	Moderate monitoring area, industrial and agricultural activities	Small monitoring area, complex terrain
CO_2 sources	Estimated CO_2 emissions from power generation and other industrial processes:		
	Total emissions within 50 miles: 7.8 Mt/year Total emissions within 100 miles: 42.5 Mt/year	Total emissions within 50 miles: 3.2 Mt/year Total emissions within 100 miles: 68.1 Mt/year	Total emissions within 50 miles: 18.5 Mt/year Total emissions within 100 miles: 126.5 Mt/year

Finally, Table 35 is the final ranking matrix used to evaluate all quantitative and qualitative parameters used in this preliminary analysis. The final scores listed in this table

are derived by multiplying site's rank with corresponding weight coefficient. The coefficients for each performance parameter are based on parameter's impact on overall feasibility of the project. For example, the maximum of 5 points are awarded to the best ranked storage site in the "capacity" and "injectivity" categories since those two performance parameters have the highest impact on the project. On the other hand, only 3 points are awarded to the best ranked site in the "topography" category since of all parameters listed in Table 34 this category has the lowest overall impact on the project.

Based on this methodology, the best overall score has the Site I, located in Dickenson County, Virginia. As can be seen from the ranking matrix, this site has multiple advantages compared to the other two storage options.

Table 35: Ranking matrix.

Performance Parameter	**Site 1 Dickenson County, Virginia**	**Site 2 Wyoming County, West Virginia**	**Site 3 Clay County, West Virginia**	**Coefficient**		
				1	**2**	**3**
Capacity and storage availability	**1**	**2**	**3**	5 pt	4 pt	3 pt
Size of the monitoring area	**3**	**2**	**1**	4 pt	3 pt	2 pt
Site topography and land cover	**3**	**1**	**2**	3 pt	2 pt	1 pt
Available infrastructure at the site - ease of access	**1**	**3**	**1**	4 pt	3 pt	2 pt
Injectivity	**1**	**2**	**3**	5 pt	4 pt	3 pt
ECBM-EGR potential	**1**	**1**	**0**	5 pt	4 pt	3 pt
Proximity to CO_2 sources	**1**	**3**	**2**	5 pt	4 pt	3 pt
Costs of MVA program	**2**	**2**	**3**	4 pt	3 pt	2 pt
Probability of seismic events	**2**	**2**	**1**	5 pt	4 pt	3 pt
Completed/abandoned wells around storage site	**1**	**3**	**2**	5 pt	4 pt	3 pt
Cap rock/sealing properties	**2**	**1**	**2**	5 pt	4 pt	3 pt
Final Score	***42 pt.***	***37 pt.***	***33pt.***			

Chapter 6.
CONCLUSIONS AND RECOMMENDATIONS

Compared to other GHG mitigation options, CCS is an emerging technology that has significant potential to reduce CO_2 emissions. Although current CCS technology is based on a combination of well-known and emerging technologies and processes, many performance and safety aspects must be addressed before CCS is introduced to the market and commercially deployed.

The decisions related to development and implementation of the commercial-scale CO_2 sequestration projects must take into account both technical and economic parameters and constraints, while considering a number of related risks and safety issues. For that reason, there is a need for a systematic methodology that can help project designers, policymakers, and other parties involved in CCS process to evaluate all available data and make knowledgeable decisions. With this in mind, the focus of this research effort was to identify all parameters and constraints related to CO_2 storage in unmineable coal seams.

From a comprehensive analysis of technical aspects of CO_2 sequestration in deep unmineable coal seams, it was found that the method for capacity estimation is the main source of the uncertainty, and has the largest impact on the technical feasibility of the project development. It was observed that in some cases, when using different methods for the storage capacity calculation, the capacity estimates differ in orders of magnitude for the same

storage site. For that reason, it is important that the government, industry, and the relevant scientific community agree on how to standardize capacity estimation procedures and related reporting rules.

There are many open issues related to CO_2 sequestration in unmineable coal seams that has to be understood and addressed before commercial deployment of the technology. The most important issues include: transmissivity between fracture and matrix pore systems; geometry and structure of confining formations near targeted seam; and coal cleat structure and its response to pressure changes. Hence, the large-scale injection tests and monitoring studies are a necessary step before commercial application of CCS technology.

Results from the real option analysis show that even with extra earnings from ECBM production, under current policy framework, an investment risk is very high. Of all uncertainties, the climate policy and carbon price have the most significant impact. On the other hand, decreasing the costs of CO_2 capture, which accounts for more than 90% of total CCS costs, would probably lead to a profitability of such investment.

The decision making framework presented in this work incorporates critical parameters and assessment procedures necessary for the adequate techno-economic assessment of CO_2 sequestration. Although this holistic framework does not provide a decision rule or a "right" solution to a set of complex problems expected in commercial-scale CO_2 storage operations, it provides recommendations and guidelines that can help a decision maker in early characterization and site selection phases. The framework is designed to be flexible and expandable so that new modules and empirical data can be easily incorporated. This approach provides the user with the capability to develop and implement new

knowledge and available data, and furthermore, to build a computer-based decision support system that can automatize the entire process.

This decision making platform can be applied consistently at diverse sites as well as at different times with varying complexity at a single site. It can be initially used as a screening tool that can help to quickly decide on the suitability of storage sites. As site selection proceeds, this expert tool can be modified for individual sites as detailed site specific information become available.

There are many possible future research directions for this research. This is a first step towards the development of the computer-based simulator or decision support system that can make stochastic projections and detailed cost estimates for geological CO_2 sequestration.

Additional research direction would involve assessment of socio-economic factors and benefits that can arise from the implementation of a CCS project within a certain region. For example, adding a parameter related to job creation would help provide another perspective on the role of these projects and their importance for the region and local communities.

REFERENCES

1. Benson, S.M. and T. Surles, *Carbon dioxide capture and storage: An overview with emphasis on capture and storage in deep geological formations.* Proceedings of the Ieee, 2006. **94**(10): p. 1795-1805.
2. Watson, R.T.a.t.C.W.T., *IPCC Third Assessment Report: Climate Change 2001*, 2001, Intergovernmental Panel on Climate Change. p. 398.
3. United States. Congress. Senate. Committee on Commerce Science and Transportation., *Climate change research and scientific integrity : hearing before the Committee on Commerce, Science, and Transportation, United States Senate, One Hundred Tenth Congress, first session, February 7, 2007*. S hrg2010, Washington: U.S. G.P.O. : For sale by the Supt. of Docs., U.S. G.P.O. iii, 89 p.
4. Metz, B. and W.G.I. Intergovernmental Panel on Climate Change, *IPCC special report on carbon dioxide capture and storage*2005: Cambridge University Press for the Intergovernmental Panel on Climate Change.
5. Houghton, J.T., *Global warming: the complete briefing*2004: Cambridge University.
6. Sabine, C.L., et al., *The Oceanic Sink for Anthropogenic CO2.* Science, 2004. **305**(5682): p. 367-371.
7. Administration, U.S.E.I., *Annual Energy Outlook 2011*, EIA, Editor 2011.
8. Agency, I.E., *Annual World Energy Outlook 2010*, 2010, IEA.
9. Herzog, H.J., *Carbon Dioxide Capture and Storage*, in *The Economics and Politics of Climate Change*, D.H.a.C. Hepburn, Editor 2009, Oxford University Press.
10. Herzog, H.J.K., J. , *The Future of Coal in a Greenhouse Gas Constrained World*, in *8th International Conference on Greenhouse Gas Control Technologies*2006: Trondheim, Norway.
11. Metz, B.D., O. Meyer, L. de Coninck, HC., *Special Report on Carbon Dioxide Capture and Storage*, 2005, IPCC - Intergovernmental Panel on Climate Change.
12. Lewis, C., *Capturing CO2*, 2007, International Energy Agency (IEA) Greenhouse Gas R&D Programme.
13. Kohl, A.L. and R.B. Nielsen, *Gas purification*1997: Gulf Pub.
14. Rao, A.B. and E.S. Rubin, *A Technical, Economic, and Environmental Assessment of Amine-Based CO2 Capture Technology for Power Plant Greenhouse Gas Control.* Environmental Science & Technology, 2002. **36**(20): p. 4467-4475.

15. Zanganeh, K.E. and A. Shafeen, *A novel process integration, optimization and design approach for large-scale implementation of oxy-fired coal power plants with CO2 capture.* International Journal of Greenhouse Gas Control, 2007. **1**(1): p. 47-54.

16. Varagani, R., Chatel-Pelage, F., Gautier, F., Pranda, P., McDonald, D., Devault, D., Farzan, H., Schoff, R., Ciferno, J., Bose, A. *Oxy-combustion process for CO2 capture from coal fired power plants: An overview of techno-economic study and engineering feasibility analysis*. in *Proceedings of Inter. Con. GHG Con. Tech.* 2006. Trondheim, Norway.

17. Svensson, R., et al., *Transportation infrastructure for CCS --Experiences and expected development*, in *Greenhouse Gas Control Technologies 7*, E.S. Rubin, et al., Editors. 2005, Elsevier Science Ltd: Oxford. p. 2531-2534.

18. Barrie, J., et al., *Carbon dioxide pipelines: A preliminary review of design and risks*, in *Greenhouse Gas Control Technologies 7*, E.S. Rubin, et al., Editors. 2005, Elsevier Science Ltd: Oxford. p. 315-320.

19. Bachu, S., et al., *CO2 storage capacity estimation: Methodology and gaps.* International Journal of Greenhouse Gas Control, 2007. **1**(4): p. 430-443.

20. Ennis-King, J., Paterson, L, . *Reservoir engineering issues in the geological disposal of carbon dioxide*. in *Greenhouse Gas Control Technologies: Proceedings of the Fifth International Conference on Greenhouse Gas Control Technologies*. 2001. Cairns, Australia: CSIRO Publishing.

21. Gunter, W.D., Gentzis, T., Rottenfusser, B. A., Richardson, R. J. H., *Deep coalbed methane in Alberta, Canada: A fuel resource with the potential of zero greenhouse gas emissions.* Energy Conversion and Management, 1997. **38**(Supplement 1): p. S217-S222.

22. Bradshaw, J., Rigg, A., *The GEODISC Program: Research into Geological Sequestration of CO2 in Australia.* Environmental Geosciences, 2001. **8**(3): p. 166-176.

23. NETL, U.S.D.-. *Carbon Sequestration Atlas of the United States and Canada*, in *Atlas III*2010.

24. Holloway, S., Savage, D., *The potential for aquifer disposal of carbon dioxide in the UK.* Energy Conversion and Management. **34**(9-11): p. 925-932.

25. Celia, M.A. and S. Bachu, *Geological Sequestration of CO2: Is Leakage Unavoidable and Acceptable?*, in *Greenhouse Gas Control Technologies - 6th International Conference*, J. Gale and Y. Kaya, Editors. 2003, Pergamon: Oxford. p. 477-482.

26. Damen, K., et al., *Identification of early opportunities for CO2 sequestration--worldwide screening for CO2-EOR and CO2-ECBM projects.* Energy, 2005. **30**(10): p. 1931-1952.

27. Frailey, S.M. and R.J. Finley, *Classification of CO2 Geologic Storage: Resource and Capacity.* Energy Procedia, 2009. **1**(1): p. 2623-2630.

28. Hepple, R.P. and S.M. Benson, *Geologic storage of carbon dioxide as a climate change mitigation strategy: performance requirements and the implications of surface seepage.* Environmental Geology, 2005. **47**(4): p. 576-585.

29. Aydin, G., I. Karakurt, and K. Aydiner, *Evaluation of geologic storage options of CO2: Applicability, cost, storage capacity and safety.* Energy Policy, 2010. **38**(9): p. 5072-5080.

30. Vangkilde-Pedersen, T., et al., *Assessing European capacity for geological storage of carbon dioxide-the EU GeoCapacity project.* Energy Procedia, 2009. **1**(1): p. 2663-2670.

31. Benson, S.M. and D.R. Cole, *CO2 Sequestration in Deep Sedimentary Formations.* Elements, 2008. **4**(5): p. 325-331.

32. Bentham, M. and G. Kirby, *CO2 storage in saline aquifers.* Oil & Gas Science and Technology-Revue De L Institut Francais Du Petrole, 2005. **60**(3): p. 559-567.

33. Hermanrud, C., et al., *Storage of CO2 in saline aquifers-Lessons learned from 10 years of injection into the Utsira Formation in the Sleipner area.* Energy Procedia, 2009. **1**(1): p. 1997-2004.

34. Law, D.H.S. and S. Bachu, *Hydrogeological and numerical analysis of CO2 disposal in deep aquifers in the Alberta sedimentary basin.* Energy Conversion and Management. **37**(6-8): p. 1167-1174.

35. Cailly, B., et al., *Geological storage of CO2: A state-of-the-art of injection processes and technologies.* Oil & Gas Science and Technology-Revue De L Institut Francais Du Petrole, 2005. **60**(3): p. 517-525.

36. Solomon, S., et al., *A Simplified, Semi-analytical Method to Handle Uncertainty in Long-term Containment in Geologic CO2 Storage Sites.* Energy Procedia, 2009. **1**(1): p. 2533-2540.

37. Pawar, R.J., et al., *Geologic sequestration of CO2 in a depleted oil reservoir.* Abstracts of Papers of the American Chemical Society, 2003. **226**: p. U605-U605.

38. Zhang, Y.Q., C.M. Oldenburg, and S.M. Benson, *Vadose zone remediation of carbon dioxide leakage from geologic carbon dioxide sequestration sites.* Vadose Zone Journal, 2005. **3**(3): p. 858-866.

39. Wiese, B., et al., *Hydraulic characterisation of the Stuttgart formation at the pilot test site for CO2 storage, Ketzin, Germany.* International Journal of Greenhouse Gas Control, 2010. **4**(6): p. 960-971.

40. Würdemann, H., et al., *CO2SINK--From site characterisation and risk assessment to monitoring and verification: One year of operational experience with the field laboratory for CO2 storage at Ketzin, Germany.* International Journal of Greenhouse Gas Control, 2010. **4**(6): p. 938-951.

41. Doughty, C. and K. Pruess, *Modeling Supercritical Carbon Dioxide Injection in Heterogeneous Porous Media.* Vadose Zone J, 2004. **3**(3): p. 837-847.

42. Flett, M., R. Gurton, and G. Weir, *Heterogeneous saline formations for carbon dioxide disposal: Impact of varying heterogeneity on containment and trapping.* Journal of Petroleum Science and Engineering, 2007. **57**(1-2): p. 106-118.

43. Litynski, J., et al., *An Overview of Terrestrial Sequestration of Carbon Dioxide: the United States Department of Energy's Fossil Energy R&D Program.* Climatic Change, 2006. **74**(1): p. 81-95.

44. Vivalda, C., M. Loizzo, and Y. Lefebvre, *Building CO2 Storage Risk Profiles With The Help Of Quantitative Simulations.* Energy Procedia, 2009. **1**(1): p. 2471-2477.

45. Damen, K., A. Faaij, and W. Turkenburg, *Health, Safety and Environmental Risks of Underground Co2 Storage – Overview of Mechanisms and Current Knowledge.* Climatic Change, 2006. **74**(1): p. 289-318.

46. Gale, J., *Geological storage of CO2: What do we know, where are the gaps and what more needs to be done?* Energy, 2004. **29**(9-10): p. 1329-1338.

47. Bachu, S., *CO2 storage in geological media: Role, means, status and barriers to deployment.* Progress in Energy and Combustion Science, 2008. **34**(2): p. 254-273.

48. Cooper, C., *A technical basis for carbon dioxide storage.* Energy Procedia, 2009. **1**(1): p. 1727-1733.

49. Simone, A.M., E.; Jenvey, N., *CO2 geological storage field development-Application of baseline, monitoring and verification technology.* Energy Procedia, 2009. **1**(1): p. 2219-2226.

50. NETL, U.S.D.-. *Monitoring, Verification, and Accounting of CO2 Stored in Deep Geologic Formations*, 2009.

51. Jones, D.G., et al., *New and established techniques for surface gas monitoring at onshore CO2 storage sites.* Energy Procedia, 2009. **1**(1): p. 2127-2134.

52. Fabriol, H., et al., *Results of investigations to design a monitoring program for a CO2 storage project in the Paris Basin (France).* Energy Procedia, 2009. **1**(1): p. 2285-2291.

53. White, D.J. and J.W. Johnson, *Integrated geophysical and geochemical research programs of the IEA GHG Weyburn-Midale CO2 monitoring and storage project.* Energy Procedia, 2009. **1**(1): p. 2349-2356.

54. Herzog, H.J., *Scaling up carbon dioxide capture and storage: From megatons to gigatons.* Energy Economics, 2011. **In Press, Corrected Proof**.

55. Bohm, M.C., et al., *Capture-ready coal plants - Options, technologies and economics.* International Journal of Greenhouse Gas Control, 2007. **1**(1): p. 113-120.

56. Hamilton, M.R., H.J. Herzog, and J.E. Parsons, *Cost and U.S. public policy for new coal power plants with carbon capture and sequestration.* Energy Procedia, 2009. **1**(1): p. 4487-4494.

57. IEA Energy Technology Analysis, *Prospects for CO2 Capture and Storage* 2004, Paris Washington, D.C: OECD/IEA.

58. McCoy, S.T. and E.S. Rubin, *An engineering-economic model of pipeline transport of CO2 with application to carbon capture and storage.* International Journal of Greenhouse Gas Control, 2008. **2**(2): p. 219-229.

59. Laughton, D., Hyndman, R., Weaver, A., Gillett, N., Webster, M., Allen, M., Koehler, J., *A Real Options Analysis of a GHG Sequestration Project*. 2004.

60. Rammerstorfer, M. and R. Eisl, *Carbon capture and storage—Investment strategies for the future?* Energy Policy, 2011. **39**(11): p. 7103-7111.

61. Dixit, A.K. and R.S. Pindyck, *Investment under uncertainty*1994: Princeton University Press.

62. Kodukula, P. and C. Papudesu, *Project valuation using real options: a practitioner's guide*2006: J. Ross Pub.

63. Damodaran, A., *THE PROMISE OF REAL OPTIONS.* Journal of Applied Corporate Finance, 2000. **13**(2): p. 29-44.

64. Harrison, R., et al. *A Decision Support System for Filtering and Analysis of Carbon Dioxide Capture Data*. in *Electrical and Computer Engineering, 2007. CCECE 2007. Canadian Conference on*. 2007.

65. Fox, J., et al., *Safe and sound: artificial intelligence in hazardous applications*2000: AAAI Press/MIT Press.

66. Druzdzel, M., Flynn, R., *Decision Support Systems*, in *Encyclopedia of library and information science*2002.

67. Szladow, A.J., Mills, D. *Intelligent system in heavy industry*. in *Proceedings of intelligent systems in process engineering*. 1995. Denver, CO.

68. Liqiang Geng, Z.C., Christine W. Chan, Gordon H. Huang. , *An intelligent decision support system for management of petroleum-contaminated sites.* Expert Syst. Appl., 2001: p. 251~260

69. Flores, J.J., *Engineering Applications of Artificial Intelligence*2000: Elsevier.

70. Kritpiphat, W., An, A., Chan, C.W., Tontiwachwuthikul, P., & Cercone, N. , *Supervisory and decision-support system for intelligent monitoring and control of a pipeline network*, in *ISPE*1995.

71. Gentzis, T., *Economic coalbed methane production in the Canadian Foothills: Solving the puzzle.* International Journal of Coal Geology, 2006. **65**(1-2): p. 79-92.

72. Gunter, W.D., S. Wong, and T. Gentzis, *Field-testing CO2 sequestration and enhanced coalbed methane recovery in Alberta, Canada - Historical perspective and future plans.* Abstracts of Papers of the American Chemical Society, 2000. **220**: p. U396-U396.

73. Koperna, G.J., Riestenberg, D.E. *Carbon Dioxide Enhanced Coalbed Methane and Storage: Is There Promise?* in *SPE International Conference on CO2 Capture, Storage and Utilization*. 2009. San Diego, California, USA.

74. Mavor, M.J., Gunter, W.D., Robinson, J.R., Law, D.H.S., Gale, J. *Testing for CO2 Sequestration and Enhanced Methane Production from Coal*. in *SPE Gas Technology Symposium*. 2002. Calgary, Alberta, Canada.

75. Wong, S., Gunter, B., *Testing CO2-Enhanced Coalbed Methane Recovery*, in *Greenhouse Issues, v. 45*1999.

76. Korre, A., et al., *Modelling the uncertainty and risks associated with the design and life cycle of CO2 storage in coalbed reservoirs.* Energy Procedia, 2009. **1**(1): p. 2525-2532.

77. Stevens, S.H., Spector, D., *Enhanced Coalbed Methane Recovery: Worldwide Application and CO2 Sequestration Potential*, 1998, Report prepared for IEA Greenhouse Gas R&D Programme.

78. Cook, P.J., Rigg, A., Bradshaw, J. , *Putting it back where it came from: Is geological disposal of carbon dioxide an option for Australia?* . Australian Petroleum Production and Exploration Association Journal 2000. **40** (1): p. 654-666.

79. van Bergen, F., Pagnier, H. , *CO2 sequestration in coal - a potentially clean energy cycle*, in *Greenhouse issues*2001, IEA. p. 3-6.

80. Holditch, S.A., et al., *Coal seam stimulation manual: topical report*1990: The Institute.

81. Langmuir, I., *The Evaporation, Condensation and Reflection of Molecules and the Mechanism of Adsorption.* Physical Review, 1916. **8**(2): p. 149-176.

82. Hildenbrand, A., et al., *Evolution of methane sorption capacity of coal seams as a function of burial history — a case study from the Campine Basin, NE Belgium.* International Journal of Coal Geology, 2006. **66**(3): p. 179-203.

83. Arri, L.E., Yee, D., *Modeling Coalbed Methane Production with Binary Gas Sorption*, in *SPE Rocky Mountain Regional Meeting*1992: Casper, Wyoming.

84. Conrad, J.M., Miller, M. J., Ripepi, N., *Potential for Carbon Sequestration in the Central Appalachian Basin*, in *Air and Waste Management Association Conference*2007.

85. Marshall Miller & Associates, *FINAL REPORT: Characterization and Preliminary Engineering and Design Of Potential Sites for a Large-Volume Carbon Sequestration Test In Coal Seams with Enhanced Coalbed Methane Recovery and In Other Secondary Geological Reservoirs In Central Appalachia*, 2011: Bluefield, Virginia.

86. Ripepi, N., *Carbon Dioxide Storage in Coal Seams with Enhanced Coalbed Methane Recovery: Geologic Evaluation, Capacity Assessment and Field Validation of the Central Appalachian Basin*, 2009, Virginia Polytechnic Institute & State University: Blacksburg, VA.

87. Virginia Center for Coal and Energy Research, V., *Final Technical Report: Characterization and Field Validation of the Carbon Sequestration Potential of Coal Seams in the Central Appalachian Basin*, 2011: Blacksburg, VA

88. Durucan, S. and J.-Q. Shi, *Improving the CO2 well injectivity and enhanced coalbed methane production performance in coal seams.* International Journal of Coal Geology, 2009. **77**(1-2): p. 214-221.

89. Fokker, P.A. and L.G.H. van der Meer, *The injectivity of coalbed CO2 injection wells.* Energy, 2004. **29**(9-10): p. 1423-1429.

90. Siriwardane, H.J., R.K. Gondle, and D.H. Smith, *Shrinkage and swelling of coal induced by desorption and sorption of fluids: Theoretical model and interpretation of a field project.* International Journal of Coal Geology, 2009. **77**(1-2): p. 188-202.

91. Stanton, R., Flores, R., Warwick, P.D., Gluskoter, H., Stricker, G.D. , *Coalbed sequestration of carbon dioxide*, in *1st National Conference on Carbon Sequestration*2001: Washington, USA

92. Reeves, S., Taillefert, A., Pekot, L., Clarkson, C. , *Topical Report: The Allison Unit CO2-ECBM pilot: a reservoir modeling study*, 2003, U.S. Department of Energy.

93. Xie, X. and M.J. Economides, *The impact of carbon geological sequestration.* Journal of Natural Gas Science and Engineering, 2009. **1**(3): p. 103-111.

94. Carroll, R.E., Pashin, J.C., *Relationship of Sorption Capacity to Coal Quality: CO2 Sequestration Potential of Coal Bed methane Reservoirs in the Black Warrior Basin*, in *Proceedings of the International Coal Bed Methane Symposium*2003, paper 0317. p. 11p.

95. Chalmers, G.R.L. and R. Marc Bustin, *On the effects of petrographic composition on coalbed methane sorption.* International Journal of Coal Geology, 2007. **69**(4): p. 288-304.

96. Reeves, S., *Topical Report - Assessment of CO2 Sequestration and ECBM Potential of U.S. Coalbeds*, February, 2003, Advanced Resources International.

97. DMME. *Virginia Gas and Oil Production Statistics*. 2008.

98. Conrad, J.M., Miller, M.J., Phillips, J., Ripepi, N. , *Characterization of Central Appalachian Basin CBM Development: Potential for Carbon Sequestration and Enhanced CBM Recovery*, in *International Coalbed Methane Symposium*2006 Tuscaloosa, Alabama.

99. Grimm, R.P., et al., *Seal evaluation and confinement screening criteria for beneficial carbon dioxide storage with enhanced coal bed methane recovery in the Pocahontas Basin, Virginia.* International Journal of Coal Geology, (0).

100. (USDA), U.S.D.o.A., *Soil Survey of Russell County, Virginia*, 1945.

101. (USDA), U.S.D.o.A. *Web Soil Survey*. 2008; Available from: http://websoilsurvey.nrcs.usda.gov/.

102. (USDA), U.S.D.o.A. *National Cooperative Soil Survey*. 2001; Available from: http://www2.ftw.nrcs.usda.gov/osd/dat/S/SHELOCTA.html.

103. (USDA), U.S.D.o.A. *National Cooperative Soil Survey*. 2000; Available from: http://www2.ftw.nrcs.usda.gov/osd/dat/C/CEDARCREEK.html.

104. Harlow, G.E., Jr., and LeCain, G.D., *Hydraulic characteristics of, and ground-water flow in, coal-bearing rocks of southwestern Virginia*, in *U.S. Geological Survey Water Supply*1993. p. 36 p.

105. Matthews, C.S. and D.G. Russell, *Pressure buildup and flow tests in wells*1967: Henry L. Doherty Memorial Fund of AIME.

106. Stauffer, P.H., et al., *A System Model for Geologic Sequestration of Carbon Dioxide.* Environmental Science & Technology, 2008. **43**(3): p. 565-570.

107. Teisberg, E.O., *Capital Investment Strategies under Uncertain Regulation.* The RAND Journal of Economics, 1993. **24**(4): p. 591-604.

108. Teisberg, E.O., *An Option Valuation Analysis of Investment Choices by a Regulated Firm.* Management Science, 1994. **40**(4): p. 535-548.

109. Brennan, M.J., *The supply of storage*, in *The American economic review*1958, American Economic Association.

110. Nagel, T. and M. Rammerstorfer, *Modeling investment behavior under price cap regulation.* Central European Journal of Operations Research, 2009. **17**(2): p. 111-129.

111. Roques, F.A. and N. Savva, *Investment under uncertainty with price ceilings in oligopolies.* Journal of Economic Dynamics and Control, 2009. **33**(2): p. 507-524.

112. Abadie, L.M. and J.M.C. Gómez, *Long-term dynamics in CO2 allowance prices and carbon capture investments*2007: Universidad del País Vasco.

113. Benz, E.A. and S. Trueck, *Modeling the Price Dynamics of Co2 Emission Allowances.* SSRN eLibrary, 2008.

114. Daskalakis, G., D. Psychoyios, and R.N. Markellos, *Modeling CO2 Emission Allowance Prices and Derivatives: Evidence from the European Trading Scheme.* Journal of Banking & Finance, Vol. 33, No. 7, pp. 1230-1241, 2009, 2008.

115. Szymon, B., et al., *Convenience Yields for CO2 Emission Allowance Futures Contracts*, 2006, Sonderforschungsbereich 649, Humboldt University, Berlin, Germany.

116. Bock, B., et al., *ECONOMIC EVALUATION OF CO2 STORAGE AND SINK ENHANCEMENT OPTIONS*, in *Other Information: PBD: 1 Feb 2003*2003. p. Medium: ED; Size: 462 pages.

117. Dooley, J.J., R.T. Dahowski, and C.L. Davidson, *On the Long-Term Average Cost of CO2 Transport and Storage*, March 2008.

118. Gale, J. and J. Davison, *Transmission of CO2—safety and economic considerations.* Energy. **29**(9-10): p. 1319-1328.

119. Rubin, E.S., C. Chen, and A.B. Rao, *Cost and performance of fossil fuel power plants with CO2 capture and storage.* Energy Policy, 2007. **35**(9): p. 4444-4454.

120. Rubin, E.S., et al., *Use of experience curves to estimate the future cost of power plants with CO2 capture.* International Journal of Greenhouse Gas Control, 2007. **1**(2): p. 188-197.

121. (EPA), E.P.A., *Geologic CO2 Sequestration Technology and Cost Analysis*, in *Technical Support Document*2008.